BULLETIN 60

Geology and Mineral Deposits of the Northern Big Burro Mountains-Redrock Area, Grant County, New Mexico

by CHARLES H. HEWITT

STATE BUREAU OF MINES AND MINERAL RESOURCES
NEW MEXICO INSTITUTE OF MINING & TECHNOLOGY
CAMPUS STATION SOCORRO, NEW MEXICO

BULLETIN 60

Geology and Mineral Deposits of the Northern Big Burro Mountains-Redrock Area, Grant County, New Mexico

by CHARLES H. HEWITT

1959

STATE BUREAU OF MINES AND MINERAL RESOURCES
NEW MEXICO INSTITUTE OF MINING & TECHNOLOGY
CAMPUS STATION SOCORRO, NEW MEXICO

NEW MEXICO INSTITUTE OF MINING & TECHNOLOGY

E. J. Workman, *President*

STATE BUREAU OF MINES AND MINERAL RESOURCES

Alvin J. Thompson, *Director*

THE REGENTS

MEMBERS EX OFFICIO

The Honorable John Burroughs ..... *Governor of New Mexico*

Tom Wiley ..... *Superintendent of Public Instruction*

APPOINTED MEMBERS

Robert W. Botts ..... Albuquerque

Holm O. Bursum, Jr. ..... Socorro

Thomas M. Cramer ..... Carlsbad

John N. Mathews, Jr. ..... Socorro

Richard A. Matuszeski ..... Albuquerque

NORTHERN BIG BURRO MOUNTAINS-REDROCK AREA

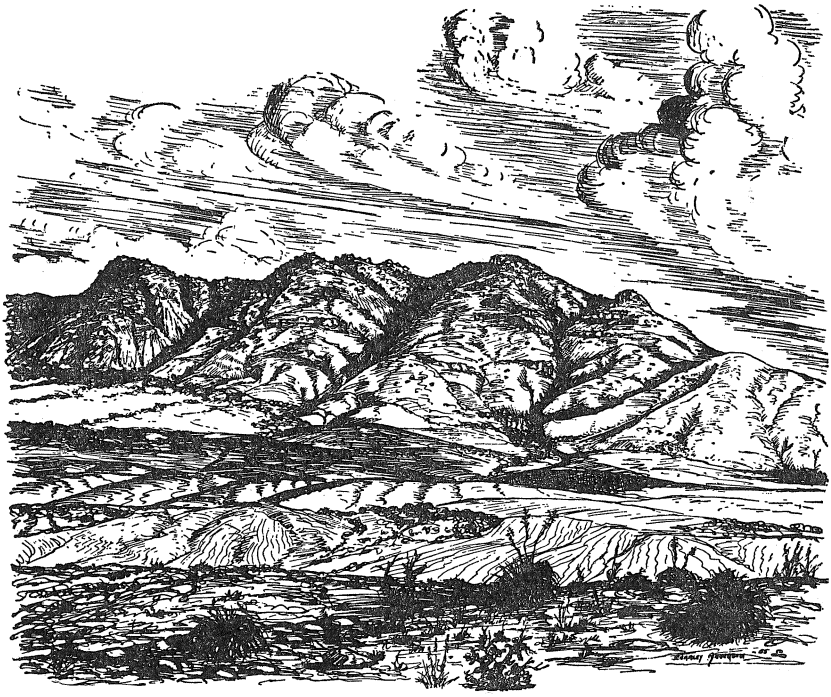

Plate 13

West Side of Northern Big Burro Mountains

Typical steep, narrow valleys. Pediment (left) at base of mountains; dissected Gila conglomerate (foreground). *Sketch by courtesy of Charley Anderson, Jr.*

Contents

	Page
ABSTRACT	1
INTRODUCTION	3
Nature of investigation	3
Previous work	3
Acknowledgments	4
GEOGRAPHY AND GEOMORPHOLOGY	5
Location and access	5
Climate and vegetation	5
Topography and drainage	6
Pediment surfaces	7
GENERAL GEOLOGY	8
Regional geology	8
Geology of central Grant County	8
General statement	8
Geology of the Big Burro Mountains	9
Definition of rock units	9
Precambrian metamorphic and igneous rocks	9
Cretaceous sedimentary rocks	10
Laramide and post-Laramide intrusive rocks	10
Tertiary volcanic rocks	11
Tertiary and Quaternary sedimentary rocks	11
PETROLOGY	12
Precambrian metamorphic and igneous rocks	12
General statement	12
Bullard Peak series	12
General statement	12
Quartz-feldspar gneiss and related rocks	14
Sillimanite gneiss	21
Hornblende gneiss and related rocks	22
Granite gneiss	27
Migmatite	30
Origin of the Bullard Peak series	32

Page

Ash Creek series 33
General statement 33
Sericite phyllite 36
Andalusite-sericite schist 37
Cordierite hornfels 38
Spotted andalusite hornfels 39
Biotite hornfels 41
Diopside quartzite 42
Serpentine-carbonate rocks 44
Origin of the Ash Creek series 53
Comparison of the Bullard Peak and Ash Creek series 57

Precambrian igneous rocks 58
Anorthosite 58
Occurrence 58
Petrography 59
Origin 60
Age 60
Metadiabase 60
General statement 60
Occurrence 60
Petrography 61
Origin 62
Granite and related rocks 63
General statement 63
Tonalite 65
Granite 66
Orbicular rock 69
Pegmatite 73
Aplite 76
Age relations in the Burro Mountains batholith 77

Cretaceous sedimentary rocks 78
Beartooth quartzite 78
General statement 78
Stratigraphy 78
Petrogenesis 79
Colorado shale 80
General statement 80
Stratigraphy 80
Petrogenesis 81

Page

Laramide and post-Laramide intrusive rocks 81
General statement 81
Diabase 82
Occurrence 82
Petrography 83
Origin and age 83
Andesite 84
Occurrence 84
Petrography 84
Age 84
Monzonite porphyry 85
Occurrence 85
Petrography 85
Age 85
Andesite porphyry 85
Occurrence 85
Petrography 86
Origin and age 86
Rhyolite and rhyolite porphyry 87
Occurrence 87
Petrography 87
Age 88
Basalt 88
Occurrence and petrography 88
Age 88

Tertiary volcanic rocks 89
General statement 89
Quartz latite and rhyolite 89
Occurrence 89
Petrography 89
Origin and age 90

Tertiary and Quaternary sedimentary rocks 91
General statement 91
Gila conglomerate 92
Occurrence 92
Petrology 92
Origin 94

Page

Bajada deposits 94
Terrace gravels 94
Bolson deposits 94
Quaternary alluvium 95

STRUCTURAL GEOLOGY 96
General statement 96
Precambrian structural features 96
Banding, layering, and foliation 96
Lineation 98
Folds 98
Igneous-metamorphic relations 99
Contacts 99
Xenoliths 99

Laramide and post-Laramide structural features 100
Faults, joints, and fractures 100
Dikes and stocks 102

Relation of Precambrian and Laramide structures 103

GEOLOGICAL HISTORY 104
Precambrian history 104
Paleozoic and Mesozoic history 105
Laramide and post-Laramide history 106

ECONOMIC GEOLOGY 107
History of mining 107
Precambrian metamorphic deposits 108
Serpentinite (ricolite) 108
Asbestos 108
Magnetite 108

Precambrian pegmatites 109
Mica 109

Laramide and post-Laramide hydrothermal veins 109
General statement 109
Tungsten 110
Rice-Graves claim 110
S. Harper claim 112

Page

Copper 113
Lead 113
Lead Mountain 113
Slate Creek Canyon 113
Little Bear Canyon 114
Live Oak prospect 114

Silver 115
Telegraph district 115
Black Hawk district 115
Astrologer mine 116

Fluorite 116
General features 116
Great Eagle mine 117
Hope prospect 119
Redrock area 119
Long Lost Brother prospect 120
Wild Horse Mesa and vicinity 121

Manganese 122
General features 122
Black Eagle mine 122

Radioactive minerals 124

Laramide and post-Laramide replacement deposits 126

Magnesite 126

Economic potential of the mineral deposits 127

REFERENCES 129

INDEX 145

Illustrations

TABLES

		Page
1.	Comparison of Bullard Peak series and Ash Creek series	13
2.	Modes of Precambrian hornblende gneiss and amphibolite	25
3.	Modes of Precambrian granite gneiss	29
4.	Comparison of the derivation of the Bullard Peak metamorphic rocks	34
5.	Comparison of serpentine minerals	49
6.	Comparison of the derivation of the Ash Creek metasediments	54
7.	Modes of Precambrian metadiabase	61
8.	Modes of Precambrian granite	68
9.	Minerals in pegmatites in the Big Burro Mountains	74
10.	Comparison of the occurrence of Laramide and post-Laramide intrusive rocks	82

FIGURES

1. Geological sketch map of scheelite deposit 111
2. Geological sketch map of the Black Eagle mine 123
3. Geological sketch map of radioactive deposit 125

PLATES

1. Geology of the northern Big Burro Mountains, Redrock area, New Mexico ..... In pocket
2. Burro Mountains 135
3. Granite and gneiss 136
4. Photomicrographs 137
5. Photomicrographs 138
6. Serpentinite 139
7. Photomicrographs 140
8. Igneous rocks 141
9. Migmatites 142
10. Gila conglomerate 143
11. Ore minerals 144
12. Geologic map of the Ash Creek area, Grant Co., New Mexico ..... In pocket
13. West side of northern Big Burro Mountains ..... Frontispiece

Page

Copper 113
Lead 113
Lead Mountain 113
Slate Creek Canyon 113
Little Bear Canyon 114
Live Oak prospect 114

Silver 115
Telegraph district 115
Black Hawk district 115
Astrologer mine 116

Fluorite 116
General features 116
Great Eagle mine 117
Hope prospect 119
Redrock area 119
Long Lost Brother prospect 120
Wild Horse Mesa and vicinity 121

Manganese 122
General features 122
Black Eagle mine 122
Radioactive minerals 124

Laramide and post-Laramide replacement deposits 126
Magnesite 126

Economic potential of the mineral deposits 127

REFERENCES 129

INDEX 145

Abstract

The northern Big Burro Mountains-Redrock area, part of the Basin and Range province, is in Grant County, southwestern New Mexico. Precambrian metamorphic and igneous rocks underlie the northwest-trending mountains; Pliocene(?) Gila conglomerate and younger, unconsolidated gravels underlie the desert basin southwest of the mountains. North-dipping, Upper Cretaceous Beartooth quartzite and Colorado shale beds and early- to middle-Tertiary quartz latite-rhyolite flows cover the northern end of the mountains. Laramide and post-Laramide stocks and dikes have been intruded into Precambrian, Cretaceous, and early-Tertiary rocks.

The Precambrian metamorphic rocks include an older Bullard Peak series and a younger Ash Creek series, both of which occur as xenoliths and roof pendants in the Burro Mountains batholith. The Bullard Peak series is made up of interlayered quartz-feldspar gneiss, biotite gneiss, mica schists, hornblende gneiss, and amphibolite that were formed by dynamic metamorphism (amphibolite facies) of argillaceous feldspathic sandstone, calcareous argillaceous siltstone, shale, and dolomitic shale. These source sediments were intruded by diabase and leucogranite that were metamorphosed to hornblende gneiss and granite gneiss along with the sediments prior to the deposition and metamorphism of the Ash Creek rocks.

The Ash Creek series was derived from a sequence of shales, quartzose shale, feldspathic argillaceous sandstone, dolomitic sandstone, and siliceous dolomite that were first subjected to mild regional metamorphism, and then to three periods of contact metamorphism successively by anorthosite, diabase, and the Burro Mountains granite. The intrusion of diabase was primarily responsible for the formation of sericite phyllite; andalusite-sericite schist; cordierite, andalusite, and biotite hornfelses; diopside quartzite; and several varieties of serpentine-carbonate rocks.

Intrusion of the Burro Mountains batholith resulted in the development of metasomatic muscovite, microcline, and sillimanite and, by lit-par-lit injection, converted part of the Bullard Peak hornblende gneiss and biotite schist to migmatite. Part of one migmatized hornblende gneiss xenolith contains orbicules. The granite enclosed mixed xenoliths of Ash Creek metasediments and diabase and converted the latter to metadiabase. The complex batholith is made up of several varieties of granite and lesser amounts of tonalite, granodiorite, pegmatite, and aplite.

Bullard Peak rocks have a well-developed bedding foliation; lineation is minor. Local contortions and minor folds appear on northeast-

trending major folds. The Ash Creek rocks are poorly foliated and not folded. Northwest- and northeast-striking normal faults of post-Upper Cretaceous age, which are partly controlled by Precambrian structures, are the dominant structural features. Dikes of diabase, andesite, monzonite porphyry, andesite porphyry, rhyolite and rhyolite porphyry, and basalt of Laramide and post-Laramide age have been localized by northeast-, northwest-, west-, and north-trending faults and shears.

Uplift of the Big Burro Mountains by means of faulting along northwesterly faults and along northeasterly cross faults began in late-Cretaceous/early-Tertiary time. The Gila conglomerate formed by the merging of fanglomerates on the mountain flanks. Continued uplift and a change to an arid climate in late-Tertiary/Quaternary time resulted in pedimentation on the western mountain flank, dissection of Gila conglomerate, and deposition of bajada and bolson deposits in the basin to the southwest.

Precambrian metamorphic deposits of serpentinite, asbestos, and magnetite in the Ash Creek rocks are of mineralogical significance only. Laramide and post-Laramide hydrothermal veins related to stocks and dikes of intermediate composition contain fluorite and manganese oxides, as well as minerals containing W, Cu, Pb, Zn, Ag, and U. Over a million dollars in silver and several thousand tons of fluorite have been produced from the area. Significant production in the future is dependent upon the discovery of new ore bodies or extensions of deposits already known.

Introduction

The Big Burro Mountains, which lie about 20 miles west of the Silver City mining district in Grant County, contain the largest exposure of Precambrian rocks in southwestern New Mexico. The local geology of several mining districts on the east flank of the mountains is well known, but prior to this investigation few studies had been made of the petrology, structure, and mineral deposits of the northern Big Burro Mountains.

NATURE OF INVESTIGATION

This report is revised from the writer's doctoral dissertation in the Department of Mineralogy, University of Michigan. The work was sponsored by the New Mexico Bureau of Mines and Mineral Resources under its field assistance fellowship program. Additional details of the study will be found in the original thesis on file with the Bureau in Socorro.

During the summers of 1954, 1955, and 1957, the writer mapped the area of this report on aerial photographs having mean scales of 1:31,680 and 1:8,000. The geologic information was transferred to a base map prepared from the New Mexico State Highway Department quadrangle map SW 9C. Pace and compass sketch maps were made of mineral deposits of possible economic value; prospects and mines were checked with a Geiger counter for significant radioactivity. Investigations carried on at the University of Michigan Mineralogical Laboratory included examination of characteristic hand specimens, thinsections, and polished sections; some mineral identifications were made by oil immersion and X-ray diffraction techniques. Modal estimates of thinsections were made with a Hunt-Wentworth recording micrometer.

PREVIOUS WORK

Gilbert (1875), in the first published report of this area, described the desert ranges of western New Mexico and eastern Arizona as islands of deep-red Archean granite and Paleozoic rocks in basins of Gila conglomerate and other gravel deposits. Lindgren and Graton (1906) and Lindgren et al. (1910) described red and gray gneisses, amphibolite, schist, and pegmatites in the cores of a few of the ridges (Burro Mountains) of the desert range province.

Early studies of the copper deposits in the southern part of the range were made by Reid (1902), Lang (1906), Wade (1907), Stauber (1910), and Somers (1915). Paige (1911) also studied these copper deposits and mapped the geology and ore deposits of Silver City quadrangle, which lies east of the mapped area of this report (Paige, 1916). Snow (1891), Hidden (1893), and Zalinski (1907) examined several small turquoise deposits in the southern Big Burro Mountains; Zalinski (1908)

described the exploitation of these deposits, and Paige (1912) their origin.

A. A. Leach (1916) and Lasky and Wootton (1933) studied the geology of the Black Hawk district in the northern Big Burro Mountains. In late 1951 and early 1952, Gillerman and Whitebread (1956) investigated the uranium-nickel-cobalt-silver deposits and mapped in detail a small area surrounding the Black Hawk mine. F. I. Leach (1920) studied a small radium deposit in the White Signal district in the southern Big Burro Mountains; A. A. Leach (1927) investigated the geology and mining of these deposits. In 1949 and 1950, Granger and Bauer (1950, 1952) investigated the known uranium deposits in this district. Lovering (1956) described uranium mineralization in the White Signal and Black Hawk districts and in seven other localities in the Big Burro Mountains. None of the localities mentioned by Lovering is within the area covered by this report.

Johnston (1928) and Rothrock et al. (1946) investigated fluorite deposits of the Big Burro Mountains. Gillerman (1951) mapped many of these deposits in detail and studied their local geology. Within the Redrock area, serpentine rocks have been investigated by Talmage and Wootton (1937), magnesite by Yale and Stone (1921, 1922), and magnetite by Kelley (1949). Elston (1955b, 1956) did reconnaissance mapping in parts of Virden quadrangle that lie north, west, and south of the area of this report. Wargo (1958) mapped the structure and stratigraphy of the volcanic rocks in the Schoolhouse Mountain area to the north of the Big Burro Mountains.

ACKNOWLEDGMENTS

The writer is indebted to E. Wm. Heinrich of the Mineralogy Department, University of Michigan, for helpful advice throughout the field and laboratory investigation and for critically reviewing the thesis manuscript. R. M. Denning, L. S. Ramsdell, C. B. Slawson, L. I. Briggs, and D. F. Eschman, at the University of Michigan, offered many helpful suggestions and reviewed the original manuscript. Eugene Callaghan, former director, and the late Robert Balk, of the New Mexico Bureau of Mines and Mineral Resources, aided in various problems encountered during the field investigation. Janice L. Hewitt provided invaluable assistance in preparing the manuscript.

The writer is grateful to the residents of Redrock, New Mexico, particularly Mr. and Mrs. Charley Anderson, Jr. and Mr. and Mrs. Fred Anderson, for their many kindnesses during the field investigation.

Sincere appreciation is extended to the New Mexico Bureau of Mines for financial assistance and to the Mineralogy Department, University of Michigan, for providing thin and polished sections. The Ohio Oil Company facilitated preparation of the revised manuscript.

Geography and Geomorphology

LOCATION AND ACCESS

The area of this report lies at the northern end of the Big Burro Mountains, in Grant County, New Mexico (pl. 1). The eastern and western boundaries respectively are the 108°30′ and 108°45′ meridians. The eastern boundary is approximately 15 miles west of Silver City and about 8 miles west of Tyrone. The survey line between T. 19 S. and T. 20 S. marks the southern boundary. Mapping was extended approximately 13 miles north from this line to include the contacts of Precambrian rocks with overlying Cretaceous sediments or Tertiary lavas. Wherever possible, contacts along the eastern edge of the area have been joined with those of Silver City quadrangle (Paige, 1916; Elston, 1955b; Gillerman and Whitebread, 1956).

Two roads which service the community of Redrock enter the area from the east and south. The route from Silver City is as follows: U. S. Highway 260 to the Mangas Valley, a dirt road along the Mangas Valley for 3.7 miles, and a dirt road across the Big Burro Mountains to Redrock, a total distance of 40 miles. The alternate route extends northeast from Lordsburg on U. S. Highway 70 to an oiled county road leading north to Redrock, a total of 30 miles. Several roads and jeep trails from Redrock lead to various prospects and ranches. Main dirt roads are graded and except for periods of heavy rainfall are passable to automobiles. Jeep or truck transportation is desirable for less accessible parts of the area.

CLIMATE AND VEGETATION

Southwestern New Mexico has a continental semiarid to semidesert climate. Although average temperature ranges from 72°F in the summer to 36°F in the winter, daily variations may be as great as 60 degrees. Yearly precipitation averages 16 inches, most of which falls during July and August in widely scattered local thunderstorms. During a single storm, as much as 3 inches of rain may fall and flood the larger canyons and occasionally parts of the Gila Valley.

The flora and fauna of the Burro Mountains clearly reflect the semiarid to semidesert climate. According to Merriam's life zone system of the United States Biological Survey, the higher mountains of the area are in the Transition zone, and the gravel basins are in the Upper Sonoran zone (Corle, 1951). Within the Gila National Forest, the peaks support a moderate growth of piñon, oak, and scrub juniper, with scattered birch, oak, and cottonwood along the mountain valleys. Patches of yucca, agave, catsclaw, mesquite, and numerous species of cacti and grasses grow between the larger trees. The sparse vegetation that dots the gravel basin includes only a few of the above-mentioned shrubs and

grasses and a few large oaks or cottonwoods which are widely scattered along the larger dry washes.

An early pioneer's comment (Corle, 1951) on the flora and fauna of the Gila Valley applies to this area as well: "If you touch it, it stings you; if you pet it, it bites you; if you eat it, it kills you."

TOPOGRAPHY AND DRAINAGE

The Burro Mountains range trends N. 40° W. and is 40 miles long and as much as 15 miles wide. It consists of two distinct topographic masses separated by the Mangas Valley. The larger and western mass is called the Big Burro Mountains, the smaller and eastern mass, the Little Burro Mountains.

The Continental Divide follows the crest of the southern half of the Big Burro Mountains, then swings sharply east across the Little Burro Mountains, and passes north of Silver City. The maximum altitude along the mountain crest is at Burro Peak, 8,035 feet above sea level. The southwestern mountain flank slopes into a gravel-covered basin (pl. 2A). Maximum relief between the mountains and the basin is about 3,000 feet.

The Gila River, which flows southwestward across the area, drains the part of the Big Burro Mountains that lies west of the Continental Divide. The small portion east of the divide is drained ultimately to the Gulf of Mexico through the Rio Grande. Where the Gila cuts across the north end of the Burro Mountains, its canyon averages 40 feet wide at the bottom, with walls as much as 500 feet high. Between Cliff, New Mexico, and Duncan, Arizona, a distance of 55 miles, the river has a gradient of 20 feet per mile. Through the igneous and metamorphic rocks, the course of the Gila is generally straight, but 4 miles northeast of Redrock, where the river leaves the crystalline rocks and flows onto Gila conglomerate, the nature of the channel changes markedly. For a distance of approximately 8 miles, the Gila meanders across a mile-wide valley flat cut into Gila conglomerate. River terraces and meander scars mark meander spurs along both sides of the river.

Intermittent streams entering the Gila River from areas underlain by crystalline rocks have a dendritic pattern that is modified by less resistant bands of metamorphic rocks and by joints, shear zones, and faults in igneous rocks. None of the intermittent streams are spring fed. For a period of several days to several weeks after a heavy rainfall, running water percolates along canyons characterized by a shallow alluvial cover and a large gathering area. Long subparallel washes with wide sandy bottoms, meandering channels, and gentle gradients typify the basin drainage. Many short gullies with relatively steep gradients enter at right angles to the main washes. These basin drainages are dry except for a few hours after a heavy rainfall. The intermittent streams that flow out of the mountains and across the basin before entering the Gila

River decrease sharply in gradient where they enter the basin. These streams trend generally southwest in the mountains and on the steeper slopes of the Gila conglomerate immediately adjacent to the mountains. On the flatter basin surface of the conglomerate, however, the washes trend generally northwest and enter the southwestward flowing Gila River at right angles. This northwest trend of the basin drainages may be the result of fault control.

PEDIMENT SURFACES

A pediment surface along the western flank of the mountains between the mountain slope and the basin gravel is about three-quarters of a mile wide and extends north to northwest in a gentle arc for about 6 miles (pl. 1). It slopes southwest toward the basin at a maximum angle of 13 degrees; the mountain slopes 30 degrees or more. The actual contact of the pediment and the Gila conglomerate is obscured by a bajada of talus and debris derived from the mountains and pediment in post-Gila time.

Although the southern portion of the pediment coincides closely with the surface exposure of granite, and the break in slope coincides with the contact of granite and metamorphic rocks, field evidence indicates pedimentation rather than differential erosion: (1) Along the central and northern parts of the pediment, both the pediment and mountain slopes are underlain by granite and metamorphic rocks; and (2) at Bullard Peak Canyon, metamorphic rocks exposed on the pediment are cut to the same slope as the granite. Inasmuch as the topographic break between the pediment and mountain slopes does not follow a contact for its entire length, the gently sloping surface is most likely a true erosional pediment.

General Geology

REGIONAL GEOLOGY

Eastern Arizona and western New Mexico include parts of three geological provinces: The Colorado Plateau, the Rocky Mountains, and the Basin and Range province. The Colorado Plateau is bounded on the east and southeast by north-trending mountain ranges of the Colorado and New Mexico Rocky Mountains and on the southwest by northwest-trending mountains of the Basin and Range type. The structural relations between the Colorado Plateau and these mountain ranges are obscured to the south by the Tertiary Datil lava field.

In central New Mexico, the north-trending Rocky Mountains extend south from Colorado in two subparallel uplifts of late Laramide age (Eardley, 1951). The eastern uplift is a southern extension of the Sangre de Cristo Range and extends to the Sacramento uplift. The western uplift extends from the Sandia Mountains, at the north, to the Franklin Mountains. These north-trending ranges are characteristically elongate asymmetrical folds, some of which have Precambrian igneous and metamorphic rocks exposed along their crests where Paleozoic and Mesozoic sediments have been eroded away.

The northwest-trending ranges are generally small, distinct, subparallel masses that are closely spaced but separated by relatively narrow valleys filled with Tertiary and Quaternary clastic sediments and interlayered volcanic rocks. These ranges are made up of Precambrian igneous and metamorphic rocks, a thin series of Paleozoic sediments, and a relatively thick series of Cretaceous sediments. Some ranges exhibit extensive folding and thrusting similar to that in northern Utah and western Wyoming; others show numerous high-angle faults but few or no folds or thrust faults (Eardley, 1951).

In southwestern New Mexico, these two types of mountain ranges merge gradually to form dominantly northwest-trending ranges that extend into northern Mexico. The Big Burro Mountains are in the area of convergence but are structurally related to the northwest-trending Basin and Range type of Arizona.

GEOLOGY OF CENTRAL GRANT COUNTY

General Statement

East of the Big Burro Mountains in Silver City quadrangle, two small mountain masses parallel the northwest-trending axis of the Big Burro Mountains. The larger of the two is the Silver City range, which includes Treasure Mountain. This range is characterized by a complex pattern of steeply dipping, northwest-striking normal faults that mark the southwest edge of the range. A Precambrian complex, which is ex-

posed along part of the southwest flank, is overlain by northeast-dipping Paleozoic and Mesozoic sediments. To the north and east, the Silver City range is covered by flat-lying Tertiary flows of rhyolite, andesite, and basalt that have been offset by faults that strike northwest. Northeast-trending normal faults offset the sediments and Precambrian granite and locally transect the northwesterly faults.

The Little Burro Mountains, a similar but smaller and less complex range, lie between the Silver City range and the Big Burro Mountains to the southwest. The Little Burro Mountains, about 8 miles long and 2 miles wide, are bounded on the southwest by a northwest-striking normal fault. Northeast-dipping Cretaceous sediments overlie the Precambrian core, which is exposed along the crest and southwest flank. Stocks and dikes of Laramide age with associated mineral deposits have been intruded into both the Little Burro and Silver City ranges. Tertiary and Quaternary conglomerate, gravel, and alluvium underlie the intermontane valleys.

Geology of the Big Burro Mountains

The Big Burro Mountains are bounded on the southwest, south, and east by a desert plain. Unlike the ranges that lie to the northeast, the Big Burro Mountains are not flanked by Paleozoic or Mesozoic sediments. The range is made up predominantly of the Precambrian Burro Mountains granite batholith which has been intruded into two series of metamorphic rocks. At the northern end of the range, the Precambrian rocks disappear beneath north-dipping Cretaceous sediments and Tertiary lavas. The Precambrian rocks are generally confined to the topographic limits of the mountains. However, they are poorly exposed in a few dry washes in the basin as much as a mile west of the mountain front.

Definition of Rock Units

The rock types in the northern Big Burro Mountains-Redrock area have been grouped into 25 mappable units. Of these, the Precambrian rocks that make up most of the mountains and the Tertiary and Quaternary sediments that floor the desert basin are most widespread. The major groups are as follows: (1) Tertiary and Quaternary sedimentary rocks, (2) Tertiary volcanic rocks, (3) Laramide and post-Laramide intrusive rocks, (4) Cretaceous sedimentary rocks, (5) Precambrian granite and related rocks, (6) Precambrian basic intrusive rocks, and (7) Precambrian metamorphic rocks.

Precambrian Metamorphic and Igneous Rocks

Two series of metamorphic rocks occur in the Big Burro Mountains. The more extensive of these is made up of interlayered quartz-feldspar, hornblende, and sillimanite gneisses, granite gneiss, mica schists, and migmatite. These rocks are exposed in an irregular mass that underlies

about 20 square miles in the northwest part of the range. Structurally this exposed mass is part of a poorly defined and complex overturned fold. The trace of the axial plane of this fold trends about N. 30° E. Xenoliths of these metamorphic rocks are locally abundant in granite throughout the north-central part of the mountains.

A less extensive series of metamorphic rocks is made up of several mineralogical varieties of hornfels and serpentinite. It occurs only as xenoliths in Precambrian granite and metadiabase at the northwest end of the mountains in the vicinity of Ash Creek. The largest xenolith is about a mile long; smaller xenoliths are scattered near its edges.

Small xenoliths of coarse-grained anorthosite are enclosed in granite and metadiabase in the vicinity of Ash Creek canyon. Sills of metadiabase, some as much as 1,000 feet thick, transect the metasedimentary rocks. Precambrian granite encloses small xenoliths of metadiabase and mixed xenoliths of metadiabase and metasediments.

The complex Burro Mountains batholith has been intruded into all other Precambrian rocks in the area. Although granite is the most abundant rock type, tonalite, granodiorite, pegmatite, and aplite occur locally as gradational facies and as separate intrusions. Along a part of the crest and the west flank of the mountains, hornblende gneiss and biotite schist have been extensively migmatized by lit-par-lit intrusions of the granite.

Cretaceous Sedimentary Rocks

Hogbacks of the Upper Cretaceous(?) Beartooth quartzite and Colorado shale overlie Precambrian rocks along the northern end of the Big Burro Mountains. The north-dipping sediments have been displaced by northwest- and northeast-trending normal faults that also cut the overlying volcanic rocks. Outliers of quartzite cap a few peaks south of the main exposures.

Laramide and Post-Laramide Intrusive Rocks

The largest occurrence of Laramide intrusive rocks in the Big Burro Mountains is the Tyrone stock of monzonite porphyry which crops out on the southeast side of the mountains. This stock is roughly circular in outcrop and about 6 miles across. A smaller stock of monzonite porphyry, the Twin Peaks stock, crops out along the northeast edge of the mountains and extends into the area of this report. Both stocks have been intruded into the Burro Mountains granite.

Dikes of diabase have been emplaced along northwest-trending tension fractures that transect the Precambrian complex. The similarity in attitude between the diabase dikes and Laramide faults suggests that they may be of the same age. Dikes of andesite porphyry, rhyolite, and rhyolite porphyry, up to 200 feet thick, have been emplaced in generally west-trending fractures. Andesite porphyry and rhyolite porphyry also occur as plugs and irregular dikes in Burro Mountains granite, Bear-

tooth quartzite, and Colorado shale. Small dikes of andesite cut Precambrian granite; small dikes of basalt cut the granite and Tertiary volcanic rocks.

The relative ages of these rocks, as far as contact relations permit their determination, are as follows (in order of increasing age): Basalt, rhyolite and rhyolite porphyry, andesite porphyry, monzonite porphyry, andesite, and diabase.

Tertiary Volcanic Rocks

A series of Tertiary andesite and rhyolite flows, tuffs, and agglomerates overlies the Colorado shale along the northern end of the Big Burro Mountains. These rocks are the southern limit of the extensive Datil lava field. Northwest-, north-, and northeast-trending faults offset the lavas. In the northeast corner of the area of this report, these lavas are probably in fault contact with the Burro Mountains granite.

Tertiary and Quaternary Sedimentary Rocks

The Gila conglomerate and younger terrace gravels, bajada deposits, bolson deposits, and ash beds underlie the extensive desert basin southeast, south, and west of the Big Burro Mountains. These deposits locally overlie Precambrian rocks along the flanks of the mountains and are in contact with them along extensive northwest- and northeast-trending faults.

Petrology

PRECAMBRIAN METAMORPHIC AND IGNEOUS ROCKS

General Statement

The Precambrian metamorphic rocks crop out in the northern Big Burro Mountains and in the area northwest of the mountains. Paige (1916) described these metamorphic rocks in the Silver City quadrangle as ". . . minor ill-defined schistose and quartzitic masses, which are metamorphosed ancient sediments." Gillerman (1951) described inclusions of schists and quartzites in the Precambrian granite in the southern part of the Big Burro Mountains and lenses of schist, amphibolite, quartzite, and other metamorphic rocks in the northern part of the mountains. In the Black Hawk mining district, Gillerman and Whitebread (1956) mapped two units of Precambrian rocks older than the Burro Mountains batholith: (1) Thinly bedded quartzite that contains thin layers of mica schist, amphibolite, and knotted schist, and (2) rocks of monzonitic and quartz monzonitic composition which may be migmatized sedimentary rocks.

The two metamorphic series that the writer has differentiated differ in petrology, structure, and degree of metamorphism. The more extensive and probably the older of the two has been designated the Bullard Peak series from the characteristic exposures in the general area south of Bullard Peak. The younger series is named after Ash Creek Canyon, where xenoliths of these rocks are well exposed. Characteristics that serve to distinguish the two series are compared in Table 1.

Bullard Peak Series

General Statement

The Bullard Peak metamorphic rocks crop out along the crest, west flank, and north end of the Big Burro Mountains in parts of T. 18 S., R. 17 W.; T. 18 S., R. 16 W.; T. 19 S., R. 17 W; and T. 19 S., R. 16 W. (pl. 1). The metasedimentary and meta-igneous rocks that make up this series have been intruded and are bounded by granite and related rocks of the Burro Mountains batholith. The largest exposure of these rocks in this area is an irregular mass, probably a roof pendant, 5½ miles long and 4 miles wide. Xenoliths of these rocks occur in granite several miles from the edges of this main exposure.

The structural pattern of the Bullard Peak series has been complicated by intrusions prior to metamorphism, by several periods of regional metamorphism, and by postmetamorphic intrusions. North of Eccles Canyon, the bedding and foliation strike northeast and are nearly vertical. Near the confluence of Eccles and Bar Six Canyons, the trend becomes north, and the dip is vertical, steeply east, or steeply west.

TABLE 1. COMPARISON OF BULLARD PEAK SERIES AND ASH CREEK SERIES

	BULLARD PEAK SERIES	ASH CREEK SERIES
MAIN ROCK TYPES	quartz-feldspar and sillimanite gneisses	cordierite, andalusite, and biotite hornfelses
	mica schists and gneisses	phyllite
	hornblende gneiss and amphibolite	serpentine-carbonate rocks
RELATION TO BURRO MOUNTAINS GRANITE	extensive lit-par-lit injection	minor lit-par-lit injection
	migmatite	
	feldspar metacrysts	
	some sharp contacts	sharp contacts
METAMORPHISM	high stress	mild stress
	high temperature	moderate temperature
STRUCTURES	well-developed foliation	foliation moderate to absent
	locally intensely contorted	

Southeast of Bullard Peak, this north trend veers west along the base of the peak. The general structure approximates a large overturned fold, with the trace of the axial plane striking northeast. Smaller structures occur on this large fold. Toward the western edge of the exposure and north and east of Bullard Peak, the metamorphic rocks are contorted and extensively migmatized.

The rock types that make up the Bullard Peak series have been grouped as follows into five mappable units: (1) Quartz-feldspar gneiss, biotite gneiss, quartzite, muscovite schist, and biotite schist; (2) sillimanite gneiss; (3) hornblende gneiss and amphibolite; (4) granite gneiss; and (5) migmatite and undifferentiated metamorphic rocks.

The rocks in the first two units are clearly metasedimentary and show characteristic gradational contacts, lensing, and interlayering. The hornblende gneiss and amphibolite unit contains some rocks whose parent material was sedimentary and, as shown by crosscutting field relationships, some whose parent material was igneous. The granite gneiss has been interpreted, on the basis of field and petrographic evidence, as a metaigneous rock. The fifth unit contains hornblende, biotite, and quartz-feldspar gneisses, some of which have been altered to migmatite by lit-par-lit injection and by development of feldspar and mica metacrysts.

Because of gradational contacts, interlayering of metasedimentary and meta-igneous rocks, disruption by igneous intrusions, development

of migmatite, and occurrence of some rock types exclusively as xenoliths, the thickness of individual units changes from place to place.

Quartz-Feldspar Gneiss and Related Rocks

Occurrence. Quartz-feldspar gneiss, one of the most abundant of the Bullard Peak metasedimentary rocks, crops out along the south slope and crest of the ridge north of Eccles Canyon and as low ridges along the north and east sides of Bullard Peak. In the unit mapped as migmatite and undifferentiated metamorphic rocks, quartz-feldspar gneiss is exposed around the southeast and west sides of an irregular mass of granite gneiss and along the flank of the mountains north of Kelley Chimney Canyon (pl. 1). Xenoliths of quartz-feldspar gneiss, some too small to be mapped, are scattered through the Burro Mountains granite east of Bullard Peak Canyon and in the general area of Bear and Little Bear Canyons. Larger exposures occur around the head of Joe Harris Canyon and southwest of Rough Canyon in secs. 20, 21, and 29, T. 18 S., R. 17 W., where a consistent northeast trend of isolated masses suggests that they may be roof pendants.

Within the quartz-feldspar gneiss are thin layers and lenses, from a few inches to a few feet thick, of biotite gneiss, quartzite, mica and sillimanite schists, hornblende gneiss, and amphibolite. Quartzite layers a few feet thick are interlayered with quartz-feldspar gneiss along the ridge north of Eccles Canyon and in the area around Bullard Peak. Lenses and layers of biotite gneiss are abundant east and southeast of Bullard Peak in the Black Hawk Canyon area. Lenses of muscovite schist are more abundant than those of biotite schist; both types are well exposed in the Bullard Peak and Black Hawk Canyon areas and in small canyons north of Eccles Canyon.

Where the quartz-feldspar gneiss occurs with other units of this series, it is interlayered with and transected by hornblende gneiss and granite gneiss. The contacts between quartz-feldspar gneiss and granite gneiss are sharp; those between quartz-feldspar gneiss and hornblende gneiss are gradational in some areas and sharp in others.

Petrography. From Eccles Canyon to Bullard Peak, the quartz-feldspar gneiss crops out as a rounded ridge. The position of less resistant schistose layers in the gneiss locally controls drainages. Exposures are usually deeply weathered to tan blocks that are loosely consolidated to friable; locally a weathered surface is cream or dark red. In a few canyons that transect the ridges of quartz-feldspar gneiss, the fresh gneiss is commonly compact, subvitreous, and light to dark gray.

The gneiss is fine to medium grained and varies widely in mineral composition. The most abundant, and locally the only, constituents are quartz and feldspar. Tiny flakes of biotite in parallel orientation give the rock a crude foliation. Ragged plates of muscovite up to several centimeters across, and rarely thin lenses of fibrous sillimanite, are developed locally. Mineralogical banding is common. Bands rich in

quartz, quartz and feldspar, magnetite, muscovite, and biotite, commonly less than an inch to several inches in thickness, were observed in various areas. The nature of the banding is such that by variation in amounts of quartz and mica, the gneiss grades along and across strike into lenses and layers of quartzite, biotite gneiss, and mica schist. Where the quartz-feldspar gneiss has been contorted, the micaceous layers are lensoid, discontinuous, or crenulated.

Quartz-feldspar gneiss. In thinsections, the typical quartz-feldspar gneiss shows a texture that is granoblastic with interlocking boundaries. The average grain size is about 0.5 mm; locally the grains are as much as 1.5 mm across. Quartz, microcline, and oligoclase-andesine are the main constituents. Quartz exceeds feldspar; microcline generally exceeds plagioclase and is slightly altered to sericite and kaolinite. Twinning in the plagioclase is poorly developed; the mineral is locally extensively altered to sericite and kaolinite.

In some thinsections, about 2 to 3 percent of magnetite and 5 percent of biotite are the only additional constituents. Relict bedding may be represented by discontinuous bands of magnetite about 0.2 mm thick. Brown biotite flakes, about 0.2 mm long, are oriented parallel with this assumed relict bedding. Where muscovite and biotite occur together, muscovite is the coarser and the younger (pl. 4A). Accessory minerals are cordierite, which is interlocked with quartz and feldspar, and zircon euhedra that are included in biotite. The cordierite shows pinitic alteration.

Quartz-feldspar gneiss from the roof pendants at the head of Joe Harris Canyon contains quartz, oligoclase-andesine(Ab_{65-75}), and microcline, all from 0.2 to 0.4 mm across, arranged in a granoblastic mosaic. Plagioclase, however, is more abundant than microcline. Lenses of coarse-grained quartz and plagioclase probably represent relict bedding. Tiny biotite flakes are interstitial to quartz and feldspar anhedra. Ragged muscovite poikiloblasts, several centimeters long, include quartz and feldspar. The muscovite is oriented parallel or nearly parallel to the foliation caused by the planar arrangement of biotite flakes. The sequence of mineral formation in the most common variety of quartz-feldspar gneiss is: (1) Quartz, feldspars, magnetite; (2) biotite; and (3) muscovite.

A schistose variety of quartz-feldspar gneiss, which occurs east of Bullard Peak close to an area of migmatization, contains alternating, contorted quartz-rich and mica-rich layers. Thinsection examination shows strings and lenses of granoblastic quartz and minor cordierite interstitial to patches of sericite and poorly oriented plates of muscovite, biotite, and chlorite. Muscovite and biotite are intergrown along (001); muscovite occurs as slightly poikiloblastic flakes that include quartz and magnetite. Chlorite and magnetite replace biotite. Pale-pink to colorless almandite anhedra occur in accessory amounts with granoblastic quartz. Sillimanite needles are molded between quartz anhedra and muscovite

plates. Patches of sericite appear to have formed by replacement of bundles and trains of fibrous sillimanite. Quartz and magnetite appear to be the oldest constituents in the rock. Both biotite and muscovite transect quartz; muscovite transects and replaces biotite. Both garnet and sillimanite seem to have formed at the expense of the micas. The sequence of mineral formation is thus: (1) Quartz and magnetite; (2) biotite; (3) muscovite; (4) garnet and sillimanite; and (5) sericite after sillimanite, chlorite and magnetite after biotite.

Sillimanite was observed also in a deeply weathered quartz-feldspar gneiss in Black Hawk Canyon. Sillimanite lenses, locally making up 10 to 20 percent of the rock, have weathered out as rounded knobs up to an inch across. These knobs are made up of a felted mass of tiny needles partially altered to sericite. Sillimanite was also observed in quartz-feldspar gneiss from the ridge west of Black Hawk Canyon, where it occurs in millimeter-thick discontinuous lenses parallel to the foliation. Microscopically, these lenses appear as a felted aggregate of needles. Weathering gives the sillimanite a dull, mottled, blue-gray surface; patches of sericite up to a centimeter across have partly replaced it.

Biotite gneiss and schist. The quartz-feldspar gneiss grades locally into lenses and layers of biotite gneiss and schist. Typical biotite gneiss is fine to medium grained and contains from about 25 to 50 percent biotite; it is particularly abundant in the Bullard Peak area and in Black Hawk Canyon. An example of fine-grained biotite gneiss from a lens that crops out on the ridge east of Bullard Peak is made up of dark-olive biotite thinly interlayered with a fine-grained aggregate of quartz and feldspar. Locally, the gneiss shows fine crenulations, the crests of which are spaced about a centimeter apart. In thinsection, this gneiss shows crenulated layers of biotite and epidote about a millimeter thick, interlayered with an interlocking aggregate of quartz and plagioclase (Ab_{68-73}). The biotite flakes include anhedra of quartz, plagioclase, apatite, zircon, and sphene that is coated with leucoxene. Slightly pleochroic, light-green chlorite rims biotite and forms intergrowths along (001) planes in biotite. Elongate epidote anhedra are wrapped by biotite flakes and occur rarely along biotite-quartz-plagioclase boundaries. The granular quartz and plagioclase, which make up about 50 percent of the rock, have an average grain size of 0.3 mm. Sericite and kaolinite coat the poorly twinned plagioclase.

A coarser grained biotite gneiss from Black Hawk Canyon contains patches and lenses of biotite, some up to 2 cm across, in parallel orientation in a fine-grained quartz-plagioclase-biotite matrix. Thinsection examination shows biotite flakes from 0.2 to 2 mm long. The smaller flakes are along quartz-plagioclase boundaries; the larger ones are grouped in patches and have an irregular outline. Biotite includes anhedra of quartz, apatite, and epidote and clusters of zircon and sphene euhedra. A few of the epidote anhedra show color zoning, with a lighter rim that shows slightly lower birefringence than the core. The

quartz-plagioclase (oligoclase-andesine) aggregate, about 70 percent of the rock, is equigranular-anhedral, with an average grain size of about a millimeter. Plagioclase shows albite and Carlsbad twinning and patchy alteration to sericite and kaolinite.

A spotted biotite-magnetite gneiss is interlayered with quartz-feldspar gneiss in a xenolith, about 1,000 feet long and 400 feet wide, in the SE¼ sec. 18, T. 18 S., R. 17 W. (pl. 1). A weathered surface shows evenly distributed magnetite anhedra, about a millimeter across, in a fine-grained, biotite-rich matrix. Light-colored rims, about 0.4 mm thick, that surround each of the magnetite anhedra are slightly elongate parallel to the foliation produced by the planar orientation of biotite flakes. Thinsections show that the matrix is composed of a granoblastic aggregate of quartz, microcline, oligoclase, and minor cordierite, each about 0.25 mm across. Plates of dark-brown biotite, up to 0.5 mm long, are evenly distributed interstitial to quartz and feldspar grains. A foliation is apparent in the parallel orientation of biotite plates and in a crude elongation of quartz and feldspar grains. Near the magnetite porphyroblasts, the grain size of quartz and feldspar anhedra is larger, cordierite is more abundant, and biotite is absent. The magnetite subhedra are poikiloblastic with quartz and feldspar, and are discontinuously rimmed with muscovite. The poikiloblastic nature of the magnetite, the abundance of cordierite, and the absence of biotite in the rims that surround magnetite suggest that magnetite and cordierite formed late in the history of the rock, and partially at the expense of biotite. The sequence of formation of the essential constituents is thus: (1) Quartz, feldspars, and magnetite; (2) biotite; and (3) magnetite, muscovite, and cordierite.

The biotite schists locally contain oriented biotite flakes up to several millimeters long as the only essential constituent. Deeply weathered schist contains biotite that has a bronze luster and is coated with patches of limonite. Unaltered schist exposed in walls and beds of canyons is black to green black. Some schists contain lenses of fine granoblastic quartz. An example in Black Hawk Canyon, sec. 32, T. 18 S., R. 16 W., contains elongate pods of recrystallized quartz, up to an inch long and three-quarters of an inch thick, that lie in the plane of foliation.

Muscovite schist. Muscovite schist commonly crops out in small canyons. On the low ridge separating Eccles Canyon drainage from that of Black Hawk Canyon, float of hematite-stained muscovite schist is scattered in talus debris. Lenses of muscovite schist, gradational into quartz-feldspar gneiss, are made up of oriented plates of muscovite, less than a centimeter long, that include quartz and, less commonly, feldspar anhedra. A thinsection of coarse-grained muscovite schist from the ridge west of Black Hawk Canyon, in sec. 6, T. 19 S., R. 16 W., shows muscovite as the only essential constituent. A few biotite flakes, some in parallel orientation, are included in poorly oriented muscovite plates

as much as 2 cm long. Apatite, magnetite, and quartz anhedra in accessory amounts are included in muscovite.

Where granite has been intimately intruded into muscovite schist, particularly in the zone of lit-par-lit injection south of Bullard Peak, clusters and trains of sillimanite needles have developed generally parallel to the foliation of the schist. The lenses that are rich in sillimanite are only a few feet long; they grade along and across strike to typical muscovite schist. A deeply weathered sillimanite-muscovite schist from a small xenolith of quartz-feldspar gneiss in Little Bear Canyon has inch-long sillimanite crystals coated and partly replaced by sericite. The sillimanite crystals lie in the plane of foliation but show no preferred linear arrangement.

A spotted, chlorite-muscovite schist is interlayered with the quartz-feldspar gneiss north of Bullard Peak in a tributary to Black Hawk Canyon near the east edge of the area. Ragged patches of dark-green chlorite are evenly distributed in a fine-grained, light-tan to brown matrix. The equidimensional chlorite patches are as much as a centimeter across; some are as small as 0.5 mm. Thinsections show rosettes of pennine poikiloblastic with quartz and zircon. The matrix is made up of about equal amounts of quartz and muscovite, and accessory amounts of sillimanite and hematite after magnetite(?). Quartz grains, which average 0.3 mm across and are slightly elongate parallel to the foliation, form a granoblastic aggregate. Muscovite occurs as ragged poikiloblastic plates that include quartz, as individual flakes interstitial to quartz, and rarely as symplectic intergrowths with quartz. Aggregates of sillimanite needles in accessory amounts are wrapped around and embedded in quartz anhedra.

Origin. The mineral composition, texture, and field relations of the quartz-feldspar gneisses and related rocks indicate that they have been derived by regional metamorphism of a series of quartzo-feldspathic and pelitic sediments. Evidence that specifically points to a sedimentary origin is as follows:

1. Relict bedding, which appears as:
   a. Mineralogical banding among layers of quartz, quartz-feldspar, quartz-mica, mica, and magnetite,
   b. Textural banding—relict graded bedding;
2. Gradation along strike and interlayering among quartz-feldspar gneiss, quartzite, mica schists, and hornblende gneiss;
3. General preponderance of quartz over feldspars;
4. Variation in the composition of plagioclase;
5. Presence of the aluminous minerals sillimanite and cordierite.

The parent material for typical quartz-feldspar gneiss was most likely a fine- to medium-grained feldspathic sandstone with small amounts of argillaceous material. Local variation in the composition and texture of the sediment resulted in mineralogical and textural banding and

gradation among metamorphic rock types. The preservation of a relict texture is evidence that in some of the gneiss metamorphism involved recrystallization, but not complete reconstitution. The size of quartz, feldspar, and some magnetite grains is probably close to that of the clastic particles in the parent sediment.

During metamorphism, chlorite, sericite, and quartz are produced by reaction among magnesian montmorillonite, illite, and quartz or among illite, aluminous serpentine, and quartz (Yoder, 1955). Further reactions between sericite and chlorite result in the formation of biotite; recrystallization of sericite results in muscovite (Harker, 1939). The relative amounts of chlorite, muscovite, and biotite are thus controlled by the composition of the argillaceous material in the parent sediment, as well as by the degree of metamorphism.

Textural relations between muscovite and biotite in some of the quartz-feldspar gneiss consistently indicate that muscovite is the younger, is not as well oriented, and generally is the coarser grained of the two. This relation may be explained by: (1) Growth of biotite until the supply of chlorite was exhausted, followed by recrystallization of excess sericite to muscovite; (2) formation of muscovite by metasomatism related to intrusion of the Burro Mountains batholith. Some of the fine-grained muscovite, particularly that in the muscovite schist and quartz-feldspar gneiss in the Bullard Peak and Eccles Canyon areas, resulted from recrystallization of original argillaceous constituents in the parent sediments. However, the coarse muscovite in the roof pendants of quartz-feldspar gneiss at the head of Joe Harris Canyon may be the result of addition of K, OH, and possibly Al during intrusion of the granite.

Accessory amounts of cordierite in the quartz-feldspar gneiss are apparently not related to igneous contacts. Although cordierite is commonly an antistress mineral, it has been reported from rocks of the sillimanite-almandite subfacies whose origin is unconnected with igneous intrusions (Turner, 1948). Turner (1948) interpreted the presence of cordierite under these conditions as perhaps representing a stress that is lower than usual for this subfacies. The cordierite in the Bullard Peak rocks may indicate conditions of lower stress; it may have formed late in the metamorphic history of the quartz-feldspar gneiss, when stress had diminished but temperature was still elevated, or even later when the temperature was again raised by intrusion of the Burro Mountains batholith.

Sillimanite occurs in the quartz-feldspar gneiss and muscovite schist in areas close to granite contacts and in areas of lit-par-lit injection and migmatization. This relationship indicates that the intrusion of granite was instrumental in development of sillimanite. Textural evidence indicates that sillimanite formed primarily at the expense of biotite and muscovite and, to a lesser degree, of quartz. Turner (1948) cites this type of replacement as an example of metasomatism involving removal of

K and other bases. Sillimanite in quartz-feldspar gneiss probably formed after the development of biotite by regional metamorphism. The intrusion of the Burro Mountains batholith raised the temperature of the country rock and may have introduced solutions that, by adding Al and Si and removing K, Fe, and Mg, brought about the formation of sillimanite from muscovite and biotite.

The biotite gneiss originated from metamorphism of a siltstone or sandstone that contained abundant argillaceous material. The presence of epidote in regionally metamorphosed rocks indicates the presence of calcium in the source rock. The parent material of the biotite gneiss was calcareous, argillaceous siltstone lenses and layers in feldspathic sandstone. The ultimate origin of the biotite-magnetite gneiss is similar to that of the typical quartz-feldspar gneiss. The quartz-feldspar-biotite matrix that encloses the magnetite porphyroblasts is identical to some biotite-rich layers in the quartz-feldspar gneiss, and thus originated by regional metamorphism of argillaceous, quartzo-feldspathic sediments. The magnetite porphyroblasts are clearly the youngest mineral in the rock; their origin may be related to thermal metamorphism at the time the xenolith was enclosed by granitic magma. At least some of the iron that formed the magnetite seems to have been drawn from surrounding biotite. The effect of thermal metamorphism was apparently a breakdown of biotite to form magnetite and muscovite. This reaction may have begun around detrital grains of magnetite. The coarser grain size of the quartz and feldspar that rim the magnetite shows that the small area surrounding the magnetite porphyroblasts suffered local recrystallization.

In summary, the quartz-feldspar gneiss and its related rock types originated from metamorphism of a series of pelitic and quartzo-feldspathic sediments. The banding, layering, and lensing among metamorphic rock types are the result of interlayering and lensing in the parent sediment. The most likely parent material for each of the metamorphic rock types is as follows: (1) Quartz-feldspar gneiss—feldspathic sandstone with varying amounts of argillaceous material; (2) quartzite—pure quartz sandstone; (3) biotite gneiss—calcareous, argillaceous siltstone or sandstone; (4) muscovite schist—shale rich in illite, montmorillonite, or kaolinite; (5) biotite schist—shale rich in chloritic mica, magnesian montmorillonite, or aluminous serpentine.

The mineral composition and well-developed foliation in rocks that contain orientable minerals indicate that they belong to the amphibolite facies. Since sillimanite probably formed later than the regional metamorphism that produced the various schists and gneisses, its presence does not necessarily denote a general attainment of conditions of the sillimanite-almandite subfacies. However, the assemblage almandite-plagioclase-biotite-quartz, all apparently produced by dynamic metamorphism and all present in the quartz-feldspar gneiss, tends to indicate that the regional metamorphism did attain an intensity only

slightly lower than that of the sillimanite-almandite subfacies. The distinguishing mineral assemblage of this subfacies is sillimanite-almandite-orthoclase-plagioclase-biotite-quartz. However, Turner (1948) points out that this ideal assemblage is seldom attained. In the Bullard Peak metamorphic rocks, the presence of muscovite may indicate disequilibrium or, more likely, the late development of metacrysts. The regional metamorphic conditions that produce rocks of this subfacies are high temperature and high pressure in a stress environment. The relationship in time between the regional metamorphism and the intrusion of the Burro Mountains batholith is discussed at the end of the section on Precambrian metamorphic rocks.

Sillimanite Gneiss

Occurrence. Xenoliths of quartz-feldspar gneiss and other related rocks characterized by abundant sillimanite have been mapped in a separate unit of sillimanite gneiss. The largest xenolith, about 2,000 feet long and 1,200 feet wide, crops out on the west slope of Fox Tail Canyon, in sec. 6, T. 18 S., R. 17 W. (pl. 1). Smaller xenoliths of sillimanite gneiss, all less than a quarter of a mile long, crop out on both sides of the Gila River, in secs. 12, 13, 23, and 24, T. 18 S., R. 18 W., and in a tributary to House Canyon, in sec. 28, T. 18 S., R. 17 W. All these xenoliths are enclosed in the Burro Mountains granite; those in Fox Tail Canyon have been intruded intimately in a lit-par-lit manner.

Sillimanite gneiss xenoliths crop out above the granite as low mounds flanked by talus. Where topographic relief is high, the xenoliths are inconspicuously exposed in steep slopes and canyon walls. Weathering gives the gneiss a dark-red, red-brown, or brown surface that is commonly pitted or knobby. Mineralogical banding is emphasized on a weathered surface by the light-brown color of feldspar-rich bands. Irregular spots, mottling, and hematite and manganese oxide stains are common on weathered surfaces.

On a freshly broken surface, which is usually light tan, dark gray, or brown, the rock appears as a fine-grained aggregate of quartz and feldspars, with tiny, poorly oriented muscovite flakes. A few dark-red garnet euhedra were observed in the sillimanite gneiss from a small xenolith in a tributary to Joe Harris Canyon. Banding is apparent on a freshly broken surface by the alternation of inch-thick, dark-gray, vitreous, quartz-rich bands with light-tan, feldspar-rich bands. Sillimanite gneiss from Fox Tail Canyon shows a marked irregular mottling of light-tan areas, up to a few centimeters across, in a dark-gray to black matrix. In general, the sillimanite gneiss is more compact, shows a darker color, and is not as well foliated as quartz-feldspar gneiss.

Petrography. Thinsections show that typical sillimanite gneiss consists of quartz, sillimanite, andalusite, biotite, muscovite, and accessory magnetite (pl. 4B). Quartz anhedra, about 0.2 mm across, are arranged in a mosaic that makes up about 50 percent of the rock. Dark-olive bio-

tite plates, up to 0.4 mm long, lie along quartz grain boundaries. Ragged, strongly poikiloblastic muscovite plates include quartz, magnetite, and biotite anhedra and form symplectic intergrowths with andalusite. Irregular masses of andalusite up to a millimeter long are poikiloblastic with magnetite and minor quartz, and transect biotite and muscovite. Colorless to light-tan sillimanite needles in bundles, sheaves, and trains transect biotite, muscovite, and possibly andalusite. Minute sillimanite needles are molded along grain boundaries of the quartz mosaic and project into quartz anhedra. The paragenetic sequence is: (1) Quartz and magnetite; (2) biotite; (3) muscovite and andalusite; (4) sillimanite; and (5) chlorite and magnetite after biotite.

In a thinsection of mottled sillimanite gneiss from the ridge west of Fox Tail Canyon, the light-tan areas appear as a granoblastic aggregate of quartz and microcline anhedra that are about 0.5 mm across. Microcline anhedra with well-developed gridiron twinning include biotite. Biotite flakes, which are interstitial to quartz and microcline anhedra, are replaced along (001) by chlorite and magnetite. Muscovite is included in microcline and forms a spongy network between quartz and microcline anhedra. Some of the light-colored areas show a concentration of biotite and quartz near the center and a finer grained quartz-microcline mosaic at the margin. The areas that are dark gray megascopically contain as much as 50 percent of tiny, light-tan to brown sillimanite needles that have partially replaced both muscovite and biotite and that also wrap and penetrate quartz anhedra. Sillimanite, the youngest metamorphic mineral, seems to have formed in patches made up of an aggregate of quartz, muscovite, and biotite, all of which are about 0.2 mm across. Accessory amounts of magnetite subhedra occur in both light and dark areas.

Origin. Textural and mineralogical features, as well as field occurrences, suggest that the sillimanite gneiss formed from xenoliths of quartz-feldspar gneiss that were enclosed in granitic magma. The presence of andalusite, an antistress mineral, indicates that thermal metamorphism in a low-stress environment has been superimposed on the regional metamorphic effects that produced the quartz-feldspar gneiss. Biotite, potash feldspar, and quartz are most likely relict from the quartz-feldspar gneiss. Muscovite may be relict from the gneiss or may have developed as a result of metasomatism. Sillimanite and andalusite were both formed as a result of increased temperature, and possibly metasomatism, concomitant with intrusion of the Burro Mountains batholith. The presence of andalusite and sillimanite is characteristic of the pyroxene hornfels facies of contact metamorphism and indicates conditions of high temperature and pressure, but low stress.

Hornblende Gneiss and Related Rocks

Occurrence. Hornblende gneiss and amphibolite are intimately associated with other members of the Bullard Peak series in the part of

the Big Burro Mountains that lies north of the Redrock-Silver City road. Along the eastern edge of the area of this report, hornblende gneiss occurs in layers up to 1,000 feet thick. The northern end of the unit mapped as migmatite and undifferentiated metamorphic rocks (pl. 1) is made up largely of hornblende gneiss that passes gradationally into quartz-feldspar gneiss and migmatite. In the central and southern parts of this exposure (in sec. 12, T. 19 S., R. 17 W., and in the area north of Eccles Canyon), hornblende gneiss is interlayered with quartz-feldspar gneiss.

Xenoliths of hornblende gneiss occur in granite in Eccles Canyon, south of Bullard Peak, north and east of Wild Horse Mesa, and in Bear and Little Bear Canyons. Some of these xenoliths are as much as one-quarter of a mile long. An elongate body of hornblende gneiss, about 2¼ miles long and up to 1,000 feet wide, is enclosed in granite northwest of Bullard Peak, in secs. 13, 24, and 25, T. 18 S., R. 17 W.

Some of the contacts between hornblende gneiss and quartz-feldspar gneiss are sharp; others are gradational. The abundant lenses and layers of hornblende gneiss that have been mapped with the unit of quartz-feldspar gneiss are conformable and pass gradationally along and across strike into feldspar gneiss. In sec. 18, T. 19 S., R. 16 W., hornblende gneiss shows crosscutting relations with quartz-feldspar gneiss; in sec. 8, T. 19 S., R. 16 W., hornblende gneiss transects granite gneiss. In both of these exposures, the foliation in the hornblende gneiss is essentially parallel to that of the quartz-feldspar and granite gneisses.

The ease with which hornblende gneiss is eroded is seen by its characteristic outcrop in small canyons. Lenses and thin layers of hornblende gneiss that crop out in ridges of quartz-feldspar gneiss form a saddle or are obscured in talus on the flank of the ridge. Because of their dark color, however, these outcrops are conspicuous. A notable exception to this valley-forming characteristic is the long, narrow ridge of hornblende gneiss that crops out northwest of Bullard Peak.

Deeply weathered hornblende gneiss has a dull-green, green-black, or blue-black surface commonly marked with hematite or limonite stains. The weathering of any feldspar in the rock to a tan or brown emphasizes the texture and structure. A freshly broken surface shows that the hornblende gneiss is made up of 50 to 90 percent dark-green to green-black hornblende and varying amounts of quartz and light-gray to gray-green plagioclase.

Petrography. Several textural varieties of hornblende gneiss occur in this area. Some of the very fine-grained rocks appear megascopically to be made up entirely of hornblende. Some types show the alternation of centimeter-thick bands of fine-grained hornblende with those of coarser grained hornblende and plagioclase. A common variety contains fine-grained quartz-plagioclase layers or lenses, about a millimeter thick, set in a medium-grained hornblende matrix. Another variety contains equigranular hornblende subhedra, about a millimeter across, enclosed

in a finer grained quartz-plagioclase aggregate. Hornblende gneiss from the ridge west of Goat Canyon contains stubby hornblende porphyroblasts, about half an inch long, set in a fine-grained hornblende-plagioclase matrix.

Most of the hornblende gneisses show some type of planar structure (pl. 3A) either by mineralogical or textural banding, or by the parallel arrangement of hornblende crystals. Although hornblende needles are commonly oriented parallel to the banding, they rarely are alined. In a few areas where the hornblende gneiss has been crenulated, hornblende needles lie parallel to the axes of the crenulations.

The hornblende gneiss unit contains two petrographic varieties having the following essential mineral compositions: (1) Hornblende gneiss—hornblende, plagioclase, quartz, ± epidote, ± pyroxene; (2) amphibolite—hornblende, plagioclase, ± biotite.

Hornblende gneiss. Thinsections of hornblende gneiss show bands and lenses of varying amounts of hornblende, plagioclase, and quartz (pl. 5A). Some bands are made up of an aggregate of hornblende subhedra and anhedra up to 3 mm long; others contain hornblende euhedra and subhedra enclosed in a quartz-plagioclase aggregate. The orientation of hornblende crystals and the elongation of quartz grains give the rock a rough foliation. Not uncommonly, hornblende anhedra include rounded grains of quartz and plagioclase. In a thinsection of contorted hornblende gneiss from the northern end of the ridge northwest of Bullard Peak, the hornblende occurs as ragged porphyroblasts, up to a centimeter across, that are strongly poikiloblastic with magnetite. Some of the porphyroblasts contain corroded, irregular cores of augite.

Plagioclase(Ab_{56-75}) makes up about 30 to 40 percent of the rock. It shows poorly developed albite twinning, rare normal zoning, and alteration to kaolinite, sericite, or rarely saussurite. Quartz anhedra, from 0.2 mm to 0.5 mm across, are arranged with plagioclase in a mosaic or a slightly interlocking texture. Magnetite, the most abundant accessory mineral, occurs as subhedra and anhedra in hornblende and plagioclase and along grain boundaries between hornblende and plagioclase or quartz. Discontinuous rims of zircon were observed around magnetite in one thinsection. Apatite and sphene euhedra are enclosed in hornblende; apatite euhedra are also commonly enclosed in plagioclase or along quartz-plagioclase boundaries. Clusters of tiny epidote anhedra are included in quartz and hornblende; epidote veinlets, up to a centimeter thick, locally transect the gneiss. The modes of two typical examples of hornblende gneiss are listed in Table 2.

Amphibolite. The amphibolites differ from the hornblende gneisses in the absence of essential quartz. Some of the amphibolites are banded both texturally and mineralogically; others appear to be structurally uniform.

TABLE 2. MODES OF PRECAMBRIAN HORNBLENDE GNEISS AND AMPHIBOLITE

(In percent)

	(1)	(2)	(3)	(4)
Hornblende	57	51	50	45
Biotite	—	—	20	34
Plagioclase (Ab_{56-75})	30	39	28	18
Quartz	10	5	—	—
Accessories	3	5	2	3
Totals	100	100	100	100

1. Hornblende gneiss: NE¼ sec. 18, T. 19 S., R. 16 W.
2. Hornblende gneiss: SW¼ sec. 11, T. 19 S., R. 17 W.
3. Amphibolite: NE¼ sec. 18, T. 19 S., R. 16 W.
4. Amphibolite: SW¼ sec. 11, T. 19 S., R. 17 W.

Thinsections show hornblende subhedra and rarely euhedra, up to a few millimeters long, enclosed in an aggregate of plagioclase subhedra that are about a millimeter across. The plagioclase ranges from Ab_{48} to Ab_{68}; most commonly it is in the range of Ab_{60-65}. In some specimens, it has been almost completely saussuritized; in others, it is fresh or only slightly altered to kaolinite and sericite. Ragged plates of biotite commonly cut across and replace the hornblende. Foliation is caused by the parallel orientation of biotite and hornblende, and by the elongation of plagioclase grains. Biotite commonly is replaced by chlorite and magnetite. In one thinsection, the biotite that has replaced hornblende contains epidote(?) in tabular to lenslike masses oriented parallel to (001). Apatite euhedra are included in plagioclase; magnetite and zircon clusters are included in biotite and hornblende. Calcite as rounded grains enclosed by granular plagioclase was observed in one thinsection. The modes of two examples of typical amphibolite are listed in Table 2.

Amphibolite from the ridge northwest of Bullard Peak has a relict ophitic texture. Under the microscope, the rock shows corroded labradorite(Ab_{48}) crystals, up to 4 mm long, that are enclosed and partly replaced by hornblende anhedra and subhedra. Hornblende also occurs as tiny rounded grains enclosed in labradorite. Biotite replaces hornblende and veins hornblende and labradorite.

Both hornblende gneiss and amphibolite show certain characteristics in common. Hornblende consistently transects or replaces plagioclase. Varieties that contain augite and hornblende show cores of augite being marginally replaced by hornblende. Biotite transects hornblende and replaces it. Veinlets of epidote cut across quartz, plagioclase, hornblende, and biotite. Sericite or saussurite replaces plagioclase; chlorite and magnetite replace biotite and rarely hornblende. The order of mineral formation is: (1) Plagioclase, quartz, augite, and magnetite; (2)

hornblende; (3) biotite and epidote; and (4) sericite, saussurite, chlorite, and magnetite.

Origin. The reason for the widespread occurrence of hornblende gneiss and amphibolite, and for their association with many metamorphic rock types, lies in the fact that, under conditions of regional metamorphism, a wide variety of source rocks may be converted to hornblende gneiss and amphibolite. In a recent survey of the possible origins of these rocks, King and Flawn (1953) concluded that they may be formed as follows:

1. By regional metamorphism of:
   a. Impure carbonate rocks or marls,
   b. Tuffs or reworked tuffs,
   c. Basic intrusive or extrusive rocks, or their uncontaminated detritus;
2. By action of hydrothermal or igneous agencies on carbonate rocks; additive (and subtractive) metamorphism;
3. By action of the "basic front" produced by granitization; regional metasomatism.

The hornblende gneiss and amphibolite in the Big Burro Mountains appear to have originated by means of regional metamorphism of igneous rocks, sedimentary rocks, or both. The distinction between ortho- and para-amphibolites and gneisses cannot always be made on the basis of petrographic evidence. One of the best lines of evidence in making the distinction is a discordant contact relationship with neighboring rocks. Both types of amphibolite and hornblende gneiss are present in the Bullard Peak series. Evidence that elucidates the origin of the hornblende rocks is:

1. Paragneiss and amphibolite
   a. Occurrence as lenses and layers gradational with metasedimentary rocks,
   b. Gradation of biotite amphibolite through biotite gneiss to biotite schist,
   c. A suggestion of relict sedimentary layering apparent by variation in amounts of hornblende and feldspar,
   d. Local abundance of quartz and biotite;
2. Orthogneiss and amphibolite
   a. Crosscutting contact relations,
   b. Blastophitic texture,
   c. Augite remnants in cores of hornblende porphyroblasts,
   d. Excess of feldspar over quartz,
   e. Quartz, biotite, or epidote absent or occurring in accessory amounts.

Sedimentary rocks that could have been metamorphosed to amphibolites and gneisses having the mineral compositions of those in the

Big Burro Mountains would have been essentially dolomitic and argillaceous sediments, with lesser amounts of calcareous and arenaceous material. The hornblende and plagioclase were probably derived from sediments that contained abundant dolomite, possibly ankeritic, as well as montmorillonite or kaolinite. Biotite was derived from local concentrations of chloritic mica, illite, and possibly magnesian montmorillonite; epidote represents local abundance of calcite in argillaceous layers. Where pegmatites have been intruded into hornblende gneiss, epidote veinlets are particularly abundant and probably resulted from hydrothermal alteration. The addition of K to hornblende-bearing wallrocks of granitic intrusions results in the replacement of hornblende by biotite; the consequent release of Ca initiates lime metasomatism (Harpum, 1954) and the development of epidote.

The relict ophitic texture and cores of pyroxene indicate that the source rock of the ortho-amphibolites and gneisses was a diabase. The changes brought about in the parent diabase by metamorphism were almost complete replacement of primary augite by hornblende, and limited replacement of labradorite as well.

The exposure of amphibolite and hornblende gneiss that crops out northwest of Bullard Peak is atypical because of the shape of the outcrop and the topographic expression as a ridge. At least some of the amphibolite was derived from a medium-grained diabase; some of the hornblende gneiss shows mineralogical banding that is characteristic of metasediments. The flanks of the ridge are partly obscured by talus, so that no good contact relations with granite are observable. However, in a tributary to Saddle Rock Canyon that originates on the flank of the north end of the ridge, float blocks of hornblende gneiss were found which contain potash feldspar metacrysts and blocks of granite having schlieren of hornblende gneiss. The hornblende rocks that form the ridge are probably older than the granite and are part of the Bullard Peak series. The writer has interpreted the ridge, in spite of its dikelike appearance, as a xenolith or possibly as the remains of a once more extensive roof pendant.

Granite Gneiss

Occurrence. Three masses of granite gneiss crop out on the west flank and north end of the Big Burro Mountains. The largest of these is an irregular stocklike body that underlies about 2 square miles in parts of secs. 35 and 36, T. 18 S., R. 17 W., and secs. 1 and 2, T. 19 S., R. 17 W. This granite gneiss is slightly finer grained at the contacts with quartz-feldspar and hornblende gneisses. Precambrian granite of the Burro Mountains batholith truncates the northern end of the stock. An almost vertical sill of granite gneiss, about 3 miles long and up to 300 yards thick, crops out along the north slope of the ridge north of Eccles Canyon in parts of secs. 6, 7, and 18, T. 19 S., R. 16 W., and sec. 13, T. 19 S., R. 17 W. This sill forms the "box" in Brushy Canyon about a

mile above its confluence with Eccles Canyon (pl. 1). The Burro Mountains granite terminates both the northern and southwestern ends of the sill.

The granite gneiss that underlies Bullard Peak in secs. 30 and 31, T. 18 S., R. 16 W., is probably continuous with an irregular elongate mass of granite gneiss that parallels the eastern edge of the mapped area for about 3 miles southeast of the peak. Talus from the peak obscures the relationships, but the granite gneiss from the peak and from the ridge southeast of the peak are megascopically and microscopically similar. This gneiss is deeply weathered to various shades of red, yellow, and brown. The ridges of granite gneiss along Eccles and Bullard Peak Canyons are similarly weathered along the crest, but the walls of some deeply cut canyons exhibit excellent exposures of fresh gneiss.

A weathered surface shows about equal amounts of fine to medium-sized grains of quartz, brown potash feldspar, and white chalky plagioclase. Less than 5 percent of the rock is made up of biotite, which weathers a dark brown with a slight bronze luster. In Brushy and Bullard Peak Canyons, the fresh gneiss is rounded and grooved by stream erosion. A freshly broken surface shows vitreous quartz, light-pink potash feldspar, and white plagioclase. A surface broken parallel to the foliation shows irregular patches of green-black biotite 3 cm long; surfaces broken normal to the foliation show discontinuous, subparallel lenses of biotite about a millimeter thick.

The granite gneiss that underlies Bullard Peak differs structurally from the other occurrences of granite gneiss. Instead of a planar foliation caused by the subparallel arrangement of biotite clusters, the biotite layers of the Bullard Peak gneiss show indistinct chevron folding; the axial planes are spaced less than an inch apart. This gneiss is also locally contorted. Because of the talus and vegetation cover, no interpretation of the structure of the gneiss or its relation to the country rocks was attempted.

Petrography. Thinsections of granite gneiss show a subhedral to anhedral granular texture, interlocking grain boundaries, and an average grain size of 2 mm. The modes of granite gneiss are listed in Table 3. Microcline microperthite, the dominant mineral, occurs as subhedral or anhedral grains as much as 3 mm across; less commonly, microcline forms a network including quartz and oligoclase. A few small microcline anhedra form granophyric intergrowths with quartz. Microcline marginally replaces oligoclase. Alteration to kaolinite and sericite is not uncommon; sericite selectively replaces alternate albite twin lamellae.

Oligoclase (Ab_{68-76}) occurs as subhedra and anhedra interlocked with quartz and microcline or included in microcline. Myrmekite is uncommon as discontinuous rims on oligoclase and as individual anhedral grains. A few tiny anhedra of quartz are included in oligoclase. Some of the plagioclase, particularly that in the Bullard Peak granite gneiss,

TABLE 3. MODES OF PRECAMBRIAN GRANITE GNEISS
(In percent)

	(1)	(2)	(3)
Quartz	33	31	37
Microcline microperthite	41	33	44
Oligoclase (Ab_{68-76})	24	27	13
Hornblende-biotite	1	4	4
Accessories	1	5	2
Totals	100	100	100

1. Brushy Canyon, sec. 18, T. 19 S., R. 16 W.
2. Bullard Peak Canyon, SW¼ sec. 36, T. 18 S., R. 17 W.
3. Bullard Peak, sec. 30, T. 18 S., R. 16 W.

shows well-developed zoning, with cores of Ab_{72} and margins of Ab_{76}; normal zoning is also apparent in the preferential alteration of the core to flakes of sericite. Carlsbad and albite twinning are most abundant; pericline twins are rare.

Biotite, the only mafic mineral in the granite gneiss from Brushy and Bullard Peak Canyons, occurs as ragged plates interstitial to quartz and feldspar or included in quartz. The biotite is strongly pleochroic from light yellow tan to dark brown and commonly shows pleochroic halos around euhedral zircon. Dark-green hornblende occurs in clusters with biotite in the granite gneiss from Bullard Peak. Both hornblende and biotite are partially replaced by chlorite and magnetite.

Granite gneiss from all three occurrences contains magnetite, apatite, sphene, and zircon as accessory minerals, the first three as euhedral grains enclosed by quartz, oligoclase, and biotite; magnetite anhedra also occur along quartz-feldspar boundaries. Discontinuous rims of zircon are molded on magnetite. In addition to these accessories, the granite gneiss in Brushy Canyon also contains fluorite as euhedra included in microcline, and as irregular masses interstitial to quartz and feldspar. The sequence of crystallization is: (1) Early accessories—apatite, zircon, sphene, and some magnetite; (2) hornblende and biotite; (3) oligoclase, microcline, and quartz; (4) granophyre, myrmekite, and exsolution of perthite; and (5) alteration of hornblende and biotite to chlorite and magnetite, alteration of feldspars to sericite and kaolinite, and formation of epidote veinlets.

Origin. "Granite" gneisses may be derived by high-grade regional metamorphism of impure arenaceous sediments or of felsic igneous rocks. An igneous origin for the granite gneiss in the Big Burro Mountains is suggested by field evidence and supported by the following mineralogical and textural features: (1) Uniformity in composition and zoning of plagioclase throughout the rock; (2) uniformity in occurrence and type of perthite structure shown by microcline, the only potash

feldspar present; (3) greater abundance of microcline than quartz; (4) presence of myrmekite and granophyre, which are considered to be late-stage magmatic features (Wahlstrom, 1950).

Inasmuch as the foliation in the granite gneiss that occurs north of Eccles Canyon and in the Bullard Peak Canyon area is present throughout the exposures and is essentially parallel to that of the surrounding quartz-feldspar and hornblende gneisses, the granitic foliation is probably not a primary flow feature. The chevron folding and contortions in the gneiss that forms Bullard Peak support the view that the parent leucogranite was intruded into the source rocks of the Bullard Peak series prior to regional metamorphism.

Migmatite

General statement. Rocks in the Big Burro Mountains that are characterized by alternating bands of igneous and metamorphic material have been mapped as migmatite. The host metamorphic rock is hornblende gneiss, amphibolite, biotite schist, or rarely quartz-feldspar gneiss; the igneous component is granitic to granodioritic and may be related to the Burro Mountains batholith. Bands of igneous material, which range in thickness from less than an inch to tens of feet, have been intruded into metamorphic rocks in a lit-par-lit manner generally parallel to the banding and foliation. Where the intrusions are widely spaced, the two components show their own characteristics. Where migmatization has been intense, the resultant mixed rock is difficult to distinguish from biotite paragneiss or granite gneiss (pl. 3B). Some of the migmatite contains lenses, rather than bands, of coarse-grained igneous material. Microcline metacrysts up to an inch across are locally concentrated parallel to the foliation in the hybrid schist or gneiss (pl. 3C).

Occurrence. The largest occurrence of migmatite, which crops out in the northeast part of T. 19 S., R. 17 W., is shown on the geological map as part of the unit of migmatite and undifferentiated metamorphic rocks (pl. 1). Migmatization has been most intense at the western edge of this exposure, from Bullard Peak Canyon to the ridge south of Kelley Chimney Canyon. The migmatite grades into typical hornblende gneiss to the north and into biotite schist and quartz-feldspar gneiss to the east. Near the head of Stein Canyon, migmatite is gradational between biotite schist and Burro Mountains granite. The hornblende and quartz-feldspar gneisses north of Bullard Peak and the quartz-feldspar gneiss east and south of the peak and in Black Hawk Canyon have been migmatized locally.

Petrography. The nature of the migmatite exposure is dependent upon the relative amounts of igneous and metamorphic components. All gradations are present, from the typical dark-green to black biotite schist and hornblende gneiss that have undergone lit-par-lit injection

by pink to white granitic material, to the typical Burro Mountains granite, aplite, or pegmatite.

Migmatized biotite schist, which crops out in the canyon south of Kelley Chimney Canyon, has been intensely injected and contorted. In thinsection, the rock appears as an equigranular aggregate of quartz, microcline, and oligoclase(Ab_{72}) anhedra and biotite plates, all about a millimeter across. Oligoclase includes quartz anhedra and shows marginal development of myrmekite. Kaolinite and sericite have uniformly replaced some oligoclase anhedra; others show only marginal alteration to sericite. Microcline shows local granophyric intergrowths with quartz. Accessory amounts of zircon, apatite, and magnetite occur along quartz-feldspar boundaries; apatite euhedra are included in quartz and feldspar. Poorly oriented biotite plates, probably relict from the intruded schist, are interstitial to quartz and feldspar anhedra. Much of the biotite is replaced by pennine and magnetite.

A thinsection of migmatized biotite schist from Bullard Peak Canyon shows layers and lenses, up to a centimeter thick, of fine-grained igneous material that has been intruded parallel to the foliation. The igneous portion of the rock is made up of about equal amounts of quartz and andesine(Ab_{65}) anhedra, about a millimeter across, that have interlocking grain boundaries. Albite twinning and alteration to kaolinite and sericite characterize the plagioclase. Apatite euhedra are scattered along quartz-plagioclase grain boundaries. The quartz-plagioclase bands lie between layers of frayed and ragged biotite plates that are up to a millimeter long. Biotite includes magnetite and zircon euhedra. A few poorly oriented plates of muscovite cut across biotite. Trains and sheaves of tiny sillimanite needles occur along biotite grain boundaries, less commonly are included in biotite, and rarely are along plagioclase boundaries.

An example of migmatized hornblende gneiss from Stein Canyon (pl. 3C) contains inch-long microcline metacrysts that commonly occur in discontinuous layers parallel to the foliation. The development of individual metacrysts has disrupted the foliation of the gneiss. The area around an isolated metacryst appears microscopically as parallel, irregular bands of hornblende and minor biotite. Elongate anhedra of quartz, andesine(Ab_{68}), and microcline are wrapped and included by the hornblende layers. Quartz commonly forms a network between microcline anhedra. Plagioclase, which is much less abundant than microcline, characteristically shows albite twinnings, kaolinite and sericite alteration, marginal myrmekitic intergrowths with quartz, and marginal replacement by microcline. Accessory amounts of euhedral sphene, zircon, magnetite, and subhedral epidote are included in hornblende; euhedral apatite grains are included in microcline. The microcline metacrysts are bordered by an anhedral aggregate of microcline and include patches of unreplaced andesine and, less commonly, biotite. The

microcline shows slight sericitic alteration and poorly developed microperthite.

Origin. The gradation of hornblende gneiss and biotite schist into zones of lit-par-lit injection and migmatite clearly reveals the origin of these mixed rocks. Where injections of granite are widely spaced, the metamorphic part of the rock resembles the other Bullard Peak metasediments in the Big Burro Mountains. The presence of sillimanite, the local contortions, and the thinness of some of the injections indicate that the Bullard Peak metamorphic rocks were injected and granitized by a highly fluid magma that was probably related to the Burro Mountains batholith. This intrusion must have been accomplished at considerable depth under conditions of high temperature and high pressure. The presence of isolated microcline metacrysts that are clearly younger than the enclosing hornblende gneiss cannot be explained by simple intrusion and crystallization. Thinsections of the metacrysts show microcline replacing plagioclase, most likely as a result of potash metasomatism related to the Burro Mountains batholith.

Origin of the Bullard Peak Series

Field and petrographic evidence indicate that this series of metamorphic rocks has been derived from both igneous and sedimentary rocks that have a complex metamorphic history. The derivations of the rock types are compared in Table 4. Wherever possible, the mineral assemblage has been grouped to show the type of metamorphism under which a particular mineral was formed. A notable feature of the metasedimentary rocks is the absence of relatively thick and uniform units of pure quartzite, mica schists, or marble. The source material for the Bullard Peak metasediments was interlayered argillaceous, feldspathic sandstone and shales with admixed arenaceous, dolomitic, and calcareous material. Deposition of interbedded, fine-grained, predominantly clastic material of this type would most likely occur in the infraneritic environment of an unstable shelf area (Krumbein and Sloss, 1951).

The granite gneiss and some of the hornblende gneiss and amphibolite were derived respectively from leucogranite and diabase. Contact relations indicate that the leucogranite was intruded earlier than the diabase. Any thermal metamorphic effects that these intrusions had on their sedimentary country rocks have been obliterated by subsequent regional metamorphism. Both sedimentary and igneous rocks have been subjected to high-grade regional metamorphism. Although not all rock types are indicative of a particular metamorphic facies, mineral assemblages in some rock types indicate regional metamorphism approximating the sillimanite-almandite subfacies of the amphibolite facies.

The sequence of events that led to the formation of the Bullard Peak series is: (1) Deposition of a sedimentary series in the infraneritic

environment of an unstable shelf area; (2) intrusion of leucogranite; (3) intrusion of diabase; (4) one or more periods of regional metamorphism, one of which involved folding and metamorphism to the rank of the sillimanite-almandite subfacies; (5) intrusion of the Burro Mountains batholith, contact metamorphism, development of migmatite, and metasomatic development of sillimanite and muscovite in quartz-feldspar gneiss and of microcline in hornblende gneiss. No evidence was observed in the Bullard Peak series to indicate if these events were closely spaced or if they were separated by periods of quiescence. The relationship of these events to those that produced the Ash Creek metamorphic series is discussed in a later section.

Ash Creek Series

General Statement

The metasedimentary rocks of the Ash Creek series occur as complex xenoliths or roof pendants in the Burro Mountains granite. They underlie about 1½ square miles in secs. 9, 16, 17, 21, and 22, T. 18 S., R. 18 W. (pl. 1 and 12). The largest xenolith is about 1½ by ¾ miles; numerous smaller masses, tens of yards to a few feet in size, crop out as far as a mile from the borders of this xenolith. Granite and related aplite surround the large xenolith except along its southwest side, which is faulted against Gila conglomerate. Many of the small xenoliths are enclosed in metadiabase, which in turn is enclosed by granite. In the large xenolith, beds of the Ash Creek series strike about N. 30° E. and are vertical. Foliation is well developed only in sericite phyllite and generally parallels the bedding.

The seven metasedimentary rock types in this series were grouped into four mappable units (not in stratigraphic sequence): (1) Sericite phyllite and andalusite-sericite schist; (2) cordierite hornfels; (3) spotted andalusite hornfels, biotite hornfels, and diopside quartzite; (4) serpentine-carbonate rocks. Since the Ash Creek series has been disrupted by intrusions, only a general approximation can be made of the thickness of each unit. If one considers only the metasedimentary rocks, the maximum exposed thickness of the series is approximately 5,800 feet. Maximum thicknesses of individual units are estimated at: Sericite phyllite and associated rocks, 3,100 feet; cordierite hornfels, 1,500 feet; andalusite hornfels and associated rocks, 1,200 feet; serpentine-carbonate rocks, 100 feet.

Many of the Ash Creek rocks contain both fine- and coarse-grained muscovite. The term sericite has been widely used to include fine-grained muscovite, fine-grained phengite, and hydromuscovite. However, it is useful as a nonspecific term for fine-grained muscovite whose exact chemistry is unknown (Heinrich et al., 1953). In the following petrographic descriptions, sericite is used to indicate fine-grained muscovite.

TABLE 4. COMPARISON OF THE DERIVATION OF THE BULLARD PEAK METAMORPHIC ROCKS

ROCK	MINERAL ASSEMBLAGE	SOURCE ROCK	TYPE OF METAMORPHISM	FACIES
Quartz-feldspar gneiss	quartz, microcline, oligoclase-andesine, biotite, ± muscovite, ± sillimanite, ± almandite	argillaceous feldspathic sandstone	regional	sillimanite-almandite subfacies of amphibolite facies
	± sillimanite, ± cordierite, ± magnetite, ± muscovite		contact? and metasomatism	
	± chlorite		retrograde	
Biotite gneiss	biotite, quartz, oligoclase-andesine, ± muscovite, ± epidote	calcareous argillaceous siltstone or sandstone	regional	sillimanite-almandite subfacies
	± chlorite		retrograde	
Muscovite schist	muscovite, ± biotite, ± quartz	shale	regional	sillimanite-almandite subfacies
	± sillimanite		contact	pyroxene hornfels
	± chlorite		retrograde	

TABLE 4. COMPARISON OF THE DERIVATION OF THE BULLARD PEAK METAMORPHIC ROCKS (continued)

ROCK	MINERAL ASSEMBLAGE	SOURCE ROCK	TYPE OF METAMORPHISM	FACIES
Biotite schist	biotite, ± quartz	shale	regional	sillimanite-almandite subfacies?
Sillimanite gneiss	quartz, sillimanite?, muscovite, biotite, ± almandite, ± microcline	argillaceous feldspathic sandstone	regional	
	sillimanite, ± andalusite		contact and metasomatism	pyroxene hornfels
	chlorite		retrograde	
Hornblende gneiss and amphibolite	hornblende, oligoclase-andesine, ± quartz, ± epidote, ± biotite	dolomitic (ankeritic) shale locally calcareous	regional	amphibolite
	± epidote		contact	
Hornblende gneiss and amphibolite	hornblende, labradorite, ± augite	diabase	regional	amphibolite
Granite gneiss	microcline, quartz, oligoclase, biotite, ± hornblende	leucogranite	regional	

Sericite Phyllite

Occurrence. Sericite phyllite occurs within the largest Ash Creek xenolith as two subparallel northeast-trending layers, one about 1,800 feet thick, the other about 1,300 feet (pl. 12). The phyllite, less resistant than either the cordierite hornfels or the metadiabase in contact with it, crops out along the sides and bottom of a small valley and along the west slope of the ridge held up by cordierite hornfels.

Petrography. The silvery-gray to light-green phyllite has a velvety sheen and a well-defined foliation. Many minute hematite-filled fractures cut the phyllite at a high angle to the foliation and give the rock a distinctive reddish cast. Calcite, later than hematite, fills the larger cross fractures and also forms veinlets parallel with the foliation.

Microscopic examination shows that the phyllite is composed of sericite, quartz, and very minor chlorite, all with an average grain size of 0.05 mm. The sericite and chlorite flakes are arranged to form a lepidoblastic texture distorted by a few crenulations. Quartz is randomly distributed as anhedra between sericite flakes, in clusters up to 0.5 mm across, or in lenses along the crests of crenulations.

Origin. The simple quartz-sericite mineralogy and the lepidoblastic texture indicate that the phyllite is a product of low-grade regional metamorphism. The uniform composition, fine grain size, and abundance of minerals containing aluminum, silicon, and potassium indicate a pelitic sediment as the source rock. The dominant clay mineral in most shales is illite, which is often accompanied by chloritic mica, montmorillonite, or minor kaolinite (Grim, 1953). Few combinations of known clay minerals would form a muscovite-chlorite-quartz rock under conditions of metamorphism (Yoder, 1955); among these are (1) magnesian montmorillonite, illite, and quartz; and (2) illite having the composition of muscovite, an aluminous serpentine, and quartz. Transformation of the first group to chlorite, sericite, and quartz requires a reaction that releases water; transformation of the second group involves only recrystallization. The source rock of the sericite phyllite was probably a shale containing abundant quartz and illite, with only small amounts of chloritic mica. During metamorphism of the Ash Creek rocks, illite in the parent shale attained a higher degree of crystallinity to form sericite, which, aided by stress, recrystallized into larger oriented flakes. Quartz also recrystallized, with minor migration from the flanks to the crests of crenulations.

Sericite phyllites belong to the muscovite-chlorite subfacies of the greenschist facies as defined by Vogt (1927) and modified by Turner (1948). Relatively pure sericite phyllites may extend into the garnet zone of regional metamorphism; the grade of the phyllite in the Ash Creek series may be slightly higher than that of the greenschist facies.

Andalusite-Sericite Schist

Occurrence. Andalusite-sericite schist occurs as a marginal phase of the sericite phyllite that has been more highly metamorphosed near metadiabase contacts. The schist is particularly well exposed in a small valley southeast of the road in NE¼ sec. 21, T. 18 S., R. 18 W. (pl. 12).

Petrography. The schist is coarser grained and lacks the velvet sheen, well-developed foliation, and hematite stains characteristic of the phyllite. About 10 percent of the rock is composed of unoriented porphyroblasts of dark blue-gray andalusite, up to 4 mm across and 15 mm long, and of dark-brown biotite; both are evenly distributed in a quartz-sericite matrix.

Biotite poikiloblasts range from 0.5 to 1.0 mm and have ragged edges. Finer grained biotite rims and veins the colorless andalusite porphyroblasts (pl. 5B). Light-green chlorite replaces biotite veinlets and forms rosettes in biotite porphyroblasts. Tiny magnetite euhedra are generally associated with biotite and chlorite. The quartz-sericite matrix is similar to that of the sericite phyllite, except that in the schist the sericite is generally coarser and lenses of quartz are larger and more abundant. The perfection of foliation in the schist has been reduced by growth of the porphyroblasts. The paragenetic sequence of this rock is thus: (1) Quartz and sericite; (2) andalusite; (3) biotite; and (4) chlorite and magnetite.

Origin. The field occurrence indicates that the andalusite-sericite schist was formed by contact metamorphism resulting from intrusion of sericite phyllite by diabase. Andalusite and biotite may form during thermal metamorphism in a low-stress environment by reaction between sericite, chlorite, and iron oxides (Harker, 1939). A similar reaction, however, may produce cordierite. The relative amounts of cordierite and andalusite formed during metamorphism are dependent upon the ratio of alumina to magnesia, which in turn is dependent upon the relative amounts of chlorite and sericite. The abundance of andalusite and absence of cordierite indicate relatively little chlorite in the sericite phyllite from which this schist was derived, further supporting the hypothesis that the parent shale of the sericite phyllite was low in chloritic mica. The origin of the biotite porphyroblasts that are not associated with andalusite probably lies also in a reaction between chlorite and sericite. Replacement of biotite by chlorite and magnetite may represent retrograde metamorphism.

Rocks in which andalusite and muscovite coexist in equilibrium—and they apparently do here—belong to the cordierite-anthophyllite subfacies of the amphibolite facies (Turner, 1948). Rocks of this subfacies are formed by contact metamorphism involving moderate pressure and temperature, but low shearing stress.

Cordierite Hornfels

Occurrence. Cordierite hornfels, the most resistant rock of the Ash Creek series, crops out in the largest Ash Creek xenolith as a long, narrow, northeast-trending ridge standing 200 feet above neighboring rocks. The deeply weathered crest is capped by angular blocks that spread as talus down both sides. A smaller mass crops out in NW¼ sec. 22, T. 18 S., R. 18 W. (pl. 12). Both occurrences have been intruded by granite, and the smaller one by diabase as well.

Petrography. Weathering has left the surface a deep red brown to yellow brown with black manganese stains. A freshly broken surface shows unoriented plates of muscovite, up to 3 mm across, set in fine- to medium-grained quartz-chlorite-sericite aggregates. In the typical cordierite hornfels, quartz and chlorite-sericite aggregates comprise about 25 percent and 50 percent of the rock respectively. The anhedral quartz grains, about 0.25 mm across, occur in aggregates or, more commonly, singly within felted chlorite-sericite masses. Individual irregular masses of chlorite and sericite resemble the pinitic alteration of cordierite. Biotite and muscovite, which make up about 10 to 15 percent of the rock, are strongly poikiloblastic, with inclusions of quartz, andalusite, zircon, and apatite. Biotite, the more abundant of the two, shows incipient alteration to chlorite and magnetite.

Andalusite occurs as single anhedra about 0.05 mm in size or in irregular clusters, stringers, and lenses. Wherever andalusite is abundant, chlorite and sericite are commonly absent nearby. Accessory minerals are magnetite, apatite, zircon, ilmenite coated with leucoxene, and sphene. Magnetite, the most abundant, forms tiny euhedral to subhedral grains, usually randomly distributed or arranged in irregular, poorly defined stringers. Apatite is included in mica, zircon occurs most commonly in biotite, and sphene and ilmenite occur with granular quartz.

In one example of cordierite hornfels, ragged muscovite comprises nearly 50 percent of the rock, but no biotite is present. This muscovite forms spongy networks of unoriented poikiloblastic plates, including quartz, cordierite, and andalusite. Interspersed with the coarse-grained muscovite are fine-grained aggregates of sericite. Pennine occurs as coarse, light-green to pale-brown plates interstitial to muscovite and cordierite. Irregular poikiloblastic grains of cordierite, with pseudohexagonal "pie sector" twins and polysynthetic spear-shaped twins, locally make up as much as 30 to 40 percent of the rock. Most of the cordierite shows some degree of alteration to pinite; some is almost completely replaced by pinite. Irregular veinlets, 0.1 mm to about 1 mm thick, of hematite and finely granular calcite appear throughout the cordierite hornfels.

Origin. The presence of cordierite and andalusite indicates that this hornfels formed by contact metamorphism under conditions of moder-

ate temperature and pressure but absence of stress. The parent rock contained abundant aluminum, silicon, and potassium, as well as minor magnesium and iron. The most likely source rock for the cordierite hornfels was a shale containing abundant quartz and clay minerals (illite, montmorillonite, and chloritic mica) and possibly minor sericite and chlorite.

Early stages of metamorphism caused formation of chlorite and sericite from clay minerals in the shale. As temperature and pressure increased, reaction occurred between sericite, chlorite, and iron oxides to produce biotite alone or biotite in combination with either or both cordierite and andalusite. After formation of andalusite and cordierite, excess sericite would recrystallize to muscovite. Excess chlorite, however, would not recrystallize, but would react with any available andalusite to produce additional cordierite. Since this hornfels contains cordierite, andalusite, biotite, and coarse-grained muscovite, sericite was most likely in excess. The coarse-grained pennine is probably pseudomorphous after biotite. Similarly, the chlorite-sericite aggregates resulted from alteration of cordierite. Both probably denote retrograde metamorphism.

The association of cordierite-muscovite or andalusite-muscovite in a pelitic hornfels indicates the cordierite-anthophyllite subfacies of the amphibolite facies of metamorphism. Possible mineral assemblages for rocks with an excess of SiO_2 and a deficiency of K_2O include either andalusite, cordierite, or anthophyllite, with quartz, plagioclase, and one mica (Turner, 1948). If one considers only the minerals present in the Ash Creek cordierite hornfels, possible equilibrium assemblages are: (1) Muscovite, andalusite, cordierite, and quartz; (2) muscovite, biotite, cordierite, and quartz.

The coexistence of muscovite, biotite, andalusite, and cordierite in a small area indicates nonequilibrium conditions. Eskola (1914, 1915) cites this assemblage at the classic locality for the amphibolite facies in the Orijärvi region of Finland as not having attained equilibrium. A possible explanation for this nonequilibrium might be a relatively short time during which conditions existed for chemical reaction.

The sericite phyllite associated with the cordierite hornfels shows the effects of polymetamorphism. The cordierite hornfels must also have been subjected first to regional and then to contact metamorphism. The formation of chlorite and sericite from sedimentary clay minerals probably occurred during regional metamorphism, and the development of biotite, andalusite, and cordierite during subsequent contact metamorphism. The moderate contact metamorphism has essentially masked the effects of the earlier low-grade regional metamorphism.

Spotted Andalusite Hornfels

Occurrence. Spotted andalusite hornfels occurs at the northwest end of the largest xenolith as an irregular northeast-trending band approxi-

mately a quarter of a mile wide and three-quarters of a mile long (pl. 12). Ash Creek Canyon cuts through the southwestern end of the xenolith and exposes the hornfels in contact with Precambrian granite. Other smaller xenoliths of the hornfels are irregularly distributed in granite, aplite, and metadiabase northeast of the major occurrence. Angular talus blocks and steep walls characterize the outcrop in Ash Creek Canyon. This type of hornfels grades into biotite hornfels and diopside quartzite, both of which appear as a single unit on the geological map.

Petrography. The weathered surface shows many irregular white to light-gray spots with black rims, set in a light-tan to green matrix. The spots vary in size, shape, and sharpness of boundaries, but in general are from 2 to 15 mm across and comprise about 50 percent of the rock. On a weathered joint surface the light spots may be outlined with limonite, or the entire surface coated with fine-grained chloritic material and manganese oxide dendrites. The rock is fine grained and very difficult to break. On a fresh surface, the spots are less conspicuous, the color is generally darker, and minute specks of muscovite appear in the matrix.

In thinsection the spots can be seen to be clusters of anhedral andalusite and quartz with accessory magnetite (pl. 7A). The andalusite grains average about 0.2 mm, and the quartz about 0.1 mm in size. The irregular distribution of quartz and andalusite gives the impression of large poikiloblastic crystals of andalusite arrested in the process of forming through aggregation of smaller anhedral grains. Irregular rims of fine-grained quartz, muscovite, and biotite separate the andalusite from the matrix. The rims vary from the thickness of a single biotite flake, less than 0.1 mm, to about 0.3 mm and are usually discontinuous. Anhedral quartz and plates of chlorite and sericite, all less than 0.01 mm in size, form the matrix. Larger biotite and muscovite poikiloblasts also occur in the matrix in subparallel orientation.

Origin. The spotted texture denotes a low to moderate grade of thermal metamorphism, probably the result of reactions initiated where the combination of mineral constituents approximated the composition of the minerals that were stable under prevailing metamorphic conditions. The spotted texture also indicates a rather brief period of metamorphism, for if metamorphism prevailed for a long period of time, reaction might have continued until the entire rock mass was reconstituted.

The andalusite and biotite apparently resulted from reactions among sericite, chlorite, and possibly magnetite similar to that in the matrix. The overall composition of the hornfels, particularly the high aluminum and the excess of potassium over sodium, suggests a shale containing illite, chloritic mica, and perhaps other clay minerals, with quartz, minor hematite, and magnetite as the most likely source rock.

Crude orientation of biotite and muscovite porphyroblasts in the matrix, but not in the andalusite clusters, further supports a thesis of mild regional metamorphism prior to thermal metamorphism. The

effects of regional metamorphism on the shale were: (1) Conversion of clay minerals to sericite and chlorite; (2) formation of magnetite from hematite or limonite; (3) reaction between chlorite and sericite to form crudely oriented biotite; (4) recrystallization of sericite to produce oriented muscovite. Thermal metamorphism in the absence of stress then caused local reaction between sericite and chlorite to produce the andalusite-biotite clusters.

Biotite Hornfels

Occurrence. Biotite hornfels occurs as lenses and layers gradational with spotted andalusite hornfels and diopside quartzite in the Ash Creek xenoliths (pl. 12).

Petrography. This hornfels is fine grained and compact; numerous irregular fractures break it into sharp fragments. Some of the biotite hornfels has well-developed rock cleavage parallel to relict bedding. Weathering forms a light-olive to dark red-brown surface, with limonite stains or black dendritic coatings. A freshly broken surface has a light-cream to tan color and a subvitreous luster.

Thinsections show that about 80 percent of the rock is made up of granoblastic grains of quartz, orthoclase, and oligoclase, all about 0.05 mm in size. Biotite, muscovite, and chlorite, dispersed uniformly through the fine-grained matrix, average 0.2 mm in size. Suboriented biotite, the most abundant of the platy minerals, gives the rock a rough foliation. Ragged, poikiloblastic muscovite includes abundant quartz and feldspar. Biotite and muscovite show intergrowths subparallel to (001). Chlorite appears both as fine-grained aggregates and as larger, well-developed crystals. Wherever large flakes of muscovite, biotite, or chlorite appear, the area immediately around the flake is free of fine-grained sericite and chlorite; the result appears as small, poorly defined clear spots scattered throughout a thinsection. Andalusite, apatite, sphene, and magnetite are accessory constituents. The first two occur predominantly as inclusions in mica, but a few grains are interstitial in the quartz-feldspar mosaic. Sphene and magnetite are generally euhedral; larger skeletal crystals of magnetite occur with fine-grained chlorite.

A dark, fine-grained rock that occurs as small masses in metadiabase in Ash Creek Canyon below the ricolite quarry was considered in the field to be a variety of metadiabase. Petrographic examination showed this rock to be a hornfels somewhat similar to the biotite hornfels. A small, irregular body of this hornfels crops out as mottled, dark-green, rounded masses on the slopes of Ash Creek Canyon. The rock is made up of a light gray-green matrix that encloses scattered clusters of biotite, irregular inch-long granular masses of fine-grained magnetite and fine- to medium-grained epidote, and a few aggregates of coarse-grained silver-green chlorite. The epidote clusters stand out as knobs on a weathered surface.

Thinsections of this biotite-epidote hornfels show that about 40 percent of the rock is made up of crudely oriented plates of brown biotite set in a granoblastic aggregate of cordierite, magnetite, and minor amounts of kaolinized and sericitized feldspar. The irregular cordierite grains, less than 0.1 mm across, show hazy twinning, are partially altered to pinite, and include magnetite and apatite euhedra. Biotite flakes occur between cordierite grains and in lenslike clusters up to an inch long. Granular yellow-green epidote occurs in clusters with altered cordierite, in biotite clusters, and scattered sparsely in the matrix. About 5 to 10 percent of the rock is made up of fine-grained magnetite anhedra that are distributed both in the matrix and in the clusters of biotite and of epidote and cordierite.

Origin. The biotite hornfels represents a relatively impure fine-grained feldspathic sandstone that has been subjected to low-grade regional metamorphism and subsequent contact metamorphism. The grains in the granoblastic quartz-feldspar aggregate are probably close to the size of the original clastic particles. Small amounts of clay minerals, chloritic mica, and iron oxides reacted and recrystallized under the low pressure and low temperature of regional metamorphism to form muscovite and biotite. Andalusite, an antistress mineral, formed either during regional metamorphism, while temperature was still elevated but stress was relaxed, or, more likely, during intrusion of diabase or granite, when the temperature was again raised.

Compared with other types of hornfelses in the Ash Creek series, the biotite hornfels contains considerably less andalusite. This lesser amount of andalusite may indicate: (1) Relatively little clay material in the parent rock; (2) coarser grain size; therefore, less chance for reaction; or (3) a degree of contact metamorphism somewhat lower than that affecting the cordierite hornfels or the spotted andalusite hornfels. Since, in a single xenolith, the biotite hornfels is gradational into hornfels richer in andalusite, the amount of andalusite probably reflects a difference in original composition and grain size.

Diopside Quartzite

Occurrence. Diopside quartzite, a minor member of the spotted andalusite hornfels unit, occurs as elongate lenses and continuous layers interbedded with andalusite and biotite hornfelses in the largest Ash Creek xenolith. Outside this unit, the quartzite also occurs in two small lenses within sericite phyllite, in a xenolith with banded talc serpentinite (pl. 6A), and in several scattered xenoliths enclosed in granite and metadiabase.

Petrography. The quartzite is massive to blocky in outcrop. Two sets of joints, one parallel and another nearly normal to the bedding, cause it to break into large rectangular blocks, the surfaces of which are dull white with irregular light-green stringers. Secondary calcite coats many

of the joint surfaces. The light-green stringers either weather to a light tan or, in a few outcrops, weather out completely and leave narrow furrows. Freshly broken surfaces show bright vitreous patches of quartz between cream to pale yellow-green stringers.

Original grain boundaries are still recognizable in thinsection. A regular variation in grain size between the stringers indicates relict stratification. The largest quartz grains, 2 mm in diameter and tightly bonded by recrystallized quartz and minor interstitial feldspar, grade across the layering into a fine mixture of quartz and diopside grains about 0.1 mm in size. The colorless quartz is free of inclusions and bubble trains. Undulatory extinction and a slightly biaxial character indicate strain. The light-green stringers appear in thinsection as quartz grains enclosing diopside either as single anhedra or as aggregates. Bands of coarse-grained quartz are free from diopside, whereas bands of fine-grained quartz contain abundant diopside. Microcline occurs as thin tabular grains between quartz grains; a dusty light-tan coating of clay minerals and sericite indicates incipient alteration of the feldspar.

The diopside quartzite that occurs in a xenolith with talc serpentinite locally contains hornblende as an essential constituent. The dark-green hornblende is concentrated along fractures as blades up to an inch in length; it also appears as fine-grained whorls and irregular strings in the quartzite. Microscopic examination of a hornblende-rich part shows diopside and hornblende with accessory clinozoisite and sphene, but no quartz. Some patches up to an inch across are composed of a mosaic of diopside grains, which have a maximum size of 0.2 mm. Hornblende blades cut across and enclose diopside grains. The color distribution in hornblende is somewhat irregular parallel to γ; small colorless patches occur within the normally light blue-green hornblende blades. Sphene occurs in hornblende as euhedra up to a millimeter in length, but in diopside the sphene is subhedral to anhedral.

Origin. The diopside quartzite formed from a quartz sandstone containing thin lenses of finer grained silty quartz mixed with impurities that reacted to form diopside during contact metamorphism. Two combinations could account for the diopside and potash feldspar in the quartzite: (1) Calcite, illite, and quartz reacted to form diopside and potash feldspar; or (2) dolomite and quartz reacted to form diopside; the small amount of feldspar originated as detrital grains which were recrystallized. This second reaction is particularly likely because both dolomite and diopside have Ca:Mg = 1:1. A similar reaction between clay minerals and calcite with limited quartz could produce clinozoisite.

Coarse-grained hornblende blades are localized by fractures, and finer grained hornblende masses cut across the quartz-diopside aggregates; hence hornblende appears to have formed later than diopside. The diopside probably formed during intrusion of diabase; later, residual liquid containing aluminum and water from the diabase magma could have reacted with diopside to form hornblende.

Serpentine-Carbonate Rocks

Occurrence. Tabular xenoliths of serpentine-carbonate rocks, the least widespread unit of the Ash Creek series, crop out along Ash Creek Canyon from 2 to 3 miles above the confluence of Ash Creek and the Gila River (pl. 12). Granite, aplite, metadiabase, or a combination of these enclose the xenoliths, which range in thickness from several inches to as much as 40 yards.

Within the serpentine-carbonate unit are several petrologic types that vary in texture, mineralogy, structure, and color. Some are banded, but not foliated; therefore, the term schist is not applicable. Although "serpentinite," as originally suggested by Lodochnikov (Phillips and Hess, 1936), commonly refers to serpentine rocks derived by late magmatic alteration of basic or ultrabasic igneous rocks, it also applies to a rock composed of serpentine and/or antigorite, with no genetic connotation (Selfridge, 1936). Because several of these rocks are composed predominantly of serpentine, but with talc, chlorite, magnetite, and calcite as essential constituents, the term serpentinite has been used with modifications in the following ways: (1) Serpentine marble—ophicalcite and associated calcite-serpentine-chlorite rocks; (2) banded talc serpentinite—alternating bands of unoriented talc and serpentine, with either predominant; (3) massive serpentinite—uniform in color, massive, and composed entirely of serpentine; (4) mottled serpentinite—irregular variations in color and relative amounts of serpentine and talc; (5) magnetite serpentinite—serpentine with essential magnetite.

A single xenolith may contain one or several of these serpentine rock types. However, in only one xenolith do serpentine-carbonate rocks occur with other rocks of the Ash Creek series. Plate 6A shows a xenolith in which banded talc serpentinite is in conformable contact with diopside quartzite.

The serpentine-carbonate rocks are easily eroded, and their position in part controls the course of Ash Creek. The outcrops generally stand out as light-colored areas in contrast to surrounding darker granite and metadiabase. Smoothly abraded surfaces in the bottom of Ash Creek Canyon grade into irregularly weathered surfaces and blocks on the canyon slopes.

Petrography. Serpentine marble. Serpentine marble, as used here, includes a typical ophicalcite as well as associated rocks made up of the following mineral assemblages: (1) Calcite-serpentine; (2) calcite-serpentine-chlorite; and (3) calcite-actinolite-clinozoisite-sphene.

In the bottom of Ash Creek Canyon, the ophicalcite is typically white to light gray and marked by light green-gray mottled areas and irregularly contorted green-gray bands less than a centimeter thick. Weathered surfaces on the canyon walls are generally rough and irregular, with a light-tan color. Many evenly spaced pits, subspherical in shape and

about 0.5 mm in diameter, indicate the former presence of serpentine granules.

Thinsections of ophicalcite show rounded aggregates of light-yellow to yellow-green antigorite, up to 0.3 mm across, in a groundmass of irregularly shaped calcite grains with sutured boundaries. Some of the serpentine aggregates contain a few euhedral to subhedral magnetite grains less than 0.1 mm in size. The mode of the ophicalcite is 63 percent calcite and 36 percent serpentine. Insoluble residues from several large pieces of ophicalcite contain over 95 percent serpentine and accessory amounts of magnetite, forsterite, pennine, and spinel(?). Only a general index of refraction range of 1.535-1.540 could be measured for serpentine because of its very fine, fibrous nature. The light yellow-green forsterite occurs as single anhedra and globular aggregates. Serpentine replaces forsterite marginally and along veinlets. The forsterite has a 2V of 87° and is optically positive; these properties characterize forsterite of an approximate composition Fo_{96}– Fa_4 (Kennedy, 1947). Turbid calcite with polysynthetic twinning has $\omega = 1.661$, which indicates pure calcite (Kennedy, 1947). Dolomite was not found in ophicalcite nor in any of the other serpentine-carbonate rocks.

Abundant actinolite, clinozoisite, and accessory sphene occur in a xenolith of ophicalcite, less than one foot long, that is enclosed in metadiabase about 25 yards down Ash Creek Canyon from the ricolite quarry. Inch-wide zones of bladed actinolite and coarse, interstitial, honey-colored clinozoisite separate lenses of finely granular, tan to cream clinozoisite. The bladed actinolite is dark green, weathering to a light silvery green, with interstitial flakes of dark-brown biotite and grains of dark red-brown sphene.

Talc serpentinite. Talc serpentinite is the best known of the rock types occurring in the Ash Creek xenoliths. This material has been marketed under the trade name of ricolite and has been used as an interior-decorative building stone. Megascopically, the fine-grained talc serpentinite shows undisturbed banding similar to that of a finely bedded sediment (pl. 6B). The most common colors vary from a light green yellow to a very dark green, but shades of red, yellow, blue, and brown occur locally. The bands range from 0.1 mm to about 5 cm in thickness; the average is usually less than 1 cm. Most of the bands are of constant thickness, but not uncommonly one will pinch and swell or contain contrasting lenses. Flakes of light silver-green chlorite, up to 2 mm across, and finely granular calcite cause a rough parting parallel to the bands. Chlorite also occurs as unoriented plates, usually less than a millimeter across, in zones parallel to the banding. Fine-grained calcite and quartz fill fractures across the banding. Single veins of cross-fiber asbestiform serpentine cut the serpentinite generally parallel to the bands. Anastomotic veinlets form zones about a centimeter thick, also generally parallel to the banding.

Locally the banded talc-serpentinite grades into a light-cream to tan variety in which talc predominates over serpentine, or in which serpentine is absent. This talc-rich variety occurs in bands a few inches to several feet in thickness. The serpentinite xenolith from which the ricolite has been quarried contains such a talc-rich zone at its eastern end. On the east side of Ash Creek, a talc-rich zone 20 feet across grades along strike into the typical banded serpentinite in the canyon bottom.

A variation in mineral composition causes the characteristic megascopic banding. Thinsections of talc serpentinite show that the bands are fine-grained aggregates, with varying amounts of serpentine, talc, chlorite, clinozoisite, and quartz. Talc and serpentine are commonly the only constituents; only the type described above in talc-rich zones contains clinozoisite and quartz. The maximum size of individual grains of fibrous serpentine is 0.1 mm. Aggregates of serpentine grains form a mosaic or rarely a mesh texture. The spatial arrangement of two types of serpentine causes the mesh texture; light yellow-green, fibrous antigorite borders a central core of turbid serpentine 0.04 to 0.08 mm across. The light-green or light-brown serpentine in the core is isotropic or very slightly birefringent. Magnetite grains occur scattered within the mesh-textured serpentine.

Serpentine from the darkest of the bands has a general index of refraction range of from 1.556 to 1.560. An X-ray powder photograph of this serpentine indicates antigorite with talc impurities. The cross-fiber veinlets of asbestiform serpentine that cut the serpentinite were verified by X-ray powder photographs as chrysotile. Talc, occurring as randomly oriented plates up to 0.1 mm maximum size, generally is coarser grained than serpentine. Plates of talc with ragged edges replace and cut across serpentine. The talc-rich bands in the serpentinite appear in thinsection as a mosaic of talc plates, with minor interstitial quartz and clinozoisite, all of which are less than 0.2 mm in size. Relative amounts of these minerals vary among individual bands; the talc content ranges from 50 to 90 percent, clinozoisite from 0 to 40 percent, and quartz from 0 to 10 percent. Serpentine rarely occurs with clinozoisite and quartz.

Massive serpentinite. About 100 yards west of the ricolite quarry, banded talc serpentinite grades along the strike into a massive canary-yellow serpentinite. Widely spaced cross-fiber veinlets of chrysotile are the only features that interrupt its uniformity. The weathered surface is somewhat lighter in color and lacks the luster of the freshly broken surface. Under the microscope, the serpentinite appears compact and fine grained; crushed fragments are generally splintery to fibrous. The general refractive index ranges from 1.546 to 1.550. X-ray powder photographs show antigorite as the only constituent.

Mottled serpentinite. Contorted veins and multicolored irregular masses of mottled serpentinite occur within ophicalcite in Ash Creek Canyon above the ricolite quarry. This type of serpentinite displays

all the colors of banded talc serpentinite but lacks any regularity in color distribution. The veins are an inch to several inches thick, most commonly are dark green, and trend roughly parallel to the strike of the ophicalcite layers. The general configuration of the irregular masses of serpentinite is elongate and subparallel to the strike of the ophicalcite layers. Zones containing serpentine are as much as 5 feet thick. The most common occurrence is a central discontinuous core of ophicalcite, a few inches to several feet across, wrapped by multicolored serpentine up to several inches thick, all of which is enclosed in ophicalcite (pl. 6C). Scattered along the serpentine-ophicalcite contacts are small lenslike aggregates of coarsely crystalline white calcite and flakes of dark silvery-green pennine ranging in cross-section from less than a millimeter to several centimeters.

A specimen taken from the serpentine-ophicalcite contact shows dark green-black serpentine veining light-olive serpentine; both varieties cut ophicalcite as tiny veinlets and diffuse masses. Crushed fragments of the olive serpentine are splintery to slightly fibrous and have a general index of refraction close to 1.550. The darker serpentine has the same general index of refraction, is fibrous, and is intimately intergrown with magnetite euhedra.

Magnetite serpentinite. Several bands of magnetite serpentinite, 1 to 2 feet in width, are associated with serpentine marble and mottled serpentinite about a third of a mile above the ricolite quarry in Ash Creek Canyon. Crude bands of granular magnetite alternate with dark-green serpentine bands. The magnetite is dull black on a weathered surface and locally forms as much as 90 percent of the rock; serpentine bands weather green yellow and commonly make up less than 40 percent of the rock. The texture is somewhat similar to that of the banded talc serpentinite, but the bands of serpentine are disrupted and in some places obliterated by medium-grained magnetite anhedra. Secondary calcite coats the numerous fracture surfaces. On a fresh surface, the dark-green serpentine is inconspicuous against the black magnetite. A polished section of this serpentinite shows no evidence of exsolution in the magnetite.

Occurring with the banded magnetite serpentinite is a coarser grained, nonbanded variety. Irregularly shaped aggregates of magnetite from 1 mm to 2 cm long are evenly distributed in dark-green serpentine. The magnetite makes up a third to a half of the rock. Under the microscope, the serpentine appears as a fibrous to splintery mass, with a refractive index of 1.560-1.564. An X-ray powder photograph showed the serpentine to be antigorite.

Comparison of serpentine minerals. The various serpentinites were studied optically and by X-ray powder photographs in an attempt to account for the wide color differences. Indices of refraction were measured by immersion in liquids standardized for sodium light. Only the asbestiform serpentine occurs in units large enough so that more than a

general index range can be measured. Comparison of X-ray powder photographs with standards (Selfridge, 1936) served to identify the varieties of serpentine. Table 5 shows the tabulated results. A general correlation appears between color and index of refraction; as the color becomes darker, the index increases.

One factor that affects the variation in indices and color of the serpentinites is the chemical composition. Limited amounts of Fe^{++} and Fe^{+++} would increase the index of refraction. Increase in water would decrease the index (Selfridge, 1936). The only available chemical analysis is listed below; it was reported by Jones (1904) for "ricolite" (banded talc serpentinite):

	(In percent)
SiO_2	43.52
Al_2O_3	16.88
MgO	23.78
FeO	trace
Fe_2O_3	trace
CaO	2.22
Na_2O, K_2O	2.50
H_2O	11.10
Total	100.00

Northrup (1942) cites this analysis and notes that "the SiO_2 and H_2O are normal for serpentine, but MgO is abnormally low and Al_2O_3 is abnormally high." These abnormalities are readily explained by the variation in amounts of serpentine, talc, clinozoisite, and chlorite in the banded talc serpentinite.

Another factor contributing to the variation in color is most clearly seen in a thinsection of banded talc serpentinite. The light- and dark-green bands contain serpentine of the same color and index of refraction, but the relative amount of talc varies between bands. The colorless to light-tan talc, in effect, dilutes the color of the green serpentine. The same general effect is seen in the mottled serpentinite, where admixed magnetite darkens the apparent color of the serpentine.

Origin. Rocks in which serpentine is an abundant constituent generally originate either through serpentinization of basic and ultrabasic igneous rocks or by means of thermal metamorphism of siliceous, dolomitic rocks. The metasedimentary origin of the Ash Creek serpentine-carbonate rocks is clearly seen in the field by their conformable and gradational contact with quartzite (pl. 6A) and their close association with pelitic hornfelses. The intrusion of diabase and granite into the Ash Creek series has afforded ample opportunity for thermal metamorphism. However, any theory of origin for these rocks must also explain: (1) The genesis of the ophicalcite; (2) the formation of veins and replacements of mottled serpentinite in ophicalcite; (3) the formation of banded talc serpentinite; (4) the gradation between banded and

TABLE 5. COMPARISON OF SERPENTINE MINERALS

OCCURRENCE	TEXTURE	COLOR	INDEX OF REFRACTION	X-RAY POWDER PATTERN
Cross-fiber veinlets in talc serpentinite	absestiform fibers up to 1 cm	light yellow tan	$\alpha = 1.502$ $\gamma = 1.517$	chrysotile
Serpentine residue from ophicalcite	aggregate of fibers less than 0.1 mm	light yellow green	n = 1.535-1.540	antigorite
Massive serpentinite	massive	bright canary yellow	n = 1.545-1.550	antigorite
Dark band from talc serpentinite	plates, average size 0.1 mm	dark green	n = 1.557-1.569	antigorite with talc
Magnetite serpentinite	massive	dark green	n = 1.560-1.564	antigorite

massive serpentinites; (5) the presence of as much as 50 percent magnetite in one type of serpentinite, but its essential absence in others. Field associations indicate that the formation of the serpentinites is genetically related to the intrusion of the diabase. Xenoliths of carbonate rocks completely enclosed in metadiabase are almost wholly converted to serpentine, whereas those surrounded by metadiabase and granite or by granite alone show minor serpentine and abundant carbonate.

The various serpentinites are grouped as follows for convenience in discussing their origins: (1) Ophicalcite; (2) massive serpentinite and mottled serpentinite; (3) magnetite serpentinite; and (4) banded talc serpentinite.

Ophicalcite. Insoluble residues from ophicalcite show that serpentine granules originated by replacement of globular aggregates of forsterite. Reaction between dolomite and limited silica under conditions of thermal metamorphism will yield forsterite and calcite (Harker, 1939). The regular distribution of serpentine in calcite somewhat suggests that the silica was derived from quartz grains rather than from chert lenses or layers. The heat from intrusion of diabase caused quartz and dolomite to react to form forsterite and calcite. Later introduction of water at lowered temperatures brought about the formation of serpentine at the expense of the olivine. The small amount of magnetite in the ophicalcite is explained by the small amount of Fe^{++} in the forsterite. Apparently the parent carbonate rock was not ankeritic. Probably only local migration of the original constituents of the rocks was involved, and water was the only substance introduced.

Massive and mottled serpentinites. The textural and mineralogical features of these serpentinites cannot be explained by local reaction between quartz and dolomite, limited migration of constituents, or minor introduction of new constituents. However, the dominant minerals, primarily serpentine and talc, may be produced by the following reactions between constituents available in a siliceous dolomite:

$$6CaMg(CO_3)_2 + 4SiO_2 + 4H_2O \rightarrow \underset{\text{(serpentine)}}{Mg_6Si_4O_{11}(OH)_6 \cdot H_2O} + 6CaCO_3 + 6CO_2$$

$$3CaMg(CO_3)_2 + 4SiO_2 + H_2O \rightarrow \underset{\text{(talc)}}{Mg_3Si_4O_{10}(OH)_2} + 3CaCO_3 + 3CO_2$$

On a graphical representation of the system $MgO\text{-}SiO_2\text{-}H_2O$, in which temperature is plotted horizontally and pressure vertically, the temperature-pressure curves separating the fields of equilibrium assemblages are nearly vertical (Bowen and Tuttle, 1949). The different assemblages are thus primarily a function of temperature. Below 500°C, the equilibrium assemblage is chrysotile-talc-brucite-silica. Above approximately 500°C, pure magnesium chrysotile cannot exist, and above

approximately 800°C talc cannot exist. Formation of talc and chrysotile must occur below 800°C and 500°C respectively.

In a discussion of the serpentinization of siliceous dolomite by diabase (dolerite) intrusion, Poldervaart (1950) concluded: (1) Diabase would be essentially crystallized at a temperature (950°-1,000°C) far above the stability limit of serpentine; serpentine must form after the diabase has crystallized. (2) The thermal conductivity of dolomite is too low (5×10^{-3} cgs units) to allow heat from an intruding diabase to produce serpentine more than a few feet from the contact; therefore, heat is not the only factor active in the production of serpentine.

Poldervaart (1950) gives the following explanation for the formation of serpentine in dolomite: As the temperature is slightly increased, vadose water and possibly fluid from the basic magma are concentrated along bedding planes and joints in the dolomite. This liquid provides a highly mobile medium through which heat and ions can diffuse with comparative ease. As the temperature continues to increase, these solutions dissolve silica and dolomite from the sediment and become saturated in Si, Ca, Mg, and CO_3. Thermal diffusion concentrates Mg near the contact and Ca away from it. As the temperature decreases to within the stability limit of serpentine and talc, they begin to crystallize. Serpentine forms where the concentration of Mg is high, talc where Mg is low, and calcite where Mg is absent. Forsterite and diopside may form initially but would be converted to serpentine at a lower temperature.

This theory seems applicable to the formation of some of the Ash Creek serpentinites. Fracture and permeability control of solutions that precipitated serpentine would account for both the veins and irregular masses of mottled serpentinite. The thermal diffusion and limited differentiation of magnesium and calcium could also explain a gradation from a pure serpentine rock through a serpentine-talc rock to one in which talc predominates over serpentine.

Chrysotile asbestos associated with serpentinite could form by: (1) Direct crystallization from magnesium-rich solutions; or (2) replacement of previously formed massive serpentine either shortly after diabase intrusion at a relatively high temperature, or later when erosion has brought the serpentine into the zone of ground-water circulation. Poldervaart (1950) suggests that serpentine asbestos begins to crystallize from solution along fractures in massive serpentine. Once formation has started, fiber growth continues by replacement of massive serpentine.

Veinlets of asbestiform chrysotile cutting the Ash Creek serpentinites indicate that chrysotile is the youngest of the serpentine varieties. Inasmuch, however, as both the above conditions could have existed during the history of the serpentinite, both probably aided in growth of the asbestos after the formation of massive and banded serpentinites.

Small amounts of chlorite in the Ash Creek serpentinite usually occur at contacts between mottled serpentinite and ophicalcite. Phillips and Hess (1936) explain talc and chlorite, or talc, biotite, and actinolite

at the contact between serpentinite and siliceous wall rock as metamorphic differentiation resulting from hydrothermal alteration. Although the ophicalcite is not now siliceous, small amounts of Si and Al could have been left after the formation of serpentine. Hydrothermal alteration associated with the later intrusion of granite may have caused these to react with serpentine to produce chlorite. Actinolite and biotite occurring at the contact of ophicalcite and metadiabase may have been formed under similar circumstances.

Magnetite serpentinite. Magnetite in this serpentinite may have originated by: (1) Conversion of siliceous, ankeritic dolomite to an iron-rich olivine and subsequent alteration to serpentine and magnetite; (2) metamorphic differentiation involving a concentration of iron that was originally disseminated in the sedimentary rock; or (3) iron metasomatism associated with diabase or granite intrusion.

Two lines of evidence favor the third alternative. One is the general veinlike occurrence of magnetite later than serpentine. This characteristic is seen in the shape of the magnetite serpentinite, as well as in the tiny veinlets of magnetite-rich serpentine that cut mottled serpentinite. The other evidence is the general absence of magnetite in the other serpentine-carbonate rocks. Talc and massive serpentinites are completely free of magnetite; mottled serpentinite contains only accessory magnetite. The composition of forsterite (Fo_{96}) in the ophicalcite further supports the idea of iron-poor source rocks.

The magnetite serpentinite probably originated in a manner similar to the mottled serpentinite. Introduction of iron along joints, fractures, or relict bedding planes by residual solutions from diabase or granite led to the formation of magnetite. Since the serpentine very likely formed after diabase intrusion, and magnetite is younger than the serpentine, the formation of magnetite probably accompanied the intrusion of granite.

Banded talc serpentinite. The serpentine-talc association in the banded talc serpentinite indicates an origin not unlike that of the other Ash Creek serpentine-carbonate rocks. The source rock for the serpentine and talc rocks was probably a siliceous, dolomitic sediment. The presence of clinozoisite, a calcium-aluminum silicate, indicates the former presence of argillaceous material in the original sediment. The characteristic banding in this serpentinite doubtless reflects sedimentary layering. Prior to thermal metamorphism by diabase intrusions, the sediment was probably a finely bedded, silty dolomite with lenses or layers of argillaceous limestone. The gradation along strike of a banded serpentine-talc rock to an almost structureless talc-clinozoisite rock might represent a facies change from a silty dolomite to an argillaceous limestone.

Since the original sedimentary texture seems to be preserved in the serpentinite, formation of serpentine and talc probably occurred by

local reactions among quartz, dolomite, and introduced water. An alternate possibility is the initial formation of serpentine, some of which later was converted to talc. However, the selective alteration of only minute discontinuous layers of serpentine to talc seems unlikely. The alternation of bands rich in serpentine with those rich in talc could be the effect of alternation in the original silty sediment of magnesium-rich (dolomite) bands with magnesium-poor (dolomitic limestone) bands. Reaction of quartz and dolomite to form serpentine or talc also yields calcite. In the banded serpentinite, calcite is absent or present only in minor amounts. The production of serpentine and talc in the manner postulated above would require an open system through which circulating solutions could remove calcite.

Origin of the Ash Creek Series

Source rocks. Table 6 presents a comparison and summary of the mineralogy, source rock, and type of metamorphism undergone by the various Ash Creek rocks. Their textural features and mineral assemblages indicate the nature of the parent sediment. The association and contact relations of these sediments in turn reflect the sedimentary environment of deposition. Prior to metamorphism, the Ash Creek rocks were layered sediments containing: (1) Relatively pure medium-grained quartz sandstone with thin lenses of silty dolomite; (2) fine-grained, feldspathic, argillaceous sandstone or siltstone; (3) shale and quartzose shale; and (4) siliceous dolomite and argillaceous limestone. The stratigraphic sequence of the sediments cannot be fully established. Contact relations, however, show that a fine-grained sandstone was gradationally interbedded between shales and that siliceous dolomite was in conformable contact with medium-grained sandstone.

The lithologic association and the contact relations do not denote a specific environment of deposition. However, the source rocks postulated for the Ash Creek series compare most favorably with an association of sediments formed in the epineritic environment of a stable shelf area (Krumbein et al., 1949). Characteristics of rocks formed in such an environment are: (1) Relatively pure quartz sandstone; (2) shales containing silty quartz; (3) limestone beds, with extensive secondary chert and dolomite; and (4) sandstone gradational directly to limestone.

Metamorphism. The metamorphic history of the Ash Creek series began with low-grade regional metamorphism followed by at least two and possibly three periods of thermal metamorphism. Low-grade regional metamorphism was apparently quite uniform; all regional metamorphic mineral assemblages are typical of the greenschist facies. Foliation is well developed in the finer grained rocks and is present to some degree in all but diopside quartzite and the serpentine-carbonate rocks. Petrofabric studies might reveal relict orientation in these rocks.

TABLE 6. COMPARISON OF THE DERIVATION OF THE ASH CREEK METASEDIMENTS

ROCK	MINERAL ASSEMBLAGE	SOURCE ROCK	TYPE OF METAMORPHISM	FACIES
Sericite phyllite	sericite-quartz-chlorite	quartzose shale	regional	muscovite-chlorite subfacies of greenschist facies
Andalusite-sericite schist	sericite-quartz	quartzose shale	regional	muscovite-chlorite subfacies of greenschist facies
	andalusite-biotite		contact	cordierite-antho-phyllite subfacies of amphibolite facies
Cordierite hornfels	cordierite-andalusite-biotite-muscovite-quartz chlorite sericite-chlorite (pinite)	shale	contact retrograde	cordierite-antho-phyllite subfacies of amphibolite facies
Spotted andalusite hornfels	chlorite-sericite-quartz-muscovite	shale	regional	muscovite-chlorite subfacies of greenschist facies
	andalusite-biotite		contact	cordierite-antho-phyllite subfacies of amphibolite facies
	chlorite-magnetite		retrograde	

TABLE 6. COMPARISON OF THE DERIVATION OF THE ASH CREEK METASEDIMENTS (continued)

ROCK	MINERAL ASSEMBLAGE	SOURCE ROCK	TYPE OF METAMORPHISM	FACIES
Biotite hornfels	biotite-muscovite-chlorite-quartz-orthoclase-oligoclase	fine-grained, feldspathic, argillaceous sandstone	regional	biotite-chlorite subfacies of greenschist facies
	andalusite-biotite		contact	cordierite-anthophyllite subfacies of amphibolite facies
Diopside quartzite	quartz-diopside-potash feldspar	medium-grained sandstone, with lenses of silty dolomite	contact	pyroxene hornfels facies
Serpentine-carbonate rocks	serpentine-talc-calcite-clinozoisite-chlorite-magnetite	siliceous dolomite, with minor argillaceous limestone	contact with hydrothermal alteration	pyroxene hornfels facies

In general, rocks in the largest xenolith contain assemblages indicative of the cordierite-anthophyllite subfacies, whereas those in smaller xenoliths or in xenoliths surrounded by metadiabase contain assemblages of the higher grade pyroxene hornfels facies.

Intrusion of anorthosite, diabase, or granite may have contributed to thermal metamorphism of the Ash Creek series. Anorthosite exposures are small and field relations do not conclusively date the intrusion of the anorthosite relative to the metamorphism of the sediments. The serpentine-carbonate rocks show the relative metamorphic effects of diabase and granite intrusions. Development of serpentine and talc is much more extensive in xenoliths completely enclosed in metadiabase than in those enclosed in granite. Further evidence that diabase was more effective than granite in thermal metamorphism is the development of andalusite-sericite schist near diabase intrusions in sericite phyllite. The margin of the largest xenolith, in direct contact with granite, shows no thermal effects markedly different from those at the central part of the xenolith. The absence of feldspar metacrysts and the very limited lit-par-lit injections suggest that the xenoliths were in contact with cooling granite magma for a limited period only, probably in the upper part of the pluton. In general, field evidence supports a hypothesis of thermal metamorphism produced primarily by the intrusion of diabase.

The presence of two grades of thermal metamorphism is explained by the relative sizes of the xenoliths and the amounts of cooling diabase nearby. Rocks containing assemblages of the pyroxene hornfels facies occur only in small xenoliths, which would receive a relatively large amount of heat from the comparatively larger mass of diabase. Rocks containing assemblages of the lower grade cordierite-anthophyllite subfacies occur in the largest xenolith, where the amount of diabase is relatively small compared with the mass of the metasediments. Metasediments in the largest xenolith not only attained a lower degree of thermal metamorphism, but spotted textures and nonequilibrium assemblages indicate that conditions of thermal metamorphism lasted for a relatively short time.

In conclusion, the events significant in the formation of the Ash Creek series are:

1. Deposition of a sequence of arenaceous, argillaceous, calcareous, and dolomitic sediments in an epineritic, stable shelf environment;
2. Low-grade regional metamorphism;
3. Low- to moderate-grade thermal metamorphism of sediments by Precambrian diabase;
4. Low-grade thermal metamorphism of diabase and possibly retrograde metamorphism of metasediments by Precambrian granite, accompanied by engulfment of masses of mixed diabase-metasediments in the upper part of the granitic batholith.

Comparison of the Bullard Peak and Ash Creek Series

Rocks of the Bullard Peak and Ash Creek series do not occur together; their main exposures are approximately 9 miles apart. Thus the establishment of their relative ages must be drawn from interpretation of their metamorphic histories and of the provenance of their source sediments. The depositional environment of the source rocks of the two series has been interpreted from evidence that is somewhat fragmental, but this evidence indicates that the respective source rocks were deposited in different environments.

Some of the features of the two series are compared in Table 1. Additional features that may aid in establishing their relative ages are:

	BULLARD PEAK SERIES	ASH CREEK SERIES
Depositional environment of parent sediments	infraneritic environment of unstable shelf area	epineritic environment of stable shelf area
Highest regional metamorphic facies	sillimanite-almandite subfacies of amphibolite facies	biotite-chlorite subfacies of greenschist facies

The following age relationships may be postulated:

1. The Bullard Peak and Ash Creek series developed during a single period of metamorphism. The regional metamorphic facies resulted from: (a) Regional variation in metamorphic intensity (i. e., temperature and pressure); or (b) variation in bulk composition of the parent sediments, as shown by Yoder's experimental data for the system $MgO - Al_2O_3 - SiO_2 - H_2O$ (Yoder, 1952).
2. The Bullard Peak series is older than the Ash Creek series. The parent sediments of the Bullard Peak series were deposited and later subjected to high-grade regional metamorphism. The Ash Creek sediments were then deposited, and both series were subjected to low-grade regional metamorphism.

The writer believes that the field and petrographic evidence favors a theory of separate periods of sedimentation and metamorphism for each series. It is possible for a complete sequence of regional metamorphism from the chlorite zone through the sillimanite zone to occur within the distance between the main exposures of the two series. For example, James (1955) mapped a sequence of chlorite-biotite-garnet-staurolite-sillimanite zones in the Precambrian rocks of the Upper Peninsula of Michigan. The maximum distance between the chlorite and the sillimanite zone is 27 miles; the minimum, 4 miles. In that area,

no gaps were found in the sequence of intensity zones. In the Big Burro Mountains, even the smaller xenoliths can be assigned with some degree of certainty to either the greenschist facies or the amphibolite facies. No rocks were observed in the entire area that conclusively indicate an intermediate degree of metamorphism. Biotite and garnet are abundant, but these may both occur in equilibrium with sillimanite. Staurolite and kyanite are conspicuously absent in the Big Burro Mountains. It seems unlikely that the wide variety of rocks found in the two series could have originated during a single period of regional metamorphism. The most probable sequence of Precambrian events that led to the formation of the metasedimentary rocks was: (1) Sedimentation of the Bullard Peak source rocks; (2) high-grade regional metamorphism; (3) sedimentation of the Ash Creek source rocks; (4) low-grade regional metamorphism; (5) intrusion of the complex Burro Mountains batholith into both series, the early stages of intrusion probably having been accompanied by local stress.

PRECAMBRIAN IGNEOUS ROCKS

ANORTHOSITE

Occurrence

Anorthosite crops out as small xenoliths enclosed in Precambrian granite, aplite, and metadiabase in secs. 9, 16, and 17, T. 18 S., R. 18 W. (pl. 12). About two dozen xenoliths, the largest of which is 450 feet long, are scattered through a mile-long, northeast-trending zone. Many other xenoliths, several feet long and too small to be mapped individually, occur with the larger ones. The only association of anorthosite and metadiabase occurs in SE¼ sec. 9, T. 18 S., R. 18 W., where a xenolith of anorthosite, a few feet long, is enclosed in metadiabase. Anorthosite was not found outside the general vicinity of Ash Creek.

In areas of low relief, anorthosite outcrops, which are characterized by angular blocks up to 3 feet long, stand several feet above the surrounding aplite (pl. 8A). Anorthosite that has been deeply trenched by tributaries of Ash Creek stands up in steep cliffs. Float blocks from 5 to 10 feet across are scattered on the slope below the cliffs and along the bottom of Ash Creek Canyon.

The weathered surface displays light-tan to chalky-white euhedral plagioclase crystals up to 4 inches long; they average from 1 to 2 inches. Dark green-brown hornblende and brown biotite are interstitial to the plagioclase. Weathering usually extends from 1 to 2 cm below the exposed surfaces. Fractures are stained light to dark red brown. On a fresh surface of typical anorthosite, dark-gray euhedral plagioclase, making up about 90 percent of the rock, shows well-developed multiple twinning. Some of the larger plagioclase crystals are zoned; the dark-gray irregular core merges into a lighter gray margin.

Aplite dikes have bleached the anorthosite up to 2 feet from their

contacts. In this zone the plagioclase is white, cream, or light green, and green biotite is more abundant than hornblende. Dark-green, inch-long actinolite blades are matted along fractures in the bleached zone.

Petrography

Under the microscope, the anorthosite can be seen to consist of about 85 percent labradorite and 10 percent hornblende, with accessory amounts of biotite, chlorite, magnetite, zircon, and apatite. The plagioclase, which is somewhat saussuritized, shows both albite and pericline twinning. Normal zoning is indicated by preferential alteration of the core and by slight differences in extinction between core and margin. In general, the plagioclase ranges in composition from An_{49} to An_{55}; the average is about An_{51-53}.

Enclosed within plagioclase grains are granular aggregates of green hornblende, brown biotite, and almost colorless chlorite. The shape of some of these aggregates strongly resembles euhedral pyroxene. Hornblende veins the surrounding plagioclase and in turn is veined by biotite; chlorite and magnetite replace biotite along (001).

Most of the hornblende is tan to dark olive; it occurs within plagioclase as single crystals about a millimeter across, or as coarser euhedral to subhedral aggregates interstitial to plagioclase blades. Tiny veinlets of hornblende cut into plagioclase laths that are in contact with coarse-grained hornblende. Irregular dark-brown biotite masses transect and replace some of the larger hornblende grains and also the tiny hornblende veinlets.

Magnetite euhedra, rimmed by chlorite or less commonly by zircon, are included in plagioclase; zircon occurs in both biotite and hornblende; and euhedral apatite is included in hornblende. Textural relations among the mafic minerals indicate a paragenetic sequence of: (1) Pyroxene(?); (2) hornblende; (3) biotite; and (4) chlorite and magnetite. The mode of the anorthosite (in percent) is:

Plagioclase (Ab_{47-49})	85
Hornblende	10
Biotite	4
Accessories (chlorite, magnetite, zircon, and apatite)	1
Total	100

The presence of essential amounts of mafic minerals and of labradorite places this rock in the gabbros (2312) of Johannsen's classification. Plagioclase is more abundant than in a normal gabbro, and the coarse texture is typical of some varieties of anorthosite. The rock is best described as a gabbroic anorthosite.

Origin

This rock may have been a border facies of a pure anorthosite, or a small intrusive of gabbroic anorthosite differentiated from a larger body of magma. The anorthosite was composed originally of labradorite and probably pyroxene. Thermal metamorphism by intrusion of metadiabase or of granite and associated aplite converted pyroxene to hornblende and biotite, bleached the plagioclase near the contact, and caused formation of minor actinolite. The alteration of biotite to chlorite and magnetite may have resulted from very late stages of thermal metamorphism or from later supergene alteration.

Age

No contact relations were found between anorthosite and the Ash Creek series. The anorthosite, however, shows none of the regional metamorphic effects found in the Ash Creek metasediments; so it is probably younger than the metasediments. The occurrence of anorthosite xenoliths in Precambrian metadiabase, granite, and aplite shows that the anorthosite is Precambrian in age and is the oldest of these igneous rocks.

Metadiabase

General Statement

The unit mapped as metadiabase contains rocks that have the typical ophitic texture of a diabase. Their mineral composition, however, is amphibole and plagioclase. Although the replacement of pyroxene may be caused by uralitization, evidence cited below indicates that thermal metamorphism was instrumental in the formation of this rock.

Metadiabase crops out as intrusive masses in rocks of the Ash Creek series, as isolated masses in Precambrian granite, and in xenoliths or roof pendants of Bullard Peak rocks that are surrounded by granite. In Ash Creek Canyon, the metadiabase is cut by Precambrian granite and thus is clearly older than the granite (pl. 8B). In Black Hawk Canyon, granite cuts metadiabase and shows chilled margins at the contact. The relative ages of other metadiabase masses are not clearly established by their contact relations with granite. Because of their general similarity in texture and mineralogy, they will be discussed as a unit.

Occurrence

In addition to the Ash Creek exposures, metadiabase also occurs as small masses, averaging 200 yards in length, at the following localities (pl. 1): (1) In Joe Harris Canyon, a quarter of a mile above its confluence with the Gila River; (2) in NE¼ sec. 24, T. 18 S., R. 18 W., between the northeast-trending fault and the Gila River; (3) near the head of Joe Harris Canyon, secs. 20 and 29, T. 18 S., R. 17 W., associated with rocks of the Bullard Peak series; (4) in a tributary of Rough Canyon, sec.

18, T. 18 S., R. 17 W.; (5) in Black Hawk Canyon, sec. 6, T. 19 S., R. 16 W.; (6) south of Eccles Canyon, sec. 19, T. 19 S., R. 16 W. The metadiabase in Black Hawk Canyon is the best exposed of these occurrences; it crops out as a roughly elliptical xenolith about 250 by 500 feet.

Petrography

Ash Creek Canyon and vicinity. Smoothly abraded surfaces of metadiabase in Ash Creek Canyon are light gray to dark blue or green gray; they display a fine-grained ophitic texture. Laths of light-gray plagioclase are set in a dark matrix. A few lenses, veinlets, and knots of secondary epidote are scattered through the metadiabase. In areas of low topographic relief and on the slopes of Ash Creek Canyon, metadiabase outcrops are characterized by irregular blocks several inches long. The surfaces of the weathered blocks and of the many fractures cutting them are heavily coated with a light to dark red-brown iron stain which masks the diabasic texture. A freshly broken surface shows about equal amounts of fine- to medium-grained gray-green plagioclase and green hornblende arranged in an ophitic texture. Some metadiabase is partially converted to an aggregate of coarse-grained, dark-green amphibole; other outcrops have weathered to a soft, dark-green mass showing only sericite, clay, limonite, and relict hornblende.

In thinsection, the metadiabase in the Ash Creek area shows essential andesine(Ab_{55-58}), hornblende, and magnetite and accessory amounts of biotite and apatite. The plagioclase occurs as randomly oriented laths about a millimeter long and as aggregates of subhedral grains. Alteration to saussurite partially masks both Carlsbad and albite twinning. Aggregates of unoriented brown hornblende anhedra, about 0.2 mm in cross-section, and a few irregular biotite plates fill the interstices between plagioclase laths. Biotite wraps magnetite grains and marginally replaces hornblende. Magnetite also occurs with apatite in poikilitic plagioclase and hornblende. The mode of this metadiabase is listed in Table 7.

TABLE 7. MODES OF PRECAMBRIAN METADIABASE
(In percent)

	(1)	(2)	(3)
Plagioclase (Ab_{51-58})	43	41	41
Hornblende	45	55	53
Magnetite	9	3	5
Accessories (biotite and apatite)	3	1	1
Totals	100	100	100

1. Ash Creek Canyon.
2. Black Hawk Canyon.
3. Head of Joe Harris Canyon.

The metadiabase that has been partially replaced by amphibole shows in thinsection a few relict laths of saussuritized and sericitized plagioclase(Ab_{51}) up to 0.5 mm in length. Coarse, ragged grains of green hornblende up to several centimeters in size enclose the plagioclase. Tiny, felted needles of green hornblende protrude into the plagioclase and coarse-grained hornblende. Magnetite occurs as a few skeletal crystals, about 0.5 mm across, set in felted and coarse-grained hornblende.

Black Hawk Canyon and other localities. Metadiabase that occurs outside the Ash Creek area crops out as lenslike, elliptical bodies or elongate irregular masses surrounded by Precambrian granite. The occurrences in Black Hawk Canyon and at the head of Joe Harris Canyon are typical of the coarse-grained metadiabase. A weathered surface shows an ophitic arrangement of plagioclase laths, up to a centimeter long, set in a matrix of equally large hornblende grains. Weathering has lightened the color of the plagioclase laths to a light tan, so that they stand out in marked contrast to the green-black hornblende background. On a fresh surface, the plagioclase is light gray green, and the hornblende is dark green. Hornblende makes up about 60 percent of the rock, and plagioclase about 40 percent. Thinsections of metadiabase from these localities show coarse, unoriented plagioclase(Ab_{55}) euhedra, some of which are centrally altered to saussurite and sericite. Hornblende occurs as large single anhedral crystals, about a centimeter across, forming a spongy network between plagioclase, and as unoriented aggregates of euhedral to subhedral grains less than a millimeter in size. Hornblende grains cut across and marginally replace plagioclase. The coarse-grained hornblende seems to have formed at the expense of smaller hornblende grains. Strongly poikilitic hornblende includes tiny grains of anhedral magnetite, euhedral apatite, and rarely anhedral plagioclase.

Accessory biotite occurs most commonly interstitial to granular hornblende. In one thinsection, veinlets of biotite cut across hornblende. Magnetite also occurs as anhedra interstitial to granular hornblende. Pennine occurs in small amounts with magnetite as rosettes in biotite.

Origin

Source rock. The relict textural features indicate that the rock was derived from a diabase. The composition of the plagioclase(Ab_{51-58}) is slightly more acid than is normal for rocks of the gabbro family. The size range of the plagioclase laths at the various occurrences suggests that some of the parent diabase originated in small dikes or sills, and some in small plugs or stocks. The present xenolithic occurrence precludes a determination of the original form, size, and structure of the occurrences outside the area of the Ash Creek metasediments.

Metamorphism. An average diabase contains essential labradorite, monoclinic pyroxene, and iron oxides. Subsequent uralitization of

pyroxene is accompanied commonly by saussuritization of plagioclase. Thinsections of metadiabase contain some saussuritized plagioclase, but they show hornblende replacing plagioclase and formation of coarse poikilitic hornblende apparently by aggregation of smaller hornblende grains. The optical properties of coarse- and fine-grained hornblende in a single thinsection are similar; therefore, the distinction among primary, uralitic, and metamorphic hornblende is not feasible. Any original pyroxene may have been uralitized to some degree, but probably much of the hornblende resulted from thermal and hydrothermal metamorphism. Evidence supporting metamorphism is: (1) The field occurrence of the metadiabase principally as xenoliths in granite; (2) the absence of pyroxene, presumably replaced by hornblende; (3) the replacement of plagioclase by hornblende; (4) the absence or subordination of lower temperature effects such as widespread saussuritization and development of chlorite; (5) the local development of biotite as a posthornblende mineral.

Harker (1939) points out that the characteristics of a thermally metamorphosed diabase are: (1) Conversion of augite to hornblende; (2) patches of deep-brown biotite closely associated with hornblende; and (3) hornblende veinlets traversing plagioclase. These characteristics are common in the metadiabase of this area.

In summary, the metadiabase is thought to have originated from a diabase containing plagioclase, magnetite, and mafic minerals consisting of pyroxene alone, or of pyroxene and uralite, or of pyroxene, primary hornblende, and uralite. Thermal metamorphism and solutions accompanying the intrusion of granite caused extensive replacement of pyroxene by hornblende. In some cases, hornblende replaced plagioclase as well. The development of minor biotite around primary magnetite, chiefly at the expense of hornblende, may indicate the possible addition of minor potassium.

Age. The metadiabase in Ash Creek and Black Hawk Canyons is older than the granite. The similarity in texture, mineralogy, occurrence, and degree of metamorphism between this metadiabase and occurrences where contact relations are not clear suggests a similar age for all the metadiabase. At least some, and probably all, of the metadiabase is Precambrian in age, younger than the Ash Creek series and older than the Burro Mountains granite.

Granite and Related Rocks

General Statement

The most widespread rocks in the Burro Mountains are those that make up the complex Burro Mountains batholith. Granite is by far the most abundant rock, but at least five varieties of granite and several varieties of granodiorite and tonalite occur within the batholith.

Paige (1916) mapped part of the Burro Mountains batholith, where

it crops out in Silver City quadrangle. The Precambrian age of the batholith is well established at two small exposures, one northwest and another southeast of Silver City, where granite and included metamorphic rocks are overlain by the Upper Cambrian Bliss sandstone. Paige (1916) mapped the Precambrian rocks as a single unit. A fine- to medium-grained biotite granite is the most widespread Precambrian rock in Silver City quadrangle.

Gillerman (1951) distinguished the following varieties of granite in the vicinity of various fluorite deposits in the Big Burro Mountains: (1) Coarse-grained hornblende-biotite granite; (2) medium-grained biotite granite, locally porphyritic (most widespread); (3) alaskite; (4) porphyritic granite; and (5) pegmatite and aplite. Concerning the genetic relationships of these rocks, Gillerman (1951) states:

> The decision as to whether these represent separate intrusions or merely differentiates of the magma before or during intrusion must await additional mapping. At least one body—a coarse-grained . . . hornblende-biotite granite . . . —definitely represents a distinct intrusion and is probably the oldest of the granites.

Gillerman and Whitebread (1956) mapped on a scale of 1:6,000 about 2½ square miles of the area surrounding the Black Hawk mining district. They reported the following sequence of Precambrian igneous rocks (in order of decreasing age): (1) Monzonite and quartz monzonite (migmatized sediments?); (2) biotite-hornblende quartz diorite gneiss—most abundant rock in the Black Hawk district and a widespread phase of the Burro Mountains batholith; (3) biotite quartz diorite; (4) biotite-hornblende diorite; (5) biotite syenite; (6) biotite granite—similar to that which constitutes most of the Burro Mountains batholith south and west of the Black Hawk district.

The complexity of the Burro Mountains batholith is well shown in the detail mapping by Gillerman and Whitebread (1956, pl. 14). Differentiation of the various rock types into similar mappable units is not possible at the scale (1:31,680) on which the area of this report was mapped. The Precambrian rocks that make up the batholith were mapped as a single unit. The various members of this unit will be discussed in the following groups, which are arranged approximately in order of decreasing age: (1) Medium- to coarse-grained biotite tonalite, foliated and locally porphyritic; (2) medium- to coarse-grained hornblende-biotite granite, with porphyritic and fine-grained facies; (3) medium- to coarse-grained biotite granodiorite, locally porphyritic and/or foliated; (4) orbicular rock; (5) pegmatite; (6) aplite. Granite is by far the most abundant of these rocks in this area; tonalite, pegmatite, and aplite are locally significant. The remaining types make up only a small percentage of the batholith. The petrology of the migmatites related to the Burro Mountains batholith is discussed with the Bullard Peak metamorphic series.

Tonalite

Occurrence. Tonalite crops out along the western flank of the Big Burro Mountains in secs. 10, 11, and 15, T. 19 S., R. 17 W., where it has been intruded into schists and gneisses of the Bullard Peak series in a lit-par-lit manner (pl. 1). Small xenoliths and schlieren of schist and gneiss are common. Tonalite also occurs northeast of Bullard Peak and in the Black Hawk mining district. Contact relations with granite are generally obscure. However, a tonalite-granite contact in a tributary to Bullard Peak Canyon, sec. 11, T. 19 S., R. 17 W., suggests that tonalite has been intruded by granite. The tonalite is probably an early phase of the batholith, older than the granite, but genetically related to it.

Outcrops of tonalite are generally rounded and weathered to shades of brown, tan, or red. Feldspar phenocrysts up to an inch long stand out from the coarse-grained matrix to form a knobby weathered surface. Locally, oriented biotite plates give the rock a well-developed foliation.

Petrography. A freshly broken surface shows pink-gray phenocrysts of plagioclase set in a medium- to coarse-grained matrix of biotite, quartz, and plagioclase. The mode of the tonalite from the west flank of the mountains is (in percent):

Quartz	27
Microcline	3
Oligoclase-andesine (Ab_{74-64})	47
Biotite	22
Accessories	1
Total	100

In thinsection, andesine(Ab_{64}) appears as subhedra, up to 2 cm long, that show Carlsbad, albite, and pericline twinning. Some of the grains are selectively altered to sericite along alternate albite-twin lamellae. A few grains show bent and twisted lamellae. A medium-grained aggregate of biotite, oligoclase(Ab_{74}), quartz, and minor microcline microperthite encloses the larger andesine subhedra. Locally the matrix plagioclase is intergrown with quartz to form myrmekite. Biotite is molded between anhedra of quartz and plagioclase. A foliation is apparent in the orientation of biotite flakes and a very crude lenticular arrangement of quartz anhedra, some of which show undulatory extinction. Apatite euhedra occur along quartz and feldspar boundaries and are included in biotite; zircon is included in andesine and biotite. Magnetite occurs as euhedra in biotite and as irregular interstitial masses, a few of which contain pyrite cores. Textural evidence indicates the following sequence of mineral formation: (1) Early accessories—apatite, zircon, some magnetite; (2) andesine; (3) biotite; and (4) oligoclase, myrmekite, microcline, and quartz.

This tonalite is apparently similar in texture and mineralogy to the

quartz diorite gneiss described by Gillerman and Whitebread (1956) from the Black Hawk district. They interpreted the foliation as a primary flow structure. The orientation of biotite flakes in tonalite from the western flank of the Big Burro Mountains may be a primary flow foliation. However, the bent twin lamellae and the lenticular arrangement of quartz suggest that stress prevailed during the late stages of crystallization and possibly after solidification.

Granite

Occurrence. Granite underlies about 50 square miles in the northern and eastern parts of this area. It intrudes Precambrian metamorphic rocks and is intruded by Laramide stocks and dikes. Along the northern edge of the area, Cretaceous sediments and Tertiary volcanic rocks overlie the granite. In Ash Creek Canyon, Burro Springs Canyon, and a tributary to Joe Harris Canyon, the granite is faulted against Gila conglomerate (pl. 1).

Petrography. In the Big Burro Mountains, the granite crops out as steep ridges flanked by talus slopes. The granite is generally less resistant to erosion than the Bullard Peak metamorphic rocks, which stand in relief above it. North and northwest of the Big Burro Mountains, where topographic relief is low to moderate, the granite crops out as rounded mounds or low ridges. The "Redrock," after which the community of Redrock is named, is a rounded knob of granite deeply weathered to a brick-red color. Gentle slopes and canyon beds underlain by granite are usually veneered with a gruss of partly decomposed granite fragments.

The granite commonly weathers to spheroids, the sizes of which are largely dependent upon the spacing of joints and fractures (pl. 8C). Irregular fractures are more abundant than joints. Fracture surfaces are commonly coated with manganese oxides; the thickness of the coating ranges from thin films to several inches. Calcite and chert fillings are rare. Joint sets or systems locally control drainages in Jacks Canyon from one-quarter to one-half of a mile north of the Gila River and in a tributary to Black Hawk Canyon.

Contacts with the Ash Creek xenoliths and with some of the feldspar and hornblende gneisses of the Bullard Peak series are generally sharp. Mica schists, quartz-feldspar gneisses, and some of the hornblende gneisses have been intruded in a lit-par-lit manner, so that the granite grades through migmatite to schist and gneiss.

Deeply weathered surfaces, usually in areas of low relief, are brick red or shades of red, tan, and brown. Locally the feldspars are almost completely kaolinized, and the mafic minerals are weathered to chlorite. On a fresh surface, the feldspars are white, light pink, or pink gray. Along faults, the granite is stained by hematite and sheared, brecciated, or silicified.

The texture of the granite varies from fine to coarse equigranular; most commonly it is medium to coarse. Microcline euhedra, as much as 2 inches long, appear in a local porphyritic phase. Parallel orientation of biotite flakes, and less commonly of microcline phenocrysts, gives the rock a crude foliation. Hornblende needles are commonly oriented in the plane of foliation but show no preferred linear arrangement.

Rosiwal analyses of thinsections of granite give the following percentage ranges in essential mineral composition:

Quartz	15-25
Microcline	35-55
Oligoclase	10-30
Hornblende	0-10
Biotite	0-10

Although the essential mineral composition of the various granites is similar, the texture is variable. In general, two textural varieties can be distinguished: (1) Equigranular, fine- to coarse-grained; and (2) coarse-grained porphyritic.

In the equigranular granite, microcline is subhedral to anhedral and shows interlocking boundaries with oligoclase and quartz subhedra and anhedra. Generally, subhedra of microcline microperthite, as much as 2.5 cm long, include small amounts of quartz, oligoclase, biotite, hornblende, or accessory minerals; biotite is the most common inclusion. A few microcline anhedra show marginal granophyre or quartz inclusions zonally arranged. Carlsbad and gridiron twinning, a crude perthitic texture, and a few irregular patches of kaolinite and sericite characterize the microcline. Oligoclase(Ab_{69-74}) occurs rarely as euhedra and commonly as subhedra or anhedra up to a centimeter long. Uncommonly it shows normal zoning, with cores strongly altered to kaolinite and sericite. Some plagioclase is marginally replaced by microcline. Both Carlsbad and albite twinning are common. Biotite and hornblende occur singly or together as clusters of subhedra that are interstitial to quartz and plagioclase. Olive to dark-brown biotite is partially replaced along (001) by pennine and magnetite. Where biotite occurs with hornblende, it wraps or replaces the hornblende. Hornblende is replaced along (110) and in irregular patches by pennine and magnetite.

Apatite, zircon, magnetite, ilmenite, sphene, and epidote occur as accessory minerals generally concentrated in the hornblende-biotite clusters. Euhedra of apatite, magnetite, zircon, and sphene are included in biotite. Zircon euhedra also occur randomly or zonally included in magnetite. Leucoxene coats sphene euhedra and irregular ilmenite masses that occur interstitial to quartz and feldspar. Epidote, the least abundant of the accessories, occurs in biotite as anhedra. One thinsection of medium-grained granite from the ridge south of Eccles Canyon contains epidote and dark-brown, pleochroic allanite included in biotite.

The porphyritic granite differs from the equigranular varieties only in the size and arrangement of the microcline. Although microcline microperthite phenocrysts are as much as 2 inches long, they are usually subhedra that have interlocked, irregular, or even denticulate boundaries with the enclosing quartz-oligoclase-microcline matrix. The phenocrysts commonly include biotite, quartz, oligoclase, and accessory minerals.

Modes of the several varieties of granite are listed in Table 8. The generalized sequence of crystallization as indicated by textural evidence is: (1) Early accessories—apatite, zircon, sphene, magnetite, and ilmenite; (2) hornblende; (3) biotite; and (4) oligoclase, microcline, and quartz. Final crystallization included the growth of microcline by development of granophyre, minor replacement of oligoclase by microcline, the crystallization of interstitial grains of quartz, and development of exsolution perthite.

TABLE 8. MODES OF PRECAMBRIAN GRANITE

(In percent)

	(1)	(2)	(3)	(4)
Quartz	15	26	23	23
Microcline	42	35	57	42
Oligoclase (Ab_{69-74})	29	22	12	28
Hornblende	3	9	6	—
Biotite	9	5	—	5
Accessories	2	3	2	2
Totals	100	100	100	100

1. Wild Horse Canyon, sec. 12, T. 18 S., R. 17 W.
2. Northeast of Burro Springs Canyon, sec. 20, T. 19 S., R. 16 W.
3. Ash Creek Canyon, sec. 16, T. 18 S., R. 18 W.
4. Southeast of Eccles Canyon, sec. 19, T. 19 S., R. 16 W.

The local occurrence of the porphyritic granite and its apparent gradation into coarse equigranular granite may be the result of local growth of phenocrysts late in the crystallization history of the magma. Wahlstrom (1950) states:

> Concentrations of hyperfusables may induce the growth of large crystals by local solution and transfer or by replacement of earlier-formed minerals. Phenocrysts formed in this manner generally have ragged outlines and may contain inclusions of the replaced minerals.

The irregular outline of some of the microcline phenocrysts and the abundance of inclusions support this manner of formation. In only one thinsection, however, was microcline seen to replace oligoclase.

Granodiorite

Occurrence. The granodiorite (Johannsen 227), which occurs locally throughout the Big Burro Mountains, is a gradational facies of the

granite. The largest mass is a sill, about a mile long and less than a quarter of a mile wide, that has been intruded into the Bullard Peak series on the northwest end of the Big Burro Mountains, in sec. 35, T. 18 S., R. 17 W. (pl. 1).

Petrography. The granodiorite is similar in outcrop, weathering characteristics, and texture to the coarse-grained biotite granite described above. It differs from the granite by having more biotite and oligoclase and less microcline. The mode of granodiorite from Bullard Peak Canyon, NE¼ sec. 2, T. 19 S., R. 17 W., as measured from thin-section is (in percent):

Quartz	21
Microcline	20
Oligoclase (Ab_{72})	48
Biotite	10
Accessories	1
Total	100

Microscopically, the granodiorite is made up of coarse subhedra, up to 2 cm long, of microcline and oligoclase enclosed in an interlocked matrix of oligoclase, myrmekite, and quartz. Biotite clusters and a few hornblende blades partly replaced by biotite are molded between feldspar and quartz. Accessory minerals are apatite, sphene, zircon, magnetite, and epidote.

Orbicular Rock

Occurrence. A small xenolith of banded migmatite containing orbicules in layers and in an irregularly shaped mass crops out in NW¼ sec. 19, T. 19 S., R. 16 W. The entire exposure is only a single spur about 20 feet long that projects from the southeast slope of Eccles Canyon into the canyon bed (pl. 9A). Coarse-grained granite is exposed at the north end of the spur, in dikes that transect the orbicular rock, and on the southeast slope of Eccles Canyon. In the general area to the north of this occurrence, xenoliths of quartz-feldspar and hornblende gneisses are enclosed in the coarse-grained granite. The migmatite (pl. 9B) is made up of diffuse bands containing varying amounts of quartz, feldspar, hornblende, and biotite. Some of the bands, which are as much as 6 inches thick, are made up of unoriented biotite flakes and varying amounts of hornblende. The light bands approach a granite in texture and composition. The banding strikes N. 20° W. and dips 60° NE.

The orbicules are arranged in two 8-inch layers that are parallel to the banding in the migmatite (pl. 9B) and in an irregular cluster near the north end of the exposure (pl. 9C). The spheroidal to ellipsoidal orbicules range in diameter from 0.5 to 4.0 inches; a few are irregularly shaped, with angular corners. Most of the orbicules have a coarse-grained hornblende core, from 0.5 to 1.0 inch in diameter, and a fine-

grained plagioclase-biotite rim that ranges in thickness from 0.1 to 1.0 inch. A few of the larger orbicules have thick rims made up of alternating biotite-rich and plagioclase-rich concentric zones. In some rims, biotite or rarely hornblende is radially arranged around the core. A coarse-grained matrix of quartz, plagioclase, microcline, hornblende, and biotite encloses the orbicules. Scattered in the matrix with the orbicules are irregularly shaped lenses, from 1.0 to 5.0 inches long and 0.5 to 2.0 inches thick, that are made up of a fine-grained aggregate of plagioclase and biotite.

Petrography. Microscopic examination of the orbicule cores reveals two textural varieties. Most abundant is a polycrystalline aggregate of hornblende and biotite; a few cores are single crystals of hornblende.

In the polycrystalline cores, biotite replaces hornblende along (110) and in irregular patches; dark-green chlorite partly replaces biotite along (001). Accessory quartz is molded along hornblende grain boundaries. In one thinsection, a symplectic intergrowth was observed between quartz and biotite. Accessory amounts of euhedral sphene and magnetite are enclosed by hornblende and biotite. The sequence of crystallization of essential constituents is thus hornblende, biotite, and quartz. The mode of a typical core is (in percent):

Hornblende	85
Biotite	10
Quartz	4
Accessories	1
Total	100

The rims appear in thinsection as a fine-grained aggregate of oligoclase(Ab_{69-72}) anhedra, about 0.5 mm across, with biotite plates molded between and enclosed by oligoclase grains. The oligoclase is normally zoned and is slightly altered along alternate albite twin lamellae to kaolinite and sericite. Biotite is included in oligoclase, and transects it as well; hence the two minerals probably crystallized at the same time.

The annular nature of the rims, as seen in thinsections, makes a measurement of the mode by a linear method impractical. The method described by Mandarino (1956) was modified by offcentering a universal stage so that the axis of rotation of the inner circle coincided with the center of the orbicule core. The thinsection and universal stage were arranged so that as the inner circle was rotated, only the rim passed through the field of view. Point-count traverses were made at angular increments of 1 degree and at radii differing by 1 mm. The mode of the rim is 72 percent oligoclase and 28 percent biotite.

The fine-grained lenses appear in thinsection as an anhedral-granular aggregate of 71 percent andesine(Ab_{68}) and 28 percent biotite. Biotite plates are included by andesine and lie along andesine grain

boundaries. There is a striking similarity between these lenses and the orbicule rims.

Variation in the mineral content of the matrix is so great that a single thinsection gives no real indication of the general composition. It is made up of the following minerals; the amounts shown (in percent) are the ranges of modes measured from three thinsections:

Quartz	10-20
Microcline	5-10
Plagioclase (Ab_{69-76})	45-55
Hornblende	10-25
Biotite	10-25
Accessories	1-2

Quartz, oligoclase, hornblende, and biotite are medium to coarse grained and arranged in an equigranular anhedral texture. However, granular patches of a single constituent are locally several centimeters across. Oligoclase is normally zoned, with cores of Ab_{69} and margins of Ab_{76}; the average is Ab_{71-72}. Sericite and kaolinite selectively replace cores and alternate albite twin lamellae. Biotite and hornblende occur singly or together, with biotite replacing hornblende. Quartz anhedra are generally included within feldspars or interstitial to them. Microcline commonly occurs as subhedra or anhedra interlocked with oligoclase. Sphene, apatite, and magnetite euhedra are included in biotite and hornblende; apatite is also included in oligoclase. In one thinsection, magnetite was included in zircon; in another, magnetite was included in leucoxene-coated sphene. Epidote veins hornblende and plagioclase and occurs as anhedra with sphene enclosed in biotite.

The early formation of the accessory minerals is shown by their euhedral shape and their enclosure in biotite and hornblende. Hornblende is replaced by younger biotite. The feldspars appear to have crystallized together with quartz. The crystallization sequence of the matrix is: (1) Early accessories—sphene, apatite, magnetite, zircon; (2) hornblende; (3) biotite; (4) oligoclase, microcline, quartz; and (5) epidote veinlets. The texture and mineral composition of the matrix indicate crystallization from a calc-alkaline granitic magma.

The nature of the sharp contact between the cores and the rims suggests that the oligoclase-biotite rim formed at the expense of hornblende in the core. Contacts between rims and matrix are commonly gradational. The spatial relationship of the cores, rims, and matrix suggests that the cores are the oldest and the matrix the youngest.

Origin. The orbicular structure is one of the least common but most interesting features of igneous petrology. Elaborate systems of classification based on mineralogy, chemical composition, texture, structure, and genesis have been devised (von Chrustschoff, 1894; Loewinson-Lessing

and Vorobjeva, 1929). However, most orbicular rocks fall into one of two categories: (1) The orbicules and the matrix are essentially of the same composition; (2) the composition of the orbicules differs from that of the matrix.

The orbicular rock from the Big Burro Mountains is of the second type. Johannsen (1937) states that orbicules of this type are more abundant than those of the first type. The orbicular structure has been described in granites, granodiorites, diorites, and gabbros; the more acid types are apparently most common.

The uncommon nature of orbicular rocks and their textural and mineralogical variations have led to numerous theories of origin, which invoke a wide variety of processes. Many of these theories are summarized in the works of Sederholm (1928), Johannsen (1937), and Ray (1952). In general, orbicular rocks have been explained by various modifications of three theories: (1) Direct crystallization from a magma; (2) reaction between a magma and xenoliths, either foreign or cognate; (3) metasomatism or migmatization of a preexisting rock.

The similarity between some of the hornblende cores in the orbicules and the xenoliths of hornblende gneiss in the surrounding area suggests the second of these theories as a feasible explanation for the formation of orbicules in the Big Burro Mountains.

Bowen (1928) related the assimilation of xenoliths by a magma to his reaction series. If a magma incorporates a xenolith composed of minerals with which the magma is supersaturated (i.e., a xenolith more basic than the saturated phase), the xenolith is not dissolved, but is reacted upon and converted to minerals with which the magma is saturated. Thus (Bowen, 1928):

> . . . a granitic magma saturated with biotite cannot dissolve olivine, pyroxene, or amphibole, but can react with them to convert them into biotite, the phase with which it is saturated. . . . The reaction is not a simple subtraction from the liquid of the material necessary for this transformation, but some precipitation from the liquid itself is involved.

If, however, a magma encloses a xenolith containing minerals with which the magma is not saturated (i.e., more acid than the saturated phase), the xenolith is dissolved; the necessary heat may be supplied by crystallization of the saturated phase.

The layered biotite-hornblende rock in which the orbicules in the Big Burro Mountains occur was probably a xenolith of hornblende gneiss or amphibolite that was enclosed in granitic magma and modified by reaction with the magma, as described above. The layering may be a relict structure in the xenolith. The hornblende gneiss may have been crushed and fractured marginally and along the layering either before or during intrusion by granite. The angularity of some of the hornblende cores tends to support this view. Reaction of these hornblende fragments with the magma could have resulted in recrystallization of

the fragments and the development of reaction rims of oligoclase and biotite. In this reaction, the resorbed hornblende could contribute Ca and Na to the oligoclase, and Mg and Fe to the biotite; the magma could contribute Ca and Na to the oligoclase, and K to the biotite. The conversion of hornblende to biotite in this manner could locally lower the amount of K in the magma and thus might explain the small amount of microcline in the matrix that surrounds the orbicules.

The lensoid biotite-oligoclase aggregates that are also included in the matrix may have originated in two ways. These lenses may represent the complete reaction between hornblende gneiss fragments and granite magma, or they may be feldspar-rich layers in the hornblende gneiss which, because of their composition, did not react with the magma.

One problem concerning the genesis of the orbicular rocks in the Big Burro Mountains that remains unanswered is the extreme rarity of these rocks. Their petrology and occurrence support a formation by reaction between granite magma and xenoliths of hornblende gneiss. Hornblende gneiss xenoliths are abundant in the Burro Mountains granite, but only one occurrence of orbicular rocks was found in the entire area. The formation of the orbicular structure must require some unusual factor or combination of factors concerning temperature, pressure, composition of the magma, viscosity of the magma, or composition of the xenolith. Thermal metamorphic effects on the Ash Creek and Bullard Peak rocks suggest that the temperature of the magma increased from the northwest to the southeast. The orbicular rocks occur in the southeast and when enclosed by granite magma were probably raised to a higher temperature and subjected to a higher pressure than many of the other xenoliths. This difference in position in the batholith, and the likelihood of difference in temperature and pressure, are apparently the only differences between the environment of the orbicular rocks and that of the unaltered hornblende gneiss xenoliths.

Pegmatite

Occurrence. Lenses, dikes, and irregular masses of pegmatite occur, in the eastern part of the area of this report, in Precambrian granite and metamorphic rocks. Pegmatites are particularly abundant in the general area of Eccles, Brushy, Kelley Chimney, and Stein Canyons. Few pegmatites occur in the northeastern part of the area; practically none occurs in the northwest.

Lenslike bodies of pegmatite are usually as much as a few feet wide and a few tens of feet long. In the metamorphic rocks, some of these lenses are parallel to the foliation; others that cut across the foliation commonly have apophyses extending into the country rock parallel to the foliation. Pegmatite dikes range in thickness from a few inches to 50 or more feet. The largest of these dikes, which occur along the western flank of the Big Burro Mountains, north of the Redrock-Silver City road, strike N. 30°-55° W. and dip 10°-40° NE. Some of the pegma-

tite masses are irregular in shape and thus can be considered neither as true dikes nor lenses.

Structure. Most of the pegmatites are unzoned; none contains replacement units; and all are of simple mineralogy, having but a few uncommon accessories sparsely distributed. The most abundant variety of pegmatite is a coarse-grained rock, extremely variable in grain size, that consists of quartz, microcline, minor plagioclase, and accessory amounts of muscovite and biotite. Small aplite dikes and a few quartz veins cut some of the pegmatites. Several of the small pegmatites, notably those in a tributary to Black Hawk Canyon and near the head of Brushy Canyon, have a border zone, less than half an inch thick, of quartz, microcline, and oligoclase and a core of coarsely intergrown quartz and microcline. A few pegmatites along the mountain flank have a quartz-microcline-oligoclase border zone, a quartz-microcline-muscovite wall zone, and a lensoid quartz core.

Mineralogy. All the pegmatites observed are of granitic composition. Most consist of quartz, microcline, and plagioclase, with minor amounts of accessory minerals (table 9).

TABLE 9. MINERALS IN PEGMATITES IN THE BIG BURRO MOUNTAINS

Quartz	Garnet
Microcline	Magnetite
Oligoclase	Molybdenite
Muscovite	Allanite
Biotite	Opal

Quartz. Quartz is an abundant constituent in all the pegmatites. It occurs as coarse anhedra to subhedra usually intergrown with microcline. Most of the quartz is milky and is cut by numerous irregular hematite-stained fractures. The quartz core of a pegmatite on the south slope of the ridge north of Eccles Canyon has a definite bluish cast; a pegmatite south of Eccles Canyon contains smoky quartz. In some of the larger unzoned pegmatites, quartz is graphically intergrown with large microcline crystals.

Feldspar. Microcline, by far the most abundant of the feldspars, varies in color through shades of white, cream, or pink. Most of it is megascopically perthitic and occurs as medium to coarse subhedra intergrown with quartz and oligoclase in the unzoned pegmatites. In zoned pegmatites, it occurs in the border zone with oligoclase and quartz, in the wall zone with quartz, and rarely in the core. Microcline euhedra are not common; a few, up to 2 inches long, occur in quartz in the intermediate zone of the pegmatites in Kelley Chimney Canyon.

The pegmatitic plagioclase is oligoclase. A thinsection from an unzoned pegmatite in Eccles Canyon shows oligoclase(Ab_{87}) euhedra and subhedra up to a centimeter long enclosed by and intergrown with microcline microperthite and quartz.

Muscovite. Small books of muscovite, about half an inch across and less than an inch thick, occur as accessory constituents of many of the unzoned pegmatites. On the west flank of the Big Burro Mountains, in the wall zone of a pegmatite lens, books of silvery-white muscovite, up to an inch across, are intergrown with quartz and microcline. On the ridge between Black Hawk and Saddle Rock Canyons, just east of the mapped area, books of limonite-stained muscovite, up to 5 inches across and less than an inch thick, are scattered in debris from a prospect trench. Contact relations are obscured by the debris, but the muscovite apparently occurs with coarse quartz and microcline in the wall zone of a large irregular pegmatite.

Biotite. Biotite is less abundant than muscovite in the Burro Mountains pegmatites. It occurs with microcline and quartz as an accessory mineral in a few unzoned pegmatites and is commonly the only mica present. An unzoned pegmatite in Eccles Canyon, about a mile above the confluence of Eccles and Burro Springs Canyons, contains green-black biotite as twisted, ragged plates, up to an inch across, that are intergrown with coarse-grained quartz, microcline, and graphic granite. The biotite locally makes up about 5 percent of the pegmatite.

Magnetite. Magnetite, one of the least abundant of the pegmatite minerals, occurs in some of the larger unzoned pegmatites. Irregular masses of granular magnetite, up to 3 cm long, are enclosed in fine-grained, limonite-stained graphic granite in a pegmatite in Eccles Canyon. The magnetite, which is altered to hematite marginally and along cleavages, makes up about 15 percent of the pegmatite locally.

Garnet. Garnet was observed in Eccles Canyon in an unzoned pegmatite that is cut by small pegmatite and aplite dikes and by quartz veins. Garnet euhedra, about 2 mm in diameter, form a discontinuous border on both sides of a centimeter-thick dikelet of pegmatite that cuts the main pegmatite dike. The small dike with which the garnets are associated consists of medium-grained microcline and quartz subhedra. The garnet is dark red on a fresh surface, but weathers to a dark brown and is commonly surrounded by black manganese stains.

In thinsection, the light pink-tan garnet appears as euhedra and as aggregates of subhedra that enclose small amounts of quartz, microcline, allanite, and zircon(?). The index of refraction of the garnet is $1.801 \pm .002$, and the density, measured on a Berman density balance, is 4.16. These properties indicate a garnet that is made up of the following molecular percentages (Kennedy, 1947, fig. 9g):

Spessartite ($Mn_3Al_2Si_3O_{12}$)	65
Almandite ($Fe_3Al_2Si_3O_{12}$)	25
Grossularite ($Ca_3Al_2Si_3O_{12}$)	10

Molybdenite. Molybdenite plates, up to half an inch across, occur with quartz, microcline, and biotite in an unzoned pegmatite in Eccles Canyon. About two handfuls of molybdenite were found in the blast

debris from a prospect pit, but none could be found in place. Apparently the mineral occurred in a small lens as a primary sulfide accessory to the pegmatite, or else it was related to a small quartz vein that transects the pegmatite. This is the only occurrence of molybdenite seen by the writer in the area.

Allanite. Allanite was identified in a thinsection from the garnetiferous pegmatite in Eccles Canyon described above. The allanite occurs as euhedra, less than 0.1 mm long, enclosed in garnet. A single subhedral grain about a millimeter long was noted in microcline microperthite.

Opal. Hyalite that fluoresces a brilliant yellow green coats fractures in many of the pegmatites. The mineral is significant because it is frequently mistaken for scheelite by prospectors. Megascopically, the opal appears as irregularly distributed, light-cream to buff crusts that are rarely more than 0.5 mm thick. Under the microscope, crushed material has a characteristic conchoidal fracture, is colorless, and contains abundant brown to black inclusions. The index of refraction is $1.458 \pm .002$. The fluorescence of hyalite is commonly due to trace amounts of uranium in the form of UO_2^{++} (Pringsheim and Vogel, 1943).

Aplite

Occurrence. Aplite occurs as a gradational facies of medium- and coarse-grained granite pegmatites and as individual dikes that have been intruded into Precambrian metamorphic rocks, granite, and pegmatites. The aplite dikes are generally a few feet thick; a few are as much as 50 feet thick. Aplite and pegmatite occur in the same general areas; a notable exception is in the Ash Creek area, where pegmatites are rare but aplite dikes are abundant.

Petrography. Weathering converts the surface of aplite to dark pink, red, or brown; a freshly broken surface is pink to pink gray. Pink microcline, white to light-gray plagioclase, and colorless to light-gray quartz are arranged in a fine equigranular texture.

Under the microscope, granite aplite appears as an aggregate of interlocking subhedra and anhedra. The microcline is only slightly altered to kaolinite and sericite, and is not as perthitic as the microcline in the coarser grained Precambrian igneous rocks. Oligoclase(Ab_{89}), less abundant than microcline, shows albite twinning and is partly altered to kaolinite and sericite. A few irregular patches of granophyre are interstitial to quartz and the other feldspars. Ragged plates of biotite and muscovite include quartz and feldspar anhedra and accessory amounts of euhedral magnetite. Magnetite also is included in chlorite that has replaced biotite. The texture of the aplite indicates almost simultaneous crystallization of the essential minerals.

A west-trending dike, about 75 feet thick, in Little Bear Canyon, secs. 9 and 10, T. 18 S., R. 17 W., contains plagioclase that is more abundant and more calcic than that in the granitic aplites; the rock is thus a leucogranodiorite (Johannsen 127). Thinsections show microcline

microperthite anhedra selectively altered to sericite along gridiron twin lamellae. Quartz is included in microcline and plagioclase and is intergrown granophyrically with microcline in small anhedral units. Andesine(Ab_{66}) subhedra and anhedra are interlocked with quartz and microcline. Muscovite and biotite, commonly intergrown along (001), occur along grain boundaries of quartz and feldspar. Magnetite euhedra are enclosed in biotite; chlorite and magnetite locally replace biotite. Textural evidence indicates the following sequence of crystallization: (1) Andesine; (2) microcline, granophyre, and quartz; (3) biotite and muscovite; and (4) quartz.

The mode, measured from thinsection, is (in percent):

Quartz	33
Microcline microperthite	30
Andesine (Ab_{66})	32
Biotite and magnetite	3
Muscovite	2
Total	100

The leucogranodiorite dike is probably a late phase of the Precambrian Burro Mountains batholith and is related to the granitic aplite dikes.

Age Relations in the Burro Mountains Batholith

Age relationships among the various rocks that make up the Precambrian Burro Mountains batholith are not well established. Some of the rock types are not found in contact with each other; some of the critical contacts are obscured by talus, vegetation, or regolith. However, the following field and petrographic evidence gives some indication of the genetic history of the batholith:

1. Tonalite is the only rock of this group that shows stress metamorphism.
2. The coarse-grained granite that is the dominant rock type of the batholith has been intruded into tonalite and into the orbicular rock, and has been intruded by fine-grained granite, pegmatite, and aplite.
3. Coarse-grained granite grades locally into porphyritic granite, into coarse-grained granodiorite, and, around xenoliths, into fine-grained granite.
4. The several textural varieties of granite show similarities in essential mineralogy, particularly in species and amount of mafic constituents and in composition and zoning of plagioclase.

This evidence suggests that the tonalite is the oldest of these rocks and was probably a separate intrusion. Some of the textural variation in the granite is the effect of cooling conditions during the main intrusion of the Burro Mountains batholith. The large mass of coarse-grained

granite cooled slowly and uniformly. Some of the fine-grained granite resulted from local chilling around large xenoliths; the porphyritic phase may represent interrupted cooling, or the large microcline crystals may be metacrysts caused by a local concentration of volatiles. The gradation from granite to granodiorite could have resulted from differentiation during or after intrusion, or from the effect of assimilated country rock. The later stages of the batholith involved separate intrusion of granite and leucogranodiorite into already solidified coarse-grained granite. These later intrusions cooled rapidly enough to crystallize as fine equigranular aggregates. The youngest intrusives related to the batholith are pegmatite and aplite dikes.

CRETACEOUS SEDIMENTARY ROCKS

BEARTOOTH QUARTZITE

General Statement

The type section of Beartooth quartzite is on Beartooth Creek near Fort Bayard, about 8 miles east of Silver City, New Mexico (Paige, 1916). In Silver City quadrangle, this formation consists of 90 to 125 feet of fine- to medium-grained orthoquartzite and sandstone, with minor intercalated shale. Thin beds of chert-pebble conglomerate occur at the base and in the top 4 to 8 feet. The formation rests unconformably on rocks ranging in age from Precambrian to Pennsylvanian and is conformably overlain by the Colorado shale. The quartzite extends discontinuously westward from Silver City quadrangle into the area of this report. The age of the Beartooth quartzite has not been definitely established, because of the absence of index fossils; Paige (1916) tentatively considered it to be Upper Cretaceous.

Stratigraphy

The Beartooth quartzite crops out along the northern edge of the area as a contorted, discontinuous band displaced by several northwest-trending faults (pl. 1). It lies on a gently undulating erosion surface of Precambrian granite. The resistant quartzite caps the top or outlines the edges of uplifted fault blocks and protects the underlying granite from erosion. Where the quartzite has been undercut, as on the ridge west of Slate Creek Canyon, it breaks off in large blocks and leaves almost vertical cliffs (pl. 2B). Near the mouth of Slate Creek, erosion of the overlying Colorado shale has exposed the top of the quartzite as a smooth dip slope. Wild Horse Mesa, in parts of secs. 2, 3, 10, 11, and 12, T. 18 S., R. 17 W., is capped by Beartooth quartzite, as are several small ridges east of the mesa. Because of faulting, erosion, and intrusion by rhyolite and andesite porphyry, a complete, well-exposed section is not found in the area.

In the northwest corner of the area, in secs. 31, 32, and 33, T. 17 S.,

R. 18 W., the quartzite is about 60 feet thick, strikes approximately west, and dips 25° to 50° N. Its basal contact with Burro Mountains granite is marked by 2 to 3 feet of hematite-stained granitic debris and arkose, which grades upward into a 2-foot-thick bed of chert conglomerate. The rest of the section is made up of fine- to medium-grained sandstone and quartzite. The arkose is composed of angular fragments, up to several centimeters in length, firmly cemented by white calcite. Thinsection examination shows that the fragments are locally derived granite, quartz, altered perthitic microcline, and a few well-rounded pebbles of fine-grained argillaceous sandstone. The white calcite that occurs in the matrix also fills tiny veinlets cutting the fragments. Hematite stains the fragments and fills fractures in both matrix and fragments. The conglomerate at this locality is 10 to 15 percent hematite-stained pebbles of chert and quartz set in medium to coarse sand grains. The well-rounded pebbles are generally less than an inch across. The conglomerate grades upward into thickly bedded quartzite that is white, pink, light gray, or dark red and marked by a few dark-brown limonite-filled fractures.

The most abundant type of quartzite, both in this section and in exposures to the east, is composed of medium-grained quartz that is tightly cemented by quartz. A thinsection of this quartzite shows that it is well sorted; few grains exceed a millimeter in diameter. The grains are bound together as the result of interlocking, oriented quartz overgrowths; a dusty rim marks the outline of the original rounded grain. Aggregates of very fine-grained quartz fill any interstices not occupied by the quartz overgrowths. The only observed accessory mineral is magnetite, which occurs as dusty grains in the cement.

In the vicinity of Slate Creek and Fox Tail Creek, the quartzite forms cliffs, 100 to 125 feet high, with talus-skirted bases. Here the quartzite is uniformly massive, medium grained, and light gray. A 5-foot bed of conglomerate near the base of the formation is composed of dark-brown, well-rounded chert pebbles, about half an inch in diameter, set in coarse-grained quartz sand. The quartzite capping on Wild Horse Mesa is similar to that near Slate Creek and Fox Tail Creek. However, a few boulders of chert conglomerate were found in the soil covering the top of the mesa. Here the Beartooth apparently has a conglomeratic horizon near the top of the formation.

Petrogenesis

Features of the Beartooth quartzite indicative of its origin are:

1. The quartzite lies unconformably on Precambrian granite in this area, and in Silver City quadrangle on rocks ranging in age from Precambrian to Pennsylvanian.
2. The base of the formation is marked by a thin sheet of residual arkose or oligomictic chert conglomerate.

3. Most of the formation is made up of well-sorted, rounded, fine- to medium-grained quartz sand that is cemented with quartz.

The first two of these features are typical of sediments deposited by a transgressive sea on an area of low relief. This environment is one of stability and is characterized by considerable winnowing action, very mild subsidence during accumulation, and association of widespread unconformities (Krumbein and Sloss, 1951). The origin of the basal arkose clearly lies in the reworking of weathered residue from the underlying Precambrian granite. The chert-pebble conglomerate may have been derived from an area where cherty limestone was being weathered and eroded. Pre-Cretaceous cherty limestones that occur in southwestern New Mexico, and that may have served as source rocks for the conglomerate, are the Ordovician El Paso and Montoya limestones and the Mississippian-Pennsylvanian Fierro limestone.

Colorado Shale

General Statement

The Colorado group is the name applied by Hayden (1876) to a group of marine deposits in Colorado that underlie the Fox Hills group, conformably overlie the Dakota group, and include the Fort Benton, Niobrara, and Fort Pierre shales. The U. S. Geological Survey refers to this group, where it is undivided, as the Colorado formation (Wilmarth, 1938).

In Silver City quadrangle, the Colorado group is represented by not less than 2,000 feet of carbonaceous shale that conformably overlies the Beartooth quartzite. Faunal assemblages indicate that this shale is equivalent in age to the Benton shale (lower part of the Upper Cretaceous) of the Colorado group (Paige, 1916).

Stratigraphy

Along the northern edge of the area, the Colorado shale is truncated by an erosion surface upon which rhyolite and andesite lavas of Tertiary age were spread. The shale characteristically crops out in valleys or saddles between Beartooth quartzite and overlying lavas. Good exposures of the shale occur around the base of Clarks Peak (sec. 2, T. 18 S., R. 18 W.) and along Slate Creek, Fox Tail, and Wild Horse Canyons, east of the peak. Slate Creek, which on the State highway maps is labelled "State Creek," was erroneously named for the shale into which the canyon is cut. Remnants of Colorado shale overlie the Beartooth quartzite that caps Wild Horse Mesa, but the shale has been stripped completely from isolated outliers of quartzite east of the mesa.

In the northwest corner of the area, in sec. 32, T. 17 S., R. 18 W., the Colorado shale, about 300 feet thick, crops out in a valley between the Beartooth quartzite to the south and the Tertiary lavas to the north. The beds strike approximately west and dip 25° N. Thinly bedded,

silty, carbonaceous shale, a few feet thick, which rests on the uppermost Beartooth quartzite ledge, grades upward into thickly bedded to massive carbonaceous shale containing a few nodules of dark-gray limestone. Several 1-foot layers of black to dark-gray limestone are interbedded in the upper 20 feet of the formation.

The Colorado shale east of Clarks Peak crops out on a gentle slope between quartzite to the east and the lava that forms Clarks Peak. Here the thickness of the shale is estimated to be 1,100 feet. Thinly bedded, blue-black carbonaceous shale and a few interbedded thin layers of arenaceous shale make up most of the section. About 400 feet above the base of the formation, a 50-foot bed of light-tan, fine-grained limestone crops out as a low ridge.

In Slate Creek, Fox Tail, and Wild Horse Canyons, the shale has been faulted against Precambrian granite, Beartooth quartzite, or Tertiary lavas. At all three of these localities, the shale is the typical blue-black carbonaceous variety described above.

A carbonaceous shale similar to the Colorado shale in Slate Creek occurs in a horse block between two northwest- to west-trending normal faults in sec. 22, T. 18 S., R. 18 W. (pl. 1). The block, about three-quarters of a mile long and less than 200 feet wide, is faulted against Precambrian granite to the north and Gila conglomerate to the south. Between the faults are silicified and highly sheared slabs of fine- to medium-grained gray sandstone; gray, brown, and black limestone; and carbonaceous shale with brown and black limestone nodules. Because of the similarity in lithology to some parts of the Colorado shale, these sediments are considered to be part of that formation.

Petrogenesis

Twenhofel (1939), who reviewed the conditions necessary for formation of black shales, concluded that no single explanation can be applied, but that in general their formation requires an environment of restricted circulation or one where organic material passes through the depositional interface rapidly enough to prevent the decomposition of organic material. The Colorado shale is probably a shelf deposit formed in a shallow, possibly restricted, marine environment.

LARAMIDE AND POST-LARAMIDE INTRUSIVE ROCKS

General Statement

In southern Arizona and New Mexico, the Laramide orogeny is represented by folds and faults, stocks of intermediate composition, and associated ore deposits (Eardley, 1951). In Silver City quadrangle, the Laramide stocks and associated dikes are dated as late Cretaceous-early Tertiary because they intruded Upper Cretaceous Colorado shale and were exposed and partly eroded prior to the eruption of Tertiary rhyolite-latite-andesite lavas (Paige, 1916).

Monzonite stocks, andesite and rhyolite plugs, and diabase, rhyolite, andesite, dacite, latite, and quartz latite dikes of at least five ages intrude Precambrian granite in the Big Burro Mountains (Gillerman, 1951). The plugs and dikes are considered by Gillerman to be older than the Laramide monzonite stocks. At the southwestern end of the Big Burro Mountains, rhyolite dikes and many others of "diverse composition" transect Tertiary volcanic rocks that are apparently younger than the monzonite stocks (Gillerman, 1951). Thus the monzonite stocks and some of the dikes in the Big Burro Mountains are of Laramide age; some dikes and plugs may be older, and some are definitely younger.

The writer observed seven varieties of intrusive igneous rocks in this area. The rock types, their manner of occurrence, and the youngest rocks intruded by each are shown in Table 10. Although diabase and andesite may be pre-Laramide, and some rhyolite and basalt may be post-Laramide, all the intrusive rocks that are known to be younger than Precambrian granite are discussed together in this section.

TABLE 10. COMPARISON OF THE OCCURRENCE OF LARAMIDE AND POST-LARAMIDE INTRUSIVE ROCKS

ROCK TYPE	OCCURRENCE	YOUNGEST COUNTRY ROCK INTRUDED *
Diabase	dikes	Precambrian granite
Andesite	dikes	Precambrian granite
Monzonite porphyry	stock and dikes	Precambrian granite
Andesite porphyry	plugs and dikes	Colorado shale (diabase)
Rhyolite and rhyolite porphyry	plugs and dikes	Colorado shale (diabase, andesite porphyry, and monzonite porphyry)
Basalt	dikes	Tertiary volcanic rocks

* Transected dike rocks are in parentheses.

DIABASE

Occurrence

Diabase occurs in a large northwest-trending dike that transects Precambrian granite and the metamorphic complex in the southeast corner of the area (pl. 1), in a smaller dike that cuts the largest Ash Creek xenolith and granite in the vicinity of Ash Creek Canyon (pl. 12), and in several dikes, too small to map individually, that cut granite and other Precambrian rocks. The largest dike strikes N. 35°-40° W., dips approximately 65° SW., and ranges in thickness from 50 feet, at its northwestern end, to about 75 feet, at its southeastern end. This diabase is well exposed in Eccles Canyon along the Redrock-Silver City road, at the northern edge of sec. 19, T. 19 S., R. 16 W. The diabase dike in the Ash Creek area strikes from North to N. 50° W. and ranges in thickness from 25 to 50 feet.

Petrography

The largest diabase dike, which strikes almost normal to the valleys and ridges in the area, crops out as a shallow saddle on the ridges. It is characterized on the steep valley slopes by dark-green to dark-brown angular blocks that form extensive talus slopes. Dark-green or red-brown weathered surfaces show a fine-grained ophitic texture emphasized by the light-tan to gray coating of alteration products on millimeter-long plagioclase euhedra. Epidote veinlets, less than a millimeter thick, cut the diabase. Nearly equal amounts of dark-green pyroxene and gray-green plagioclase are seen on a freshly broken surface.

Thinsections of diabase from this dike show an ophitic arrangement of euhedral to subhedral, normally zoned, and slightly saussuritized labradorite(Ab_{44-46}) laths wrapped and included by pigeonite anhedra. A fine-grained felted aggregate of chlorite, dusty magnetite, and serpentine(?) marginally, and in some places completely, replaces the pigeonite. Primary anhedra and skeletal crystals of magnetite are molded between plagioclase laths and pyroxene anhedra. The mode of the diabase is (in percent):

Labradorite (Ab_{44-46})	45
Pigeonite	17
Chlorite, serpentine(?), dusty magnetite	29
Magnetite	9
Total	100

Because the chlorite-serpentine aggregate is secondary after pyroxene, it is concluded that the unaltered diabase contains about 46 percent pigeonite.

The diabase dike that cuts the largest Ash Creek xenolith crops out on a steep hillside partially covered by talus from the metasediments. This dike has a deeply weathered red-brown surface and commonly weathers to spheroids. A fresh surface shows a few subhedral plagioclase grains set in a very fine-grained, dark-green, ophitic matrix. Under the microscope, the matrix can be seen to consist of about 55 percent labradorite (Ab_{42}) enclosed in a felted mass of chlorite, serpentine, magnetite, and calcite. Accessory minerals are apatite, quartz, and magnetite. The subhedral to euhedral plagioclase is saussuritized along veinlets. Apparently the chlorite-serpentine aggregate is secondary after a pyroxene. A few cavities are filled by secondary calcite and euhedral quartz.

Origin and Age

The largest diabase dike was intruded along a joint that is genetically related to the extensive system of northwest-trending faults along the northern edge of the area. This type of intrusion has been described by Anderson (1942) as an opening of a joint by the pressure of an under-

lying body of magma. Emplacement of the magma was accompanied by chilling of narrow margins and subsequent crystallization of plagioclase, pyroxene, and skeletal magnetite; the euhedral magnetite may have crystallized before the pyroxene. Labradorite and pigeonite were later altered to saussurite, chlorite, serpentine, magnetite, and calcite.

Field evidence indicates that the diabase is younger than Precambrian granite and older than rhyolite and andesite porphyry dikes. Gillerman and Whitebread (1956) found the same relationship among similar dikes in the Black Hawk mining district. The diabase dikes may have been emplaced during late Precambrian time, or they may represent the earliest of the Laramide intrusions.

Andesite

Occurrence

A few dikes of andesite, usually only 2 to 3 feet thick, crop out along Eccles Canyon, on the ridge north of it, and in the Ash Creek area (pl. 1). The dikes characteristically weather to gray-green angular blocks where exposed in canyons, or are weathered to dark green-brown spheroids on hillsides.

Petrography

Fresh fine-grained andesite is composed of about 60 percent light-green plagioclase, a few needles of dark-green hornblende, and a dark-green chloritic matrix. Thinsections show unzoned euhedral to subhedral andesine(Ab_{60}) crystals that are altered in patches to kaolinite and minor sericite. The hornblende needles and a few smaller plates of brown biotite are replaced almost completely by a fibrous to granular aggregate of chlorite, epidote, calcite, and magnetite. Sericite appears near the margin of the aggregate and commonly extends into adjoining plagioclase. Aggregates of chlorite, sericite, calcite, and magnetite are also interstitial to plagioclase, as are apatite and magnetite euhedra.

Because hornblende and biotite are euhedral and andesine is both euhedral and subhedral, it appears that plagioclase may have continued to crystallize after the formation of hornblende and biotite. Apatite and magnetite euhedra crystallized early in the sequence. Dusty magnetite and the chlorite-epidote-calcite-sericite aggregates are secondary after hornblende and biotite.

Age

The youngest rock type cut by the andesite dikes is Precambrian granite. However, these dikes have not been metamorphosed and are no more altered by weathering than similar dike rocks in the area. The andesite dikes are probably also of late Cretaceous-early Tertiary age.

Monzonite Porphyry

Occurrence

The Twin Peaks monzonite porphyry stock, named for the Twin Peaks in the Black Hawk mining district (Gillerman and Whitebread, 1956), crops out in the central part of T. 18 S., R. 16 W. (pl. 1). The total surface exposure of the west-trending stock is about 5 miles long and as much as 1¼ miles wide. Approximately one-half of the stock lies in Silver City quadrangle; the remainder lies in the Black Hawk district and the area of this report.

Deeply weathered monzonite porphyry crops out along Saddle Rock Canyon, the slopes of which are characterized by white talus. Outcrops on the ridges parallel to this canyon are rounded, friable masses that have weathered light shades of gray, tan, or red brown.

Petrography

Megascopically the monzonite porphyry displays stubby, euhedral to subhedral phenocrysts of pink-white feldspar and needles of dark-green hornblende, about 1 cm long, in a fine-grained to aphanitic, pink to gray matrix. The phenocrysts occupy about 15 to 20 percent of the rock. Thinsection examination shows that most of the feldspar phenocrysts are andesine(Ab_{60-62}), with only a few of orthoclase. The plagioclase is normally zoned, shows both Carlsbad and albite twinning, and is extensively altered to kaolinite and sericite; the orthoclase shows Carlsbad twinning and is partially kaolinized. Hornblende phenocrysts are almost completely altered to a granular aggregate of chlorite, epidote, and calcite. The matrix, a microgranular mosaic of weathered feldspar and minor quartz, contains scattered subhedral to anhedral magnetite and euhedral apatite as accessory minerals.

Age

No intrusive relations with rocks younger than Precambrian were observed. However, Gillerman and Whitebread (1956) correlate the Twin Peaks stock with lithologically similar late Cretaceous-early Tertiary stocks of monzonite, quartz monzonite, and granodiorite that intrude Beartooth quartzite and Colorado shale in Silver City quadrangle (Paige, 1916).

Andesite Porphyry

Occurrence

Andesite porphyry, one of the most abundant of the Laramide intrusive rocks, occurs in two pluglike masses and several west-trending dikes which intrude Precambrian granite, Beartooth quartzite, and

Colorado shale along the northern part of the area (pl. 1). The larger plug underlies parts of secs. 10, 11, 14, and 15, T. 18 S., R. 18 W., and is about 1½ miles long and slightly less than a quarter of a mile wide; the smaller one lies just to the east and is half a mile long and less than a quarter of a mile wide. A single dike, about 300 feet thick, extends S. 80°-90° E. from each plug for 1 to 2 miles. Several west-trending dikes, about 5 miles long and 150 feet thick, extend from Little Bear Canyon to the eastern edge of the area (pl. 1). About 2½ miles north of Bullard Peak, they branch and join along west and northeast trends. A single andesite porphyry dike, about 100 feet thick and 1½ miles long, occurs along the ridge northwest of Eccles Canyon (pl. 1).

Petrography

In areas of low to moderate relief, the dikes stand above the country rock as low, rounded ridges. Along Bear and Little Bear Canyons, where topographic relief is high and erosion is active, the dikes are inconspicuous in the deeply cut tributaries to the canyon.

Weathering leaves the surface light red brown to yellow brown, with patchy limonite and hematite stains. A fresh sample contains about 20 percent light-gray to pink feldspar phenocrysts and a few hornblende needles in a mottled red-purple to red-brown aphanitic matrix.

The deeply weathered nature of the andesite porphyry is apparent microscopically. Turbid phenocrysts of zoned andesine(Ab_{62-65}), several of which contain slightly devitrified glass inclusions, are altered preferentially to kaolinite and sericite in cores and along veinlets. The subhedral feldspar phenocrysts are commonly rounded and corroded. Fine-grained aggregates of green, slightly pleochroic chlorite, dusty magnetite and, in a few places, sericite appear to be pseudomorphous after hornblende needles and biotite plates. A characteristically mottled microgranular matrix of altered feldspar anhedra, tiny quartz grains, and secondary calcite patches encloses the phenocrysts and a few accessory grains of magnetite, apatite, and zircon (pl. 7B).

Origin and Age

The strong west and northeast trend of the andesite porphyry dikes suggests that they were emplaced along joints or faults. The pluglike intrusives doubtless supplied magma to some of the dikes and may also have acted as small vents for some of the early Tertiary andesite volcanic rocks. Andesite porphyry dikes intrude Precambrian granite, Beartooth quartzite, and Colorado shale, and transect diabase dikes. The andesite porphyry is thus younger than Upper Cretaceous and may be as young as early Tertiary. No contact relations were observed between andesite porphyry and the Twin Peaks monzonite stock. Inasmuch, however, as both rock types are younger than the Upper Cretaceous Colorado shale and older than rhyolite and rhyolite porphyry dikes, they may be comagmatic.

Rhyolite and Rhyolite Porphyry

Occurrence

Rhyolite and rhyolite porphyry occur as dikes and as small, irregular intrusive masses. A west-trending pluglike mass, about 1 mile long and a quarter of a mile wide, has been intruded into granite and Cretaceous sediments in the northwest corner of the area; a similar plug in the northeast corner has been intruded into the Colorado shale. A wedge of rhyolite about 1½ miles long lies between two faults in Ash Creek Canyon, in secs. 4, 9, and 10, T. 18 S., R. 18 W. (pl. 1, 2C). In the southeastern part of the area, dikes of rhyolite porphyry, up to 125 feet thick, trend generally N. 50°-60° E. across Precambrian granite and across a diabase dike.

Small irregular rhyolite dikes that occur in the Precambrian granite in the northern and eastern parts of the area transect dikes of andesite porphyry and the Twin Peaks monzonite porphyry stock. These small dikes differ from those in the southeastern corner of the area in the following respects: The northern and eastern dikes are usually a few tens of feet thick, vary widely in dip and strike, and are commonly less than a few hundred feet long; the southeastern ones are over 100 feet thick and extend in the same direction for as much as 5 miles.

Petrography

The rhyolite and rhyolite porphyry dikes are generally highly resistant to erosion. Large dikes commonly crop out as low but distinct ridges. Smaller dikes are conspicuous in outcrop because of their light color. The weathered surface ranges from chalky white to light tan, gray, or dark brown. Numerous fractures are commonly stained dark brown or rarely brick red, with black dendritic patterns. On a freshly broken surface, the rock is white, pink, or a light shade of gray, tan, or purple. Millimeter-long phenocrysts of quartz, pink feldspar, and hematite and limonite after magnetite may locally constitute up to 20 percent of the rock. Some of the dikes have a well-developed flow structure parallel to their walls. Near large faults, the dikes are commonly brecciated and in a few localities are silicified and mineralized. The small dikes are almost completely aphanitic, with only a few feldspar microlites and very rare quartz-feldspar spherulites. Larger dikes are porphyritic, with an aphanitic or microgranular groundmass; a few are flow banded.

Thinsections of rhyolite porphyry contain rounded and corroded phenocrysts of orthoclase, oligoclase(Ab_{72}), and quartz with irregular glass inclusions. The orthoclase shows Carlsbad twinning, is partly altered to kaolinite and minor sericite, and is rarely rimmed with granophyre. The less abundant plagioclase is more extensively altered to kaolinite than is orthoclase. The matrix is made up of microgranular aggregates of quartz and orthoclase, and a few grains of apatite, zircon,

and magnetite. A eutaxitic texture in some of the rhyolite results from the parallel orientation of platelike aggregates of sericite, magnetite, and chlorite; the shape of the grains suggests that they are pseudomorphous after biotite plates.

Age

The intrusion of some of the rhyolite magma was controlled by joints trending northwest and slightly north of east. Other dikes, however, change markedly in dip and strike and thus were intruded along irregular fractures. The fine grain size of the rhyolite denotes rapid cooling and emplacement under a relatively shallow cover.

The small rhyolite dike that transects monzonite porphyry at the southwestern end of the Twin Peaks stock is younger than this late Cretaceous-early Tertiary stock. In the Burro Mountains, however, some rhyolite dikes are older than the Laramide stocks, and others are younger than Tertiary volcanics (Gillerman, 1951). The rhyolite present in this area may also have been intruded during two separate periods, one prior to the intrusion of the Twin Peaks and related stocks, the other later.

Basalt

Occurrence and Petrography

Basalt is the least widespread of the dike rocks. Most of the dikes are too small to map individually. Their size, however, has been exaggerated on the geological map to show significant age relationships. The largest occurrence of basalt is in a west-trending dike, 25 feet thick and half a mile long, that has been intruded into Precambrian granite and Tertiary volcanics in sec. 6, T. 18 S., R. 18 W. Another dike, from 5 to 10 feet thick, in E½ sec. 14, T. 18 S., R. 18 W., has been intruded into Precambrian granite and has cut dikes of andesite porphyry and rhyolite (pl. 1).

The basalt dikes are deeply weathered dark green to dark brown. A few outcrops show a suggestion of spheroidal weathering, but commonly subangular blocks characterize the surface exposures. Secondary calcite locally fills numerous fractures. The least weathered specimens are dark gray to dark purple and sharply angular. Megascopically the rock is uniformly aphanitic, with scattered microphenocrysts, about 0.1 mm long, of subhedral, dark-gray plagioclase.

Age

Basalt is the only dike rock that transects the Tertiary lavas at the northern boundary of the area. The basalt may be of late Laramide age or, more likely, it is related to late Tertiary basalts and basaltic andesites that are interbedded with Gila(?) conglomerate south of the area.

TERTIARY VOLCANIC ROCKS

General Statement

At the southern edge of the Colorado Plateau, Cretaceous sediments are overlain by erosional remnants of a series of lava flows that once were several thousand feet thick. South of the plateau, a continuous series of flows make up the Datil lava field, which is roughly circular and up to 150 miles across (Eardley, 1951). The northern edge of the area of this report is the southern limit of the Datil lava field.

A detailed study of the Datil volcanic rocks is not within the scope of this report. They are reported in the works of Paige (1916), Winchester (1920), Ferguson (1920, 1927), Callaghan (1951), Elston (1955a, b), and Wargo (1958). However, because the lower quartz latite-rhyolite members of this volcanic series occur at the northern edge of this area, they have been mapped and will be discussed as a unit of undifferentiated Tertiary volcanic rocks.

Quartz Latite and Rhyolite

Occurrence

Volcanic rocks overlie Precambrian granite and Upper Cretaceous Colorado shale along the northern edge of the area. Except for local variations where the lavas have been offset and tilted by northwest-trending faults, they strike in a westerly direction and dip from 10° to 30° N. The lavas are characteristically eroded to form peaks or long west-trending ridges with gentle, dissected dip slopes to the north and steep cliff faces to the south. Clarks Peak, the largest of the volcanic erosion peaks, rises over 1,000 feet above Slate Creek Canyon.

Petrography

Two types of volcanic rocks crop out in the area. Quartz latite flows and minor agglomerate and tuff make up the lower 300 to 400 feet of the volcanic section. In the northwest corner of the area, these intermediate lavas are in contact with granite; to the east they lie on Colorado shale. Dikes and plugs of rhyolite have been intruded into the quartz latite. Rhyolite flows and tuffs overlie quartz latite and extend northward beyond this area. At least 1,500 feet of rhyolite crops out at Clarks Peak; the maximum thickness north of the area is probably twice that figure (Elston, 1955b).

Quartz latite. At the base of the quartz latite flows is a zone of andesite flow breccia, from 30 to 40 feet thick. About 70 percent of the breccia is made up of angular fragments of aphanitic volcanic rocks that range in color from light pink to gray. The fragmental nature of the rock is made obvious on a weathered surface by the contrast of the light fragments, which are as much as 2 cm in length, to the dark-purple aphanitic matrix.

Microscopic examination shows that most of the fragments are andesite composed of microlites of andesine(Ab_{69}) in an aphanitic matrix. A few of the fragments are dacite. The matrix shows a crude flow structure, along which platy aggregates of sericite are oriented. Resorbed phenocrysts of quartz and fragments of andesine(Ab_{67}), up to 0.5 mm long, occur in the matrix between fragments of andesite and dacite.

The quartz latite weathers from a light tan to a light gray purple; its surface is marked by tiny vesicles, phenocrysts of kaolinized feldspar, and minor brown biotite. The phenocrysts are as long as 3 mm and make up 10 to 15 percent of the rock. On a fresh surface, the aphanitic matrix is light to dark purple, and the feldspar phenocrysts are light pink.

A thinsection of unaltered quartz latite from the ridge northeast of Fox Tail Canyon contains about equal amounts of sanidine and oligoclase (Ab_{73}) phenocrysts that occur as whole or broken subhedra or as clusters of subhedra. The oligoclase, slightly altered to kaolinite, shows both Carlsbad and albite twinning; sanidine is unaltered. Biotite phenocrysts have ragged edges and include magnetite euhedra. Magnetite with included zircon occurs in accessory amounts. The matrix of microgranular oligoclase(Ab_{87}) and quartz surrounds and embays the phenocrysts. Near vesicles, the matrix is slightly coarser grained, quartz is more abundant, and a few plates of tridymite, with characteristic wedge twinning, occur. Some of the vesicle margins contain spherulites.

Rhyolite. The rhyolitic volcanic rocks are made up of a series of thick flows interbedded with tuff, breccia, and agglomerate. Erosion surfaces separate some of the flows. Generally the rhyolite is white or light pink, but some is light gray to dark purple. Fragments of older rhyolite and of the andesite and quartz latite flows are not uncommon in most of these rhyolite flows. The rhyolite is typically banded and contains phenocrysts of quartz and pink feldspar that make up as much as 10 percent of the rock.

A thinsection of typical rhyolite from a small canyon about 1½ miles northeast of Wild Horse Mesa, in sec. 36, T. 17 S., R. 17 W., shows a few phenocrysts of quartz in an aphanitic to microgranular matrix of quartz and kaolinized feldspar. Contorted flow lines appear in the matrix as elongate patches of microgranular quartz. The matrix includes fragments of quartz, microcline, and sanidine, as well as fragments of the quartz latite described above, fragments of an older aphanitic rhyolite, a few glass shards, and subrounded pebbles of argillaceous sandstone.

Origin and Age

The fragmental nature of the volcanic rocks and their interlayering with tuffs and clastic sediments suggest that they accumulated over a fairly long period of time. The heterogeneous composition of some of the breccias indicates that they are accumulations of pyroclastic material. However, some of the rhyolite breccias probably resulted from

the collapse or disruption of a solidified flow crust. Plugs of rhyolite in the quartz latite flows may well be the remnants of the fillings of vents through which the rhyolite flows and tuffs were extruded.

The volcanic rocks represent a complex sequence of volcanism, during which intervals of extrusion of lava flows and abundant pyroclastic material alternated with intervals of erosion. No evidence was noted in the area that would indicate the general direction from which the flows advanced. The thickness of the lavas at the northern edge of the area indicates that prior to erosion they covered a considerably larger area and may have been continuous with the volcanic rocks in neighboring quadrangles to the south.

Contact relations in this area indicate that the volcanic rocks are younger than the Upper Cretaceous Colorado shale and older than the Upper Pliocene Gila conglomerate. Paige (1916) interpreted similar rocks in Silver City quadrangle as being early to middle Tertiary in age.

TERTIARY AND QUATERNARY SEDIMENTARY ROCKS

General Statement

The extensive deposits of coarse detrital material underlying many intermontane valleys in southern Arizona and southwestern New Mexico are known locally by various names. Gila conglomerate is the name most widely used and generally accepted. Gilbert (1875) first described these deposits in the valleys of the upper Gila as being composed of locally derived boulders interbedded with layers of slightly coherent sand. Where the Gila River intersects the troughs of the Basin and Range system, the conglomerate is continuous with the gravels which occupy the troughs and floor the desert plains. Gilbert (1875) considered the Gila conglomerate to be early Quaternary; Ransome (1919) assigned a similar age to it in the Ray and Miami districts in Arizona, as did Paige (1916) in Silver City quadrangle.

Knechtel (1936) discovered vertebrate fossils in Gila conglomerate that floors the San Simon and Gila Valleys in southeastern Arizona. He correlated the Gila conglomerate with similar deposits in the San Pedro Valley to the west and concluded that these deposits are equivalent in age. He also inferred that many of the thick valley deposits that have been described as Gila conglomerate belong to a common period of deposition, and assigned the Gila conglomerate, in part at least, to the Upper Pliocene.

The desert plain west of the Burro Mountains is underlain by various types of clastic sediments. These have been grouped, in order of decreasing age, into the following mappable units: (1) Gila conglomerate and younger related bajada deposits and dissected gravels; (2) terrace gravels; (3) unconsolidated surficial bolson deposits; (4) alluvial deposits.

Gila Conglomerate

Occurrence

Gila conglomerate and associated younger sediments underlie approximately 80 square miles in the western, southwestern, and southern parts of the area of this report. The contact of the conglomerate with Precambrian rocks along most of the western flank of the mountains is obscured by unconsolidated bajada deposits a few feet thick. Alluvial deposits overlie the conglomerate along the numerous washes that dissect it. In the southeast corner of the area, a thin veneer of bolson deposits covers the Gila conglomerate, extending for 30 miles or more southeast and south of the area.

Contact relations with the Tertiary volcanic rocks are not clear in the area. South of the area, Gila conglomerate overlies the lavas (Gillerman, 1951); northwest of the area, Gila conglomerate is faulted against the lavas (Elston, 1955b). The many boulders of rhyolite, andesite, and agglomerate in the conglomerate prove that it is younger than the volcanic rocks.

The Gila conglomerate is faulted against Precambrian rocks (pl. 1) along lower Ash Creek Canyon, Burro Springs Canyon, and a tributary to Joe Harris Canyon. Bedding is poorly defined, but dips up to 20 degrees were measured. Near large normal faults, dips up to 36 degrees were recorded. Any interpretation of apparent structure in the Gila conglomerate, however, is doubtful because the conglomerate is irregularly cemented with calcite across the crude bedding planes. The exposed surface of a calcite-cemented section gives the impression of a steeply dipping bed within the conglomerate.

Petrology

In steep-walled washes and along the Gila River, the conglomerate stands in cliffs, some of which are 100 feet high (pl. 10A). On gentle slopes, the conglomerate crops out as rounded barren hills. The color ranges from shades of red and brown, where boulders of Precambrian igneous and metamorphic rocks are dominant, to shades of light pink, gray, tan, or white, where boulders of Tertiary volcanics are abundant. Along faults in Burro Springs Canyon and north of Joe Harris Canyon, the conglomerate is stained brick red to dark brown by iron oxides. South of the area in Pines Canyon, the conglomerate is locally mineralized; chrysocolla coats some of the boulders and fills tiny veinlets that cut them.

Conglomerate. A conglomerate composed of locally derived boulders, cobbles, and pebbles set in a matrix of gravel and coarse sand is the most abundant rock type (pl. 10B). Fragments of most of the igneous and metamorphic rock types that crop out in the Burro Mountains occur in the conglomerate. The boulders, which make up from 10 to

70 percent of the rock, are commonly 1 to 2 feet in diameter; a few are as large as 12 feet across. The larger boulders are angular; those less than a few feet across are subrounded. The sand and gravel matrix is composed of quartz, feldspar, biotite, and rock fragments, locally well cemented by white calcite.

The maximum thickness of Gila conglomerate exposed in the area does not exceed 200 feet. Water wells in the conglomerate near Redrock penetrate up to 300 feet of conglomerate. A well south of the area in sec. 19, T. 21 S., R. 18 W., was drilled in Gila conglomerate to a total depth of 730 feet. Gilbert's (1875) estimate of a thickness of 1,000 to 1,500 feet does not seem unreasonable for this area.

Sandstone. Thin, irregular lenses and layers of semiconsolidated sandstone are locally interbedded with the conglomerate. Contacts between the two rock types are not sharp. The sandstone is composed of coarse, moderately sorted, angular particles of quartz and feldspar, rock fragments, and a few subrounded pebbles. The localized nature of the sandstone suggests that it probably was deposited in stream channels.

Volcanic ash. Two layers of white, semiconsolidated tuffaceous material, about 2 to 5 feet thick, are interbedded with Gila conglomerate north of the Redrock-Silver City road, in the northern part of sec. 28, T. 19 S., R. 17 W. Rounded, medium to coarse grains of quartz and potash feldspar in a silty matrix make up the basal foot of the beds. This sandy bed grades upward into thinly bedded material, which, as seen in thinsection, is composed of angular fragments, about 0.2 mm long, set in a fine-grained matrix. The most abundant fragments consist of biotite, quartz, unaltered oligoclase, and microcline, but chert, muscovite, zircon, saussuritized plagioclase, and magnetite are also present. The biotite and muscovite flakes and elongate fragments of other minerals are oriented parallel to the bedding. The isotropic to very slightly birefringent matrix is made up of very fine-grained, angular volcanic ash particles consisting of partly devitrified glass.

These arenaceous ash beds most likely were deposited in a small shallow lake. The volcanic ash was probably derived from the late stages of eruption of local Tertiary volcanoes.

Travertine. A few irregular masses of travertine, less than 5 feet long and 1 foot thick, are associated with the Gila conglomerate. The largest deposit is along the northwest-trending fault in Burro Springs Canyon, at the site of a former spring. A few masses that are scattered on the flat desert plain contain pebbles and cobbles. The light-tan travertine is porous and thinly banded; it weathers to white or dark brown.

The calcite aggregates in Burro Springs Canyon are travertine in the strict sense because they were deposited by evaporation of water from a spring. The scattered masses probably resulted from evaporation of ground water and are a type of caliche.

Origin

The following features of the Gila conglomerate and its associated rocks indicate conditions of rapid continental deposition: (1) The boulders and gravel are of local derivation; (2) the bedding, where discernible, is poorly developed; (3) irregular lenses of sand and tuff are interlayered gradationally with conglomerate; (4) the conglomerate is very poorly sorted.

The Gila conglomerate exposed in the area probably was formed by the merging of fanglomerate deposits derived from the Burro Mountains to the east and the elevated Tertiary lavas to the north. Some of the gravel may have been deposited by the Gila River. The lenses of sand were probably deposited in stream channels. Some of the sand and tuff lenses may be similar to the lake-bed facies described by Knechtel (1936), in the Gila Valley near Safford, Arizona.

Bajada Deposits

Bajada deposits (i.e., the debris derived from pedimentation) overlie Gila conglomerate along the western flank of the Big Burro Mountains. The deposits are made up of unconsolidated, locally derived material that ranges in size from coarse sand to boulders. On the gently sloping surfaces of the desert basin and in washes with gentle slopes, bajada deposits are indistinguishable from weathered Gila conglomerate. Consequently, the two deposits were mapped as a single unit. In a few steep-walled washes, however, 5 to 25 feet of unconsolidated light-brown bajada deposits can be observed overlying the darker brown, consolidated Gila conglomerate (pl. 10C).

Terrace Gravels

Matched terraces, standing about 90 feet above the flood plain of the Gila River, are cut across the Gila conglomerate on meander spurs along the river. The terrace surfaces are covered by an unconsolidated material locally derived from the conglomerate. The terrace level is an erosion surface that represents a pause in downcutting by the Gila River. Rejuvenation and renewed downcutting could have resulted from either tectonic or climatic changes. The climate during late Pliocene (Gila) time was warm and humid (Knechtel, 1936). A post-Gila arid climate is indicated by the bajada deposits that overlie the Gila conglomerate along the western flank of the mountains. The change to an arid climate that was characterized by little rainfall concentrated in heavy thundershowers during a few months of the year could account for the renewed downcutting of the Gila River.

Bolson Deposits

The edge of an extensive bolson plain overlies Gila conglomerate in the southwest corner of the area (pl. 1). The unconsolidated and undis-

sected bolson deposits are made up of locally derived sand, silt, and mud, which probably do not exceed 25 feet in thickness. The surface of the bolson plain is characterized by a relatively smooth surface, with no extensively developed drainage system or conspicuous drainage outlet.

Sedimentation is accomplished during periods of flooding of the dry washes that originate in the mountains and drain onto the bolson. Flood waters in the mountains are heavily charged with debris. As a flood recedes, larger particles are left in the bottoms of washes. The finer material is carried onto the bolson, where it settles out. These bolson deposits range in age from post-Pliocene to Recent.

Quaternary Alluvium

Recent stream alluvium floors the many washes that dissect the Gila conglomerate, the flood plain of the Gila River, and some of the canyons that are cut into igneous and metamorphic rocks in the Big Burro Mountains. The alluvium, rarely over 50 feet thick, is made up of locally derived silt, sand, and gravel that were deposited during flooding of the washes and canyons.

sected bolson deposits are made up of locally derived sand, silt, and mud, which probably do not exceed 25 feet in thickness. The surface of the bolson plain is characterized by a relatively smooth surface, with no extensively developed drainage system or conspicuous drainage outlet.

Sedimentation is accomplished during periods of flooding of the dry washes that originate in the mountains and drain onto the bolson. Flood waters in the mountains are heavily charged with debris. As a flood recedes, larger particles are left in the bottoms of washes. The finer material is carried onto the bolson, where it settles out. These bolson deposits range in age from post-Pliocene to Recent.

Quaternary Alluvium

Recent stream alluvium floors the many washes that dissect the Gila conglomerate, the flood plain of the Gila River, and some of the canyons that are cut into igneous and metamorphic rocks in the Big Burro Mountains. The alluvium, rarely over 50 feet thick, is made up of locally derived silt, sand, and gravel that were deposited during flooding of the washes and canyons.

Structural Geology

GENERAL STATEMENT

Northwest- and northeast-striking normal faults are the dominant structural features in the Big Burro Mountains. In Burro Springs Canyon, these faults mark the boundary between the mountains and the desert plain. Folding, layering, and foliation are developed in the Precambrian metamorphic rocks; foliation and jointing occur locally in the Burro Mountains granite and related igneous rocks. Joint systems generally parallel the major fault systems. The attitude of local lineation in the Bullard Peak rocks does not indicate a regional trend. Burro Mountains granite and related rocks have been intruded into the Precambrian metamorphic rocks generally parallel to layering and foliation. The northwest-striking pegmatite and aplite dikes that transect metamorphic structures commonly have apophyses extending parallel to the metamorphic layering and foliation. Some areas of migmatite are structurally very complex.

Precambrian rocks, Cretaceous sediments, and Tertiary volcanic rocks have been intruded by Laramide stocks of intermediate composition and by Laramide and post-Laramide plugs and dikes. Many of the dikes have been emplaced along fractures or joints that parallel the normal faults.

For purposes of discussion, most of the structural features fall naturally into two distinct age groups: (1) Precambrian structures and (2) Laramide and post-Laramide structures. Because some of the structural features in the Precambrian rocks closely parallel those of Laramide age, only the structures that are known to have been developed initially during Precambrian time will be discussed in the first section.

PRECAMBRIAN STRUCTURAL FEATURES

Banding, Layering, and Foliation

Banding, layering, and foliation are the dominant structural features in both the Bullard Peak and Ash Creek series, but these structures are developed to different degrees in the two series. Talc serpentinite is the only rock type in the Ash Creek series that shows distinct megascopic banding. Interlayering and lensing occur among sericite phyllite, biotite hornfels, and spotted andalusite hornfels. The planar orientation of platy minerals in the Ash Creek rocks is decidedly subordinate to layering. The planar orientation of sericite and chlorite in sericite phyllite and, to a lesser extent, of biotite in some varieties of biotite hornfels has produced a foliation that is recognizable megascopically. In the other Ash Creek rocks, planar features are either absent or recognizable only in thinsections. No orientation of the platy minerals in banded

talc serpentinite was observed either megascopically or microscopically. Foliation and layering in the largest Ash Creek xenolith strike from N. 15° E. to N. 45° E. and dip from 81° NE. to 80° NW.; both are parallel to contacts between metasedimentary units. Fracture cleavage was observed in biotite hornfels and diopside quartzite in Ash Creek Canyon. In biotite hornfels, it is parallel or at a small angle to a foliation caused by the parallel orientation of biotite flakes.

The Bullard Peak metasediments are characterized by prominent banding, layering, and lensing. Even within a single rock type, mineralogical or textural banding is apparent. The quartz-feldspar gneiss, in particular, displays conspicuous bands and lenses relatively rich in muscovite or biotite. Banding is also apparent as the result of regular variation in grain sizes. Some units of the hornblende gneiss and amphibolite contain alternating bands that are marked by varying amounts of hornblende and plagioclase. This banding is rarely continuous for any distance, but it is useful for recognizing minor folds. Crosscutting relations were observed among the Bullard Peak rocks. The generally concordant granite gneiss appears in the area southeast of Bullard Peak to transect quartz-feldspar and hornblende gneisses. Some of the hornblende gneiss and amphibolite layers northwest of Bar Six Canyon transect quartz-feldspar gneiss and granite gneiss.

The foliation in the Bullard Peak metasediments is caused by the planar orientation of muscovite, biotite, and less commonly hornblende. In the quartz-feldspar gneiss, the flattening of quartz and feldspar grains has rarely produced a crude foliation. The general attitude of foliation in the Bullard Peak series is from North to N. 45° E.; dips are as steep as 55° NW. Local variations from this general attitude occur in the area north of Bullard Peak, where the foliation strikes N. 80° W. and dips up to 75° NE. The attitude of isolated xenoliths also differs from the regional northeast trend.

In the Bullard Peak series, the foliation locally departs from exact parallelism to the bedding in the area southeast of Bullard Peak (pl. 1). Regionally, however, the foliation is more closely related to relict bedding than it is to the axial planes of folds. No evidence that would support an origin of foliation by flow, such as flattened pebbles, was observed in the area. The foliation in these rocks probably originated by mimetic recrystallization. Harker (1939) describes this process as a segregation involving solution, diffusion, and recrystallization; Mead (1940) describes it as grain enlargement, recrystallization, and replacement, with implied chemical and mineralogical changes which are dependent upon conditions of temperature and pressure and the availability of mineralizing solutions. The result is an emphasis of any preexisting planar structures in the rock. Since quartzo-feldspathic and pelitic sediments commonly are characterized by successive layers that differ somewhat in composition, mimetic recrystallization, possibly with the aid of metamorphic differentiation, would emphasize these initial

differences. Once bedding foliation has been developed, any later folding or arching would tend to accentuate it further, but it may be developed prior to folding, during folding, or subsequent to folding (Mead, 1940).

In the granite gneiss that crops out north of Eccles Canyon and in Bullard Peak Canyon, plates and patches of biotite cause a well-developed foliation. The thin lenses and layers of biotite in the granite gneiss that underlies Bullard Peak were locally compressed into chevron folds, probably concomitantly with major folding of the Bullard Peak series.

Orientation of biotite plates and elongation of quartz grains have produced a foliation in the Burro Mountains granite and related rocks. This feature is best developed in the area northeast of Bullard Peak, where the foliation in tonalite strikes N. 50°-60° E. and dips up to 80° NW. In the Black Hawk district, this northeast trend of the foliation apparently has controlled the intrusion of granite, aplite, and pegmatite dikes (Gillerman and Whitebread, 1956).

Lineation

Lineation is uncommon in the Ash Creek metasediments or in the Burro Mountains igneous rocks; it occurs only locally in the Bullard Peak rocks, but the attitude of lineations suggests no regional trend. This conclusion is supported by the detail mapping of the Black Hawk district by Gillerman and Whitebread (1956).

The alinement of hornblende needles was observed in hornblende gneiss that crops out in a tributary to House Canyon, sec. 26, T. 18 S., R. 17 W., and in the elongate xenolith northwest of Bullard Peak. A lineation is also produced by the parallel orientation of axes of minor folds on the generally southeast-dipping quartz-feldspar gneiss in sec. 5, T. 19 S., R. 16 W. A similar lineation was observed east of Bullard Peak in biotite and hornblende gneisses that show alinement of the axes of crenulations.

Folds

Folds of Precambrian age were observed only in the main exposure of the Bullard Peak rocks. The metamorphic rocks along the western part of this exposure strike from North to N. 45° E. and dip generally northwest. However, along the eastern part of the exposure, between Bullard Peak and Eccles Canyon, a distance of about 4 miles, the outcrop pattern outlines a broad fold (pl. 1); the axial plane of this fold strikes about N. 30° E. and dips northwest. The parent rock of the granite gneiss and the source rocks of some of the hornblende gneiss were intruded generally parallel to the sedimentary layering prior to folding and regional metamorphism. After folding and metamorphism, the structure was complicated further by intrusion of the Burro Mountains batholith. Prior to intrusion of the batholith, the limb of the fold

that crops out around Bullard Peak may have been continuous with the folded quartz-feldspar gneiss that partly encloses the granite gneiss stock in Bullard Peak Canyon (pl. 1). Minor asymmetric folds and tightly contorted folds occur on the south limb of the larger fold. Small asymmetric folds, probably drag folds, occur in quartz-feldspar gneiss in sec. 5, T. 19 S., R. 16 W. The axial planes are parallel, strike north, and are vertical; the axes of the folds plunge 30° S.

Near the confluence of Stein and Bullard Peak Canyons, the attitude of foliation suggests a synclinal structure, the axial plane of which strikes N. 10° E. and is vertical. In this general area and to the south, the regional northeast trend is locally disturbed by folds and contortions, but the absence of any consistent marker horizons prevents their delineation.

Ptygmatically folded layers of granitic or aplitic composition, less than an inch thick, occur in contorted migmatite in a tributary to Burro Springs Canyon, in sec. 13, T. 19 S., R. 17 W., and in a tributary to Bullard Peak Canyon, in sec. 11, T. 19 S., R. 17 W. The local contortions of the migmatite indicate that the early stages of intrusion of the Burro Mountains batholith were accompanied by stress. The ptygmatic folds were probably formed during the early stages of intrusion, while the temperature was high and stresses were still operative.

Igneous-Metamorphic Relations

Contacts

The foliation and layering of the Precambrian metamorphic rocks have partly guided intrusions of the Precambrian igneous rocks. The intrusion of the source rock of the metadiabase was controlled by layering in the source sediments of the Ash Creek series. However, the weakly foliated Ash Creek metasediments had little structural control on granitic intrusions. In most places, massive Bullard Peak rocks, such as granite gneiss and quartz-feldspar gneiss, have sharp, straight contacts with the Burro Mountains granite. Where the granite contact is parallel, or nearly so, to the layering or foliation in the Bullard Peak rocks, the contact is well defined and generally straight. Where the contact is normal to the foliation, lit-par-lit injections are common. This relationship is seen southwest of Bullard Peak (pl. 1).

Xenoliths

Along the ridge north of Eccles Canyon, the foliation in hornblende gneiss and quartz-feldspar gneiss xenoliths parallels that of the main metamorphic exposure to the north. Similarly, the foliation in a group of xenoliths of quartz-feldspar gneiss that crop out around the head of Joe Harris Canyon conforms to the regional northeast strike and steep northwest dip. The enclosing granite has no foliation parallel to that

in the isolated masses; so the masses of metamorphic rocks are either roof pendants or xenoliths that have not been rotated.

Xenoliths of sillimanite gneiss and quartz-feldspar gneiss that lie between the Gila River and Joe Harris Canyon and in the area north of the Gila River have obviously been rotated during enclosure by granite (pl. 1). Xenoliths of hornblende gneiss and quartz-feldspar gneiss south and west of Bullard Peak also show the effect of rotation. Neither the long direction of the xenoliths nor their internal structure shows a consistent orientation among xenoliths or between a xenolith and the large nearby mass of metamorphic rocks. This relationship and the absence of widespread foliation in the Burro Mountains granite support the view that stress was operative during only a part of the intrusion and cooling history of the Burro Mountains batholith.

LARAMIDE AND POST-LARAMIDE STRUCTURAL FEATURES

Normal faults, stocks, and dikes are abundant throughout the Big Burro Mountains. Although some of the faults are younger than Gila conglomerate and thus are of post-Laramide age, the parallelism between these faults and the dikes of presumed Laramide age suggests that faulting began during the late Cretaceous-early Tertiary Laramide orogeny and that movement recurred along the same faults during late Tertiary-Quaternary time.

Faults, Joints, and Fractures

Four fault systems, which trend respectively northwest, northeast, west, and north, transect the rocks in this area. Of these, the northwest-trending faults are most extensive and most numerous. They range in strike from N. 15° W. to N. 60° W.; most strike N. 45°-55° W. and dip 41°-85° SW. They are all apparently normal faults with the exception of the fault west of Slate Creek.

The northwestern end of the fault that parallels Burro Springs Canyon, in the southeast corner of the area, is obscured by bajada deposits and unconsolidated debris from the mountains. The fault that parallels a tributary to Ash Creek Canyon is covered at its southeastern end by alluvium on the Gila River flood plain. Since these two northwest-striking faults are in approximate alinement, they are very likely continuous beneath the cover of alluvium and bajada deposits. The close parallelism of parts of House and Swan Canyons with a line connecting the two faults suggests that the paths of these canyons have been structurally controlled. There may be another fault striking N. 65° W. in the area south of Bullard Peak. Aerial photographs show a strong lineament extending northwest from a point south of the Flying A ranch-house (east of the geologic map, pl. 1), across Black Hawk Canyon, and south of the granite gneiss exposed in Bullard Peak. An apparent struc-

tural discontinuity in the Bullard Peak rocks west of the Flying A ranch further suggests a fault here. Because no conclusive field evidence was found, a fault is not shown on the map.

The northeast-trending faults, which are second in abundance and extent, strike N. 20°-75° E.; some dip up to 65° SE., and others up to 68° NW. In Jacks Canyon, in the area northwest of Ash Creek Canyon, and in a tributary to Black Hawk Canyon, joint sets that strike northwest, northeast, or both, have developed locally, and their position in part controls the drainage pattern.

Only one major north-trending fault was observed. It varies along strike from N. 20° W. to due North and dips almost vertically. West-trending faults occur in the northeast part of the area. One of these, in Goat Canyon, dips steeply north; the other, which strikes about N. 80° W., is obscured by debris from the Tertiary volcanic rocks.

The longest fault in the mapped area is 4½ miles long; several of the northwest-trending faults extend beyond the limits of the area. The fault that parallels a tributary to Ash Creek is exposed discontinuously northwestward for about 10 miles (Elston, 1955b). The Malone fault, the northern end of which appears in the southeast corner of the geological map (pl. 1), extends to the southeast for at least 22 miles (Gillerman, 1951).

The surface traces of these faults are generally straight, with only local deviations from the regional trend. Either a single fault plane or a zone of parallel shears is characteristic. Brecciation, silicification, or mineralization commonly mark the fault zone. The northwest-trending fault that crosses Jacks Canyon in sec. 14, T. 18 S., R. 18 W., contains a massive quartz pod, about half a mile long and 100 feet thick.

Two of the faults contain horse blocks of sedimentary rocks. The northwest-trending fault in sec. 17, T. 18 S., R. 18 W., contains blocks of brecciated dolomite that have been partly replaced by magnesite. In sec. 22, T. 18 S., R. 18 W., a breccia of sandstone, shale, and limestone lies between two northwest-trending faults. Branching faults occur in sec. 4, T. 18 S., R. 18 W., where two parallel northwest-trending faults swing northward in a gentle arc and join in Ash Creek Canyon. Rhyolite and andesite porphyry of Laramide age have been faulted against Colorado shale to the northeast, and against Burro Mountains granite to the southwest (pl. 2C).

Movement along these faults has tilted the large blocks that lie between them. The Beartooth quartzite in the area of Goat Canyon crops out as three homoclinal blocks; two dip north and one dips east. The structure of the quartzite and shale that cap Wild Horse Mesa is essentially a broad syncline whose axis parallels the northwest-trending faults. North of the Gila River, the blocks between the northwest-trending faults are generally tilted down to the southwest. Locally, drag along the faults has produced synclinal and anticlinal structures in the remnants of sediments that overlie the granite. In lower Slate Creek Canyon,

Beartooth quartzite has been folded into a broad syncline, the axis of which trends northwest. The Gila conglomerate shows similar drag effects along the northeast-trending fault between Joe Harris Canyon and the Gila River.

Where the Cretaceous sediments have not been stripped away, it is possible to estimate the displacement along these faults. Displacement along the fault west of Slate Creek has been about 250 feet. The fault that parallels Fox Tail Canyon has a displacement of at least 700 feet.

The relative ages of the four fault systems are difficult to determine because of conflicting evidence. For example, a northwest-trending fault that crosses Slate Creek Canyon about 1¼ miles above the Gila River is offset by a northeast-trending fault. About 2 miles farther up the canyon, a northeast-trending fault is terminated by a northwest-trending fault. In the area of Wild Horse Mesa, however, the following sequence can be established (in order of decreasing age): (1) Northeast; (2) northwest and west; and (3) north. The fault systems probably originated during the same period of Laramide deformation, and some have undergone later movements that have offset Tertiary volcanic rocks and the Gila conglomerate.

Dikes and Stocks

Outstanding features of the larger dikes in this area are their uniform thickness and their straightness along strike. Very likely, these dikes have been intruded into tension fractures or into faults of small displacement which are related to the major fault systems. Large dikes have been emplaced along 3 of the 4 fracture and fault systems. Many of these dikes are as much as 3 miles long and 200 feet thick; several originate from pluglike or stocklike bodies. The largest stock in the area is the Twin Peaks monzonite porphyry stock, which is elongate in a westerly direction. Plugs of rhyolite crop out in the northeast and northwest corners of the area; plugs of andesite porphyry crop out south and southeast of Clarks Peak.

The distribution and orientation of the faults and joints in the area, and the fact that most of the faults are normal, indicate that they resulted from uplift of the Big Burro Mountains. Movement along the northwest-trending faults resulted directly from the uplift of the northwest-trending range; the northeast-trending crossfaults may have resulted from the greater uplift of some portions of the range than of others. The Big Burro Mountains are structurally similar to the Little Burro Mountains and the Silver City range to the east. The northwest-trending mountain ranges are tilted fault blocks that have been uplifted along normal faults on the southwest flank and cut by northeast-trending crossfaults.

Although Laramide deformation in some parts of the Basin and Range province involved extensive folds and thrusts, the Big Burro Mountains do not show these features. However, the absence of thrust

faults is not unique with the Big Burro Mountains. The mountain ranges of the Basin and Range in central Arizona have extensive normal faults and intrusive rocks of Laramide age but show little or no thrusting (Eardley, 1951).

From the evidence in the area of this report, the probable sequence of Laramide and post-Laramide events is as follows: (1) Doming and uplift of the Big Burro Mountains, accompanied by development of fractures, shears, and moderate faulting; (2) intrusion of Laramide stocks and dikes; (3) erosion; (4) extrusion of Tertiary volcanic rocks; (5) uplift and extensive faulting; (6) intrusion of post-Laramide dikes; (7) deposition of Gila conglomerate; (8) continued uplift and renewed movement along older faults.

RELATION OF PRECAMBRIAN AND LARAMIDE STRUCTURES

The parallelism between some of the Precambrian structures and those of Laramide and post-Laramide age suggests that the younger structures may have been controlled in part by planes of weakness in the Precambrian rocks. The normal faults and larger dikes of Laramide age are oriented along northwest and northeast directions. These directions coincide with the regional northeast trend of foliation in the Bullard Peak rocks and the Burro Mountains tonalite, and with the northwest trend of Precambrian pegmatite dikes along the west flank of the mountains.

As stated in the section on petrology, the northwest-striking diabase dike that crosses Eccles Canyon may be of pre-Laramide age. Gillerman and Whitebread (1956) consider diabase dikes in the Black Hawk district, which are similar in composition and orientation to those throughout the Burro Mountains, as being of late Precambrian or early Paleozoic age. The emplacement of these dikes during Precambrian time would further support the idea of early establishment of extensive northwest-trending fractures. Many of the small faults in the Black Hawk district follow northeast- to east-trending dikes of Precambrian granite. Gillerman and Whitebread (1956) interpret this relationship as a reopening in post-Cretaceous time of old Precambrian breaks.

Geological History

PRECAMBRIAN HISTORY

In early Precambrian time, the area now occupied by the Big Burro Mountains was the site of a shallow sea. The source sediments of the Bullard Peak series (argillaceous feldspathic sandstone, calcareous argillaceous siltstone, shale, and dolomitic shale) were probably deposited in the infraneritic area of an unstable shelf in this sea. As subsidence and deposition continued, these sediments attained a thickness of at least 10,000 feet. After their consolidation, they were intruded by thick sills and stocks of leucogranite, and later by sills of diabase that locally transected the sediments and the leucogranite. These intrusions may have been the initial phases of the orogeny that resulted in folding and dynamic metamorphism of both the sediments and the igneous rocks. The sediments were converted to pelitic schists, quartz-feldspar gneiss, hornblende gneiss, and amphibolite; the diabase was converted to hornblende gneiss and amphibolite, and the leucogranite to granite gneiss. The area probably was uplifted during the orogenic period, and subsequently the Bullard Peak rocks may have been subjected to erosion.

During a period of quiescence, when the area was again covered by a shallow sea, the source sediments of the Ash Creek series were deposited in the epineritic part of a stable shelf area to a thickness of at least 5,800 feet. After consolidation of the sediments, the rocks in the area underwent mild dynamic metamorphism, which produced only a poorly defined foliation in the Ash Creek rocks but did not involve folding or severe deformation. This second period of low-grade metamorphism apparently was not recorded in the already highly metamorphosed Bullard Peak rocks.

Anorthosite was then intruded into the Ash Creek series, and diabase was intruded into both Ash Creek and Bullard Peak rocks. The Bullard Peak rocks were not markedly affected by the small intrusions of diabase, but larger dikes and sills of diabase thermally metamorphosed the Ash Creek rocks to various hornfelses and serpentinites.

The complex Burro Mountains batholith was intruded into both series of metamorphic rocks. Early intrusions of tonalite were accompanied by local stress. The large mass of granite magma that followed cooled slowly and uniformly. Pegmatite and aplite are the youngest intrusions related to the batholith. The fluid granite magma was intimately injected into the Bullard Peak rocks along planes of foliation and layering in the deeper part of the batholith, where temperature and pressure were high. Consequently, through the formation of feldspar metacrysts, and through lit-par-lit injection, some of the high-grade metamorphic rocks were locally converted to migmatite. Some xenoliths

of Bullard Peak rocks were partly resorbed by the magma, and sillimanite was developed marginally.

The Ash Creek rocks and the diabase that had been intruded into them were enclosed as complex xenoliths in the upper part of the batholith, where temperatures were lower. The metasediments were not markedly affected by the granitic intrusion, but the diabase was thermally metamorphosed.

The area was uplifted during or shortly after the consolidation of the batholith. During the long period of erosion that followed, the Precambrian rocks were deeply dissected, and the core of the batholith was exposed. At the close of Precambrian time, the igneous and metamorphic rocks were exposed across an erosion surface of moderate relief.

PALEOZOIC AND MESOZOIC HISTORY

No record of the geologic events that occurred between Precambrian and late Cretaceous time is found in the northern Big Burro Mountains; thus the sequence of Paleozoic and Mesozoic events must be inferred from those described in reports of neighboring areas (Paige, 1916; Talmage and Wootton, 1937).

The beginning of the Paleozoic era in southwestern New Mexico was characterized by subsidence and consequent encroachment of a sea whose wave action further reduced the relief on the Precambrian surface. The Upper Cambrian Bliss sandstone, the Ordovician El Paso limestone, and the Ordovician-Silurian Fusselman and Montoya limestones were deposited in apparent conformity. The source material for some of these sediments probably was derived from an emergent area to the north. An abrupt change to conditions of uplift, erosion, and clastic deposition marked the beginning of Devonian time in the Southwest. Talmage and Wootton (1937) interpreted the Devonian Percha shale as having formed during a time of uplift and flooding that caused rapid erosion of a deeply weathered terrain and deposition of carbonaceous mud in a shallow sea. Sedimentation of the Percha shale continued until the end of Devonian time, when the muddy seas cleared. During Mississippian and Pennsylvanian time, thick beds of limestone were deposited.

No evidence of Permian, Triassic, or Jurassic events is found in southwestern New Mexico. Upper Cretaceous rocks rest unconformably on a surface of low relief that ranges in age from Precambrian at the northern end of the Big Burro Mountains, to Pennsylvanian in Silver City quadrangle. Apparently the area was uplifted and tilted during Permian time and then eroded to a low plain. Either this area was emergent during Triassic and Jurassic time, or the sediments deposited during these periods were completely removed before the encroachment of the late Cretaceous sea.

Subsidence of the land mass and the advance of the late Cretaceous

sea brought the last period of marine sedimentation to the area. The Beartooth quartzite, which was deposited as the basal unit, is overlain conformably by the Colorado shale. The later stages of the deposition of the shale were characterized by the addition of abundant volcanic material that originated as submarine extrusions or as accumulations of pyroclastic material.

LARAMIDE AND POST-LARAMIDE HISTORY

The Laramide orogeny began during late Cretaceous-early Tertiary time with a slight doming and uplift of the northwest-trending Big Burro Mountains and the development of fractures, joints, and shears along planes of weakness in Precambrian rocks. Stocks and dikes of intermediate composition were intruded into the Precambrian and Cretaceous rocks. At least five stages of intrusion are recorded in Silver City quadrangle (Paige, 1916). These stocks and dikes were probably derived by means of differentiation of a pluton that underlay the area. The relationship of Laramide intrusive rocks to the Tertiary volcanic rocks is not apparent in the area of this report, but in Silver City quadrangle, stocks of Laramide age were exposed by erosion prior to the eruption of Tertiary lavas (Paige, 1916). The general area must have undergone an extensive period of erosion after the intrusion of the Laramide rocks.

The andesite-rhyolite-basalt flows were poured out during early or middle Tertiary time onto this erosion surface. Extensive uplift along northwest- and northeast-trending normal faults followed the eruption of lavas and offset them. This uplift initiated the erosion of the Big Burro Mountains to their present topographic form and resulted in the beginning of deposition of the Upper Pliocene Gila conglomerate. Renewed uplift caused movement along previously established faults and locally exposed the Gila conglomerate to erosion along the flanks of the mountains. Continued erosion and a change to a semiarid climate in Quaternary time caused the development of pediments and bajada deposits along the flanks of the mountains, terraces along the Gila River, alluvium along drainages, and bolson deposits in basins of poorly developed drainage.

Economic Geology

HISTORY OF MINING

As early as the 15th century, turquoise deposits were mined in the Big Burro Mountains by Pueblo Indians. Although copper deposits at Santa Rita were utilized by the Apache Indians in the 17th century and systematically mined by the Spaniards in 1800, it was not until 1871, when copper was discovered near Tyrone, that the Big Burro Mountains were actively prospected (Lindgren et al., 1910). In 1881 the rich silver veins in the Black Hawk and Telegraph districts were discovered. Silver was mined in the Telegraph district until 1885. Close to a million dollars in silver was removed from the few mines in the Black Hawk district between 1881 and 1893. Both districts are now abandoned.

Additional copper discoveries in the Tyrone district, in 1902, initiated extensive prospecting and mining on the east flank of the Big Burro Mountains. The Phelps Dodge Corporation acquired the properties at Leopold in 1905 and at Tyrone in 1912. The mines were developed for large-scale production, and in 1918 the district reached a peak production of 17 million pounds of copper. Mining was discontinued by Phelps Dodge in 1921, but a small-scale leaching program was continued until 1928. Lessees continued operation of some of the small mines.

Fluorite was mined from the Burro Chief claim in the Burro Mountains in the 1880's for use as flux in the copper smelters. During World War II, the area was extensively prospected for fluorspar of metallurgical grade. About 115,000 tons of fluorspar is estimated to have been produced from the Big Burro Mountains. Of this amount, all but 5,000 tons has come from the Burro Chief and Shrine mines, both outside the area of this report (Gillerman, 1951). Within the area, the Great Eagle fluorspar mine was operated intermittently from 1911 until 1921 and again in 1943-44. A few truckloads of fluorspar ore have been produced from the Long Lost Brother and the Purple Heart deposits.

During the summers of 1954-55, no mines in the area were in production. Exploration work was in progress at a few small fluorite prospects and a scheelite deposit. However, the area is being prospected for tungsten, manganese, and radioactive minerals. The recent interest in radioactive minerals has led to the discovery of economically insignificant radioactive deposits at White Signal and in the Black Hawk district, both outside the area of this report.

PRECAMBRIAN METAMORPHIC DEPOSITS

SERPENTINITE (RICOLITE)

Banded talc serpentinite, as well as some of the massive and mottled varieties that occur in the Ash Creek xenoliths, has been used for building material and for making small decorative articles. Talmage and Wootton (1937) give the following account of ricolite:

> The New Mexico ricolite was first quarried about 1888, and a shipment was made to Chicago, where the material was used as interior wainscoting. . . . According to a statement in the Mineral Resources volume of the United States Geological Survey for 1889, the name ricolite, meaning "rich stone," was proposed for this material by Mrs. L. J. Caldwell of Chicago. At this time the material was described as resembling Mexican onyx but quite different in composition.

There is no other recorded use of this material as a building stone. Because of the striking color of ricolite, its peculiar banded and mottled texture, and the ease with which it can be carved or polished, it has had limited use by amateur lapidarists for jewelry, bookends, paper weights, and other small objects. Mr. Ernest Bennett, of Silver City, has turned lamp bases from ricolite and has experimented with the making of buttons, ash trays, and other articles.

Polished pieces of ricolite are attractive, but the softness of the material limits its use. Several attempts have been made to establish a market and exploit the ricolite deposit (E. Bennett, personal communication), but it has remained mainly a curiosity for mineral collectors and lapidarists. The geology and origin of the ricolite deposit are discussed on p. 45-46, 52-53.

ASBESTOS

Veinlets of cross-fiber chrysotile transect banded talc serpentinite and massive serpentinite in Ash Creek Canyon. The asbestos is most abundant in the xenolith from which ricolite has been quarried and in a few smaller xenoliths to the west (pl. 12). However, because the widely spaced veinlets are less than a quarter of an inch thick, the deposit is too small to be of economic significance.

MAGNETITE

Magnetite serpentinite in Ash Creek Canyon, above the ricolite quarry, locally contains up to 90 percent magnetite. The magnetite-rich serpentinite, however, occurs in a few bands only 1 to 2 feet wide and rarely longer than 10 feet. Because of the limited extent of the exposure and the inaccessibility of the deposit, any further exploration seems inadvisable. Kelley (1949) refers to this magnetite as the only recorded occurrence of "iron ore" of Precambrian age in New Mexico. The geology of the deposit is described on p. 47, 52.

PRECAMBRIAN PEGMATITES

Mica

Muscovite that might be of commercial size and quality was observed in only one pegmatite in this area. A zoned pegmatite on the ridge west of Black Hawk Canyon contains muscovite books about 5 inches across and half an inch thick. Because muscovite occurs in accessory amounts in only a few of the larger pegmatites, it does not appear to warrant consideration as an economic product in this area.

LARAMIDE AND POST-LARAMIDE HYDROTHERMAL VEINS

General Statement

Hydrothermal fissure fillings occur in the northern Big Burro Mountains-Redrock area along faults and shear zones that trend northeast or northwest, and are probably related to similarly trending major faults. Scheelite, metallic sulfides, or fluorite occur as veinlets or disseminations in a gangue of quartz, chert, jasper, or calcite.

The granite wall rocks adjacent to the veins have been subjected to argillic alteration, sericitization, or silicification. The width of the alteration zone depends largely on the thickness of the vein, but it rarely exceeds a few feet. Most commonly the feldspars are altered to sericite and clay minerals. The mafic minerals are partly replaced by chlorite and magnetite.

The most intense alteration was observed east of the Great Eagle mine, in Joe Harris Canyon, where the granite contains many small but closely spaced veinlets of fluorite and chalcedony. The surface of this altered granite shows a striking contrast of brick-red feldspar subhedra, several centimeters long, enclosed in a bright-green matrix of chlorite and magnetite. In thinsection, remnants of hematite-coated microcline are seen to be partially replaced by an aggregate of tiny sericite flakes. Plagioclase is completely replaced by sericite and coarsely granular calcite. All the mafic minerals are replaced by fibrous aggregates of chlorite and magnetite. Quartz and apatite occur in accessory amounts enclosed by sericite and chlorite. This altered rock contains much less quartz and more hematite and magnetite than does unaltered granite in the area. Magnetite, however, is more abundant than is commonly found in the alteration of hornblende or biotite to chlorite and magnetite. The alteration apparently involved the addition of OH and Fe and the removal of Si. The Si removed from the wall rock in this area may have been redeposited as chalcedony in some of the nearby fluorite veins. However, most of the altered wall rock in the area seems to have Si added rather than removed.

The conditions under which these deposits were formed range from hypothermal to low epithermal. The assemblage of scheelite-epidote-

quartz occurring at the Rice-Graves claim is indicative of hypothermal deposition. Several prospects and mines contain galena, sphalerite, chalcopyrite, and pyrite, an assemblage denoting mesothermal conditions. The deposits in the Black Hawk district, which resemble those at Great Bear Lake, Canada, and Joachimsthal, Czechoslovakia, contain an assemblage of Co-Ni-Ag-U minerals typical of mesothermal deposits (Gillerman and Whitebread, 1956). Fluorite deposits range from those that are associated with considerable galena and that may be high epithermal, to a few that contain fluorite and hypogene manganese oxides and whose texture suggests hot-spring deposits.

Most of these deposits occur in Burro Mountains granite but appear to be related to Laramide and post-Laramide stocks and dikes. Gillerman and Whitebread (1956) related deposits in the Black Hawk district to the Twin Peaks monzonite porphyry stock. A deposit of galena in Little Bear Canyon and a psilomelane deposit west of Jacks Canyon are related to Laramide andesite porphyry dikes. The fluorite deposits do not seem to show a relationship to intrusive rocks, but their localization along faults that transect Tertiary volcanic rocks indicates that they are younger than the lavas.

Gabelman (1955) states that the Big Burro Mountains are mineralogically zoned with uranium deposits on the margin and fluorite deposits in the Precambrian granite core. The distribution of mineral deposits in the northern Big Burro Mountains-Redrock area does not support this conclusion.

Tungsten

Rice-Graves Claim

Scheelite has recently been found in small amounts in the Big Burro Mountains. The largest known scheelite deposit in the area of this report is on the ridge north of Eccles Canyon, in NW¼ sec. 24, T. 19 S., R. 17 W. (pl. 1). This deposit was being explored by the owners, F. Rice, of Cliff, New Mexico, and G. Graves, of Florida, during the summer of 1955. Scheelite occurs in a silicified zone in a hornblende gneiss xenolith that is enclosed in Burro Mountains granite. The exposure of the xenolith is about a quarter of a mile long and 100 feet wide. Northeast-trending pegmatite dikes transect the hornblende gneiss and granite.

The hornblende gneiss is 100 feet thick, strikes N. 65°-80° E., and dips 46°-78° NW. A zone of silicification about 5 feet thick, parallel to the layering in the hornblende gneiss, is exposed in two 10-foot pits (fig. 1). The silicified zone is made up of veins of quartz; masses of quartz and coarse, recrystallized hornblende; and masses of fine- to medium-grained hornblende, epidote, and quartz. Scheelite occurs as millimeter-long anhedral grains in both quartz veins and quartz-epidote-hornblende masses. A few granular scheelite clusters, several centimeters across, were observed in the pits.

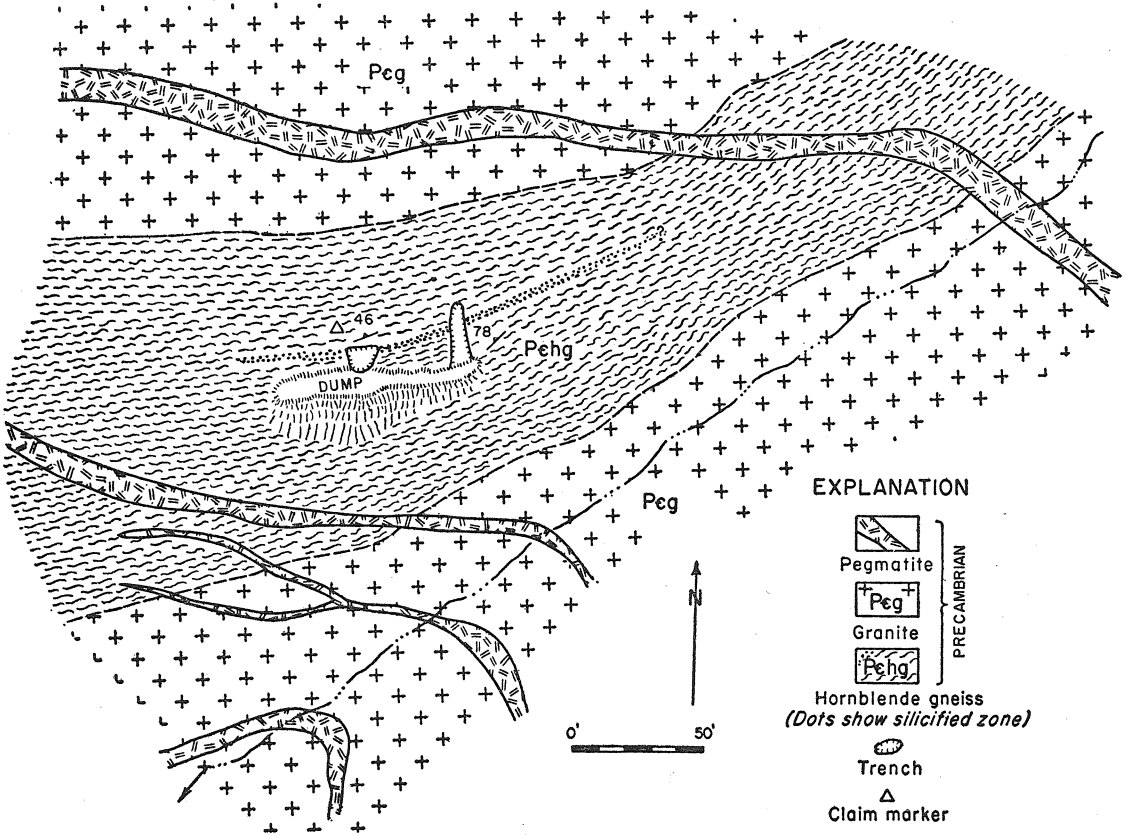

Figure 1

GEOLOGICAL SKETCH MAP OF SCHEELITE DEPOSIT

NW¼ sec. 24, T. 19 S., R. 17 W.

A thinsection from a narrow quartz vein in hornblende gneiss shows anhedral epidote grains replacing hornblende in the gneiss. Scheelite replaces hornblende and epidote along grain boundaries. Most of the scheelite occurs as subhedra enclosed in the quartz veins. Microscopically, the granular hornblende-epidote-quartz rocks show relict patches of unoriented green hornblende crystals in a mosaic of epidote, quartz, and scheelite grains about a millimeter across. Hornblende is transected by epidote, and both are partly replaced by scheelite. Quartz veins all three minerals and encloses euhedra of epidote and scheelite. The sequence of mineral formation is: (1) Hornblende; (2) epidote; (3) scheelite; and (4) quartz. The formation of this deposit involved a recrystallization of the hornblende in hornblende gneiss, replacement of some of the hornblende by epidote and scheelite, and deposition of scheelite and quartz by hydrothermal solutions. The solutions provided W and Mo, and possibly Ca and Si, for the reactions. However, Ca and Si may have come originally from the destruction of hornblende and plagioclase in the hornblende gneiss wall rock.

Two generations of scheelite in the deposit show the following differences in fluorescence and index of refraction:

AGE	FLUORESCENT COLOR	ω	ϵ
Older	yellow white	1.921	1.938
Younger	blue white	1.919	1.937

These characteristics indicate that both varieties of scheelite contain less than 1 percent Mo, but the older scheelite contains slightly more Mo than the younger scheelite (Greenwood, 1943; Cannon and Murata, 1944; Vermaas, 1952).

The age of the scheelite mineralization is not clearly indicated by field relations, because only Precambrian rocks crop out in the area around the prospect. It may have formed during Precambrian time, or it may be related to the Tertiary tungsten deposits in southwestern New Mexico described by Lindgren et al. (1910) and Kerr (1946).

The Rice-Graves prospect, as exposed at the time of the writer's visit, did not show enough scheelite for profitable mining. However, further exploration at this prospect or in the general area might reveal more extensive mineralization.

S. Harper Claim

A scheelite claim staked by Sherman Harper, of Silver City, lies southeast of Bullard Peak in a small tributary to Black Hawk Canyon, in sec. 32, T. 18 S., R. 16 W. A massive quartz vein, about 2 feet thick, that strikes N. 32° W. and is vertical in hornblende gneiss is exposed in a 20-foot shaft. Scheelite is very sparsely disseminated in the quartz vein and in the hornblende gneiss country rock.

Copper

In addition to the copper minerals associated with the lead deposits described below, copper mineralization was observed along the extensive northeast-trending fault that crops out between Joe Harris Canyon and the Gila River. No primary sulfides were found near the east end of the fault in NW¼ sec. 20, T. 18 S., R. 17 W., but chrysocolla and minor tenorite occur as veinlets and fracture coatings in fault gouge and in the granite footwall. Films of malachite and chrysocolla were observed in dump material from an adit driven through the fault into Precambrian granite and metadiabase in sec. 24, T. 18 S., R. 18 W.

Lead

Lead Mountain

Two abandoned lead mines are in a single vein on the south slope of a peak known locally as Lead Mountain. The peak lies east of Slate Creek, in SW¼ sec. 36, T. 17 S., R. 18 W. (pl. 1). The vein is a mineralized shear zone from 5 to 10 feet thick that strikes N. 30°-35° E. and dips 58°-65° SE. in Burro Mountains granite. The trace of the vein crops out about halfway up the steep slope. Two adits have been driven into the mountain along the vein; both are partly caved. For about 25 feet on both sides of the vein, feldspar in the granite has been intensely kaolinized; the altered granite contains veinlets of quartz and millimeter-long pyrite cubes.

Samples from the mine dumps contain columnar quartz and galena in lenses several inches across and as disseminated euhedral grains less than half an inch across. Crusts of coarsely crystalline violet fluorite coat fragments of kaolinized granite. No primary copper sulfides were observed, but some of the material on the dump is stained by chrysocolla, as well as by oxides of iron and manganese.

Slate Creek Canyon

The Ruth and Dorothy mines are in the bottom of Slate Creek Canyon, SW¼ sec. 36, T. 17 S., R. 18 W., on the west side of Lead Mountain (pl. 1). According to the remains of a location notice found on the property, one of the owners is John Edwards. Workings consist of an adit that is connected to the surface by a 15-foot shaft at the end of the adit. A breccia zone in Beartooth quartzite has been mineralized along a fault that strikes N. 62° E. and dips 68° NW. The trace of the fault is exposed along the east side of Slate Creek Canyon and in the mine workings. Veins of milky to pale amethyst quartz, up to a foot thick, transect the brecciated quartzite. Drusy quartz coats the breccia blocks and lines cavities between them. Coarsely crystalline galena, the most abundant sulfide, fills narrow fractures and small cavities. Associated with the galena are minor amounts of sphalerite, bornite, chalcopyrite,

and pyrite. Films of malachite, azurite, limonite, and manganese oxides coat fractures in weathered surfaces of quartz and quartzite.

These mines appear to have been worked fairly recently, but it is doubtful if any ore has been produced. The deposit, as exposed in the summer of 1955, did not seem to be of economic interest. However, further exploration may reveal larger bodies of galena in the Burro Mountains granite below the quartzite. A deterrent to further work in this area is its inaccessibility.

Little Bear Canyon

An abandoned mine lies in Little Bear Canyon, in NW¼ sec. 15, T. 18 S., R. 17 W., three-quarters of a mile above the junction of Little Bear and Bear Canyons (pl. 1). On the west slope of the canyon, three adits were driven into a single vein about 5 feet thick. The adits are inaccessible, but the size of the dumps indicates that the workings were extensive. Several shacks and an ore bin in the canyon bottom have been partly destroyed by floods. The vein is a mineralized fissure in Burro Mountains granite and in xenoliths of quartz-feldspar gneiss of the Bullard Peak series. Talus and mine dumps cover the outcrop of the vein; however, the position of adits along the vein shows that it strikes west and dips steeply south. The vein apparently parallels a thick dike of Tertiary andesite porphyry that crops out north of the mine (pl. 1). The wall rock along the vein and fragments in the vein are strongly sericitized. Specimens from the ore bin show narrow veins, nodules, and disseminations of galena and sphalerite, and lesser amounts of chalcopyrite and pyrite, in a gangue of columnar and massive quartz and white calcite. The writer observed larger masses of primary sulfides at this mine than at any other in the area. Some of the sulfide veins are as much as 6 inches across.

A polished section of the coarsely crystalline sulfides shows pyrite rimmed and embayed by sphalerite. Sphalerite encloses tiny blebs of chalcopyrite in parallel orientation. Galena occurs along sphalerite grain boundaries and as veins in sphalerite. The sequence of formation of ore minerals is: (1) Pyrite; (2) sphalerite and chalcopyrite (unmixed from solid solution?); and (3) galena. This assemblage of primary sulfides in a quartz-carbonate gangue denotes deposition under mesothermal conditions (Lindgren, 1933). The proximity of thick Tertiary andesite dikes suggests that the mineralization may also be of Tertiary age.

Live Oak Prospect

The Live Oak prospect, owned by N. P. Granfel and H. R. Eaton, of Silver City, is in NE¼ sec. 19, T. 19 S., R. 16 W. (pl. 1). A northwest-trending vertical quartz vein, about a foot thick, in Burro Mountains granite is exposed in two 15- to 20-foot shafts. The property has not been worked for many years. Granular masses, less than 4 inches long, of

galena, sphalerite, and pyrite are enclosed in massive limonite-stained quartz. Polished-section study shows that sphalerite was deposited in cavities lined with a druse of quartz. The sphalerite is similar to that from Little Bear Canyon in having tiny blebs of chalcopyrite locally arranged in trains, at random, or in parallel orientation.

A similar vein, less than a quarter of a mile southeast of the Live Oak property, is exposed in a recently excavated trench. The vein contains small amounts of galena, chalcopyrite, and pyrite, sparsely disseminated in quartz.

SILVER

Telegraph District

The Telegraph district lies on the northwest side of the Gila River, in SW¼ sec. 32, T. 17 S., R. 17 W. Silver ore was discovered in 1881, and in 1885 a stamp mill was erected on the Gila River. In 1903 a leaching plant was built near the mill site, but the small ore body was soon exhausted, and the camp was abandoned by 1905 (Lindgren et al., 1910).

In the area of the Telegraph mine, blocks of Beartooth quartzite have been faulted against the Burro Mountains granite by northwest-trending faults (pl. 1). Northeast-trending crossfaults transect both granite and quartzite. The Telegraph deposit is a mineralized crossfault striking N. 28° E. and dipping 64° SE. The fault trace crops out near the top of a steep hillside; the quartzite that caps the hill is only slightly offset by the fault. An adit was driven into the hill along the vein, and the ore was stoped upward to the surface. From the appearance of the timbering, the vein was less than 3 feet thick at the entrance to the adit and narrowed rapidly to less than a foot at the surface. The granite country rock is silicified and stained by hematite, limonite, and manganese oxides. Limonite-stained quartz is abundant. Small nodules and tiny veinlets of porous, earthy manganese oxides and a few botryoidal masses of psilomelane occur in kaolinized and silicified granite and in vein quartz. The results of tests for silver in the vein material were negative.

When L. C. Graton visited the mine in 1905, the only visible mineralization was ". . . fractured, much silicified granite, with drusy iron-stained quartz and in places minute black specks, which probably carried the silver" (Lindgren et al., 1910). Apparently there is no record of the mineralogy or the production of the mine.

Black Hawk District

The Black Hawk mining district has recently been studied and mapped in detail by Gillerman and Whitebread, of the United States Geological Survey. Since further detail work is beyond the scope of this report, the writer has abstracted some of the material in the following

description from a report of their studies (Gillerman and Whitebread, 1956).

The Black Hawk district lies in Black Hawk Canyon, at the eastern edge of the area of this report (pl. 1). Approximately $1 million in silver was produced from the several mines in the district between 1881 and 1893 (Lindgren et al., 1910). The Black Hawk mine was reopened in 1917, but there is no record of any production. The latest reported production is a small lot of silver ore from the Bronx mine in 1920 (Lasky and Wootton, 1933). In 1952, three core holes were drilled to a depth of 1,000 feet in search of nickel, cobalt, and uranium. One core showed sparse ore minerals in a carbonate gangue; the other two were barren.

The ore deposits occur in narrow northeast-trending fissure veins that transect Precambrian igneous and metamorphic rocks, as well as younger diabase, rhyolite, quartz monzonite, monzonite porphyry, quartz diorite, and andesite. The monzonite porphyry forms part of the Twin Peaks stock and appears to be related to the mineral deposits. Many minerals containing Ag, Co, Ni, and U have been reported from this district. The major ore minerals, however, are native silver, argentite, niccolite, skutterudite, nickel skutterudite (type locality), bismuthinite, pitchblende, and sphalerite in a gangue of carbonates, quartz, barite, and pyrite.

Astrologer Mine

The Astrologer mine is in SW¼ sec. 20, T. 19 S., R. 16 W., in the southeast corner of the area of this report. The mine has been inactive for many years. According to Mr. Charles Ray, of Lordsburg, the present owner, the mine has produced galena, silver, and gold. The surrounding area is underlain by the Burro Mountains granite and related pegmatite and aplite dikes, which are transected by small northeast-striking dikes of andesite.

The ore deposits are in several subparallel quartz veins that trend northeast and are vertical. The deposits were exploited through two vertical shafts on separate veins. Six drifts extend from the shafts, but none is over 75 feet long (Charles Ray, personal communication). The mine workings are now in poor condition. Specimens collected from the mine dump contain chalcopyrite, chalcocite, galena, and pyrite, disseminated in massive quartz.

Fluorite

General Features

The fluorspar deposits of New Mexico have been the subject of reports by Johnston (1928), Talmage and Wootton (1937), and Rothrock et al. (1946). Deposits in the area of the Big Burro Mountains have been studied by Gillerman (1951). Most of the deposits in the northern Big Burro Mountains-Redrock area have not been developed further since

ing. The cost of trucking ore about 30 miles from the mine to the railroad at Lordsburg is also to be considered.

Hope Prospect

The Hope prospect is an old prospect that was restaked by J. A. Moreland and Ernest Sisco in March 1955. It lies on the west slope of Joe Harris Canyon, about three-eighths of a mile southeast of the Great Eagle mine. A 20-foot pit exposes a vein of green fluorite and chert breccia, about 2 feet thick, that strikes N. 15° W. and dips 40° SW. in the Burro Mountains granite. Between this prospect and the Gila River, many small northwest-striking veinlets in granite contain a breccia of white, gray, or brown chalcedony fragments cemented with light-green fluorite.

Redrock Area

Narrow fluorite veins in Precambrian granite and Tertiary rhyolite are exposed in prospect pits and tunnels on the north side of the Gila River, about 1½ miles northeast of the Redrock post office (pl. 1). Most of the veins parallel two vertical rhyolite dikes that strike N. 40°-50° W.; a few of the veins strike northeast. Toward the southeast end of the dikes, the veins become thicker, several of them merge into larger veins, and fluorite becomes more abundant. The maximum width of the zone of mineralization is about 125 feet, but individual veins are rarely more than 2 feet thick.

The veins that parallel the westernmost rhyolite dike are fissure fillings of colorless to light-green or yellow fluorite and light-gray chert. The veins in this group are generally less than 6 inches thick; fluorite commonly fills less than half of the vein. Two shafts have been sunk on these veins, but the workings are not accessible.

At the southern end of the easternmost dike, veins of chert with small amounts of dark-purple fluorite and pyrite are exposed in two short adits and a 4-foot prospect pit. These veins have a maximum thickness of about 3 feet. The radioactive count in one of the tunnels is almost twice the background count. The vein exposed in this tunnel is predominantly chert, but several large pieces containing fine-grained fluorite and pyrite in a chert matrix were found on the dump. These pieces are weakly radioactive. The fluorite, which ranges in color from violet to dark purple, occurs as granular masses and as single millimeter-long euhedra enclosed in chert.

Thinsections show that the history of this deposit involved several periods of deposition and brecciation not unlike that of other fluorite veins in the area. The paragenesis of this deposit is: (1) Brecciation; (2) deposition of tan to brown jasper; (3) brecciation; (4) deposition of colorless quartz, followed by pyrite and fluorite; and (5) deposition of light-tan jasper, with small amounts of pyrite and fluorite.

The fluorite from this deposit shows a wide variation in color and color distribution. A few of the grains are colorless or a single shade of violet or purple. The following color distributions are also common: (1) Dark-purple halos around minute opaque inclusions in colorless fluorite; (2) colorless halos in purple fluorite, some around pyrite(?) inclusions; (3) violet to purple margins along fractures in colorless fluorite; (4) simple core-margin zoning; some grains with colorless cores and purple margins, others reversed; (5) alternating colorless and purple zones parallel to the crystal outline. The boundaries between zones are sharp, gradational, or feathery. The color in some of the zones is uniform; in others, the zone is marked by color spots or parallel streaks.

The occurrence of dark-purple fluorite as halos and along fractures suggests that the color resulted from emanations from radioactive minerals precipitated from hydrothermal solutions with the fluorite. The weak radioactivity of the area and the occurrence of radioactive minerals in the same vein system about half a mile northwest of this deposit support this origin. The distribution of the purple color in crystallographic zones may be the result of selective adsorption of trace amounts of radioactive substances during the crystal growth.

Long Lost Brother Prospect

The Long Lost Brother deposit is on the west flank of the Big Burro Mountains, about three-quarters of a mile north of the Redrock-Silver City road. The deposit was mined during 1943-44 by the owners, Charles Ray and Sid Watson, of Lordsburg, but only a few truckloads of ore were shipped (Gillerman, 1951).

A map of this deposit appears in Gillerman's (1951, pl. 53) report on fluorspar deposits in the Burro Mountains. The position of the deposit, as located by Gillerman on a United States Forest Service map of the Gila National Forest, appears in SE¼ sec. 14, T. 19 S., R. 17 W. When plotted, however, on the New Mexico Highway Department map SW 9C, which the writer used as a base, the deposit falls in NE¼ sec. 23, T. 19 S., R. 17 W. (pl. 1).

Fluorite veins, as much as 4 feet thick, occur discontinuously along two northeast-trending faults that dip steeply northwest in the Burro Mountains granite and Bullard Peak biotite gneiss. The westernmost fault has small lenses for a distance of about 1,200 feet along strike; the eastern fault is mineralized for about 400 feet. Development was by means of a 20-foot shaft at the southern end of the eastern vein, a narrow stope extending northeastward from the shaft to the surface, and several pits and trenches. Fluorite from this deposit is light yellow to green and occurs as massive or columnar types or as a breccia cemented by jasper. Veinlets of manganese oxides, as much as 2 mm thick, transect fluorite in the western vein and also occur intergrown with fluorite and jasper near the core of the vein.

Wild Horse Mesa and Vicinity

Fluorite deposits occur around the north and west slopes of Wild Horse Mesa, in secs. 2 and 3, T. 18 S., R. 17 W. (pl. 1). The mesa, underlain by Burro Mountains granite and a few xenoliths of hornblende gneiss, is capped with Beartooth quartzite and Colorado shale. Fissure fillings of fluorite, jasper, and chert occur along numerous northeast- and northwest-trending faults and shear zones. Although the faults offset the sedimentary rocks, mineralized portions of the faults are in granite.

A recently worked mine that lies at the north edge of Wild Horse Mesa was not in operation during September 1955; a detailed study of the deposit was not feasible at the time of the field investigation. The property is apparently the one described by Gillerman (1951) as the Purple Heart deposit owned by John Harrison, of Silver City. According to Gillerman, fluorite occurs as seams, fillings, and crusts in breccia zones of argillized granite. Development consists of a 65-foot shaft and a 100-foot shaft on subparallel northwest-trending veins. From 1947 to 1949, about 400 tons of fluorite ore was produced from this mine.

In September 1955, the only deposit being worked was a small prospect off the east side of the mesa, near the head of Buzzard Canyon. J. B. Tucker, who was working the mine, and C. C. Hazen, of El Paso, own the deposit, which they called the Purple Heart. According to Mr. Tucker, several carloads of fluorite ore had been produced recently from the deposit. The vein strikes N. 34° W. and dips 68° NE. Fluorite is exposed in the vein for 200 feet to the northwest of the shaft and 1,200 feet to the southeast. A 50-foot shaft has been sunk downdip on the vein; an inclined stope extends northwest from the shaft to the surface. At the bottom of the shaft, 6 inches of calcite separate a foot-thick layer of colorless, yellow, or light-green fluorite from the granite footwall. A zone of fault gouge, about 2 feet thick, lies between the fluorite layer and the granite hanging wall. The fluorite is massive to granular; some has well-developed crystal faces. No breccia ore was observed in the mine.

An abandoned mine lies about 100 yards south of the Tucker-Hazen property, across a small tributary to Buzzard Canyon. The workings consist of a 100-foot vertical shaft and caved stopes extending southward. A windmill has been erected in the shaft to pump water for cattle. The vein is covered by debris, but it apparently strikes north and is close to vertical. Specimens collected from the dump show crusts of purple fluorite on fragments of kaolinized granite. Some of the purple crusts have overgrowths of colorless fluorite that has crystallized in coarse octahedrons. Veinlets of colorless fluorite mottled with purple cut altered granite. Apparently the vein contains considerable quartz, jasper, and calcite gangue. A type of gangue which is peculiar in the area consists of calcite and milky quartz in alternating sheets usually less than a

millimeter thick and 5 cm across. Solution of calcite leaves a type of boxwork of parallel sheets of quartz.

The Clover Leaf prospect, owned by Roy Chambers, of Silver City, lies west of Wild Horse Mesa, in sec. 3, T. 18 S., R. 17 W. The writer did not see this deposit, but a 6-foot vein of fluorite and much quartz is reported to be exposed in a 10-foot prospect pit (Gillerman, 1951).

MANGANESE

General Features

Psilomelane and lesser amounts of pyrolusite and wad occur in narrow veins, as small pockets in veins, and as thin fracture coatings in the Burro Mountains granite. Botryoidal psilomelane nodules, as large as 4 inches across, occur locally as float on many of the canyon slopes in the northwest part of the area of this report. Manganese oxides were observed at the following localities, but only the Black Eagle deposit has been mined; the others do not contain manganese minerals in minable quantities: (1) Along the north side of a thick quartz vein northwest of Jacks Canyon, NW¼ sec. 14, T. 18 S., R. 18 W.; (2) Simpson prospect, about 2 miles south of Clarks Peak, SW¼ sec. 14, T. 18 S., R. 18 W.; (3) with chert in a 2-foot vein along the hanging wall of an andesite porphyry dike, NE¼ sec. 14, T. 18 S., R. 18 W.; (4) on the ridge between Joe Harris Canyon and the Gila River, NE¼ sec. 24, T. 18 S., R. 18 W., and NW¼ sec. 19, T. 18 S., R. 17 W.; (5) in the center of a fluorite vein at the Long Lost Brother claim, in NE¼ sec. 23, T. 19 S., R. 17 W.; (6) the Black Eagle mine in the SW¼ sec. 6, T. 18 S., R. 18 W.

The manganese oxides at these last two deposits are hypogene and are related to late stages of the Tertiary fluorite mineralization. Most of the other deposits resulted from concentration of manganese oxides by weathering processes and are thus supergene.

Black Eagle Mine

The Black Eagle mine, in SW¼ sec. 6, T. 18 S., R. 18 W., is on a mineralized part of a northwest-trending normal fault that extends about 4 miles southeast of the mine and northwest beyond the area of this report. A few truckloads of manganese ore have been produced by the owner, H. E. McCray, of Deming, New Mexico. The vein, from 6 to 8 feet thick and made up primarily of black, coarse, crystalline calcite and lesser amounts of manganese oxides, follows northwestward along the fault for about 375 feet, then swings westward into the hanging wall of Tertiary volcanic rock (fig. 2). At the adit entrance, the fault and vein strike N. 23° W. and dip 69° SW. A 6-inch zone of bright-orange fault gouge separates the vein from the granite footwall. The granite footwall and fragments of granite enclosed by the vein show extensively kaolinized microcline.

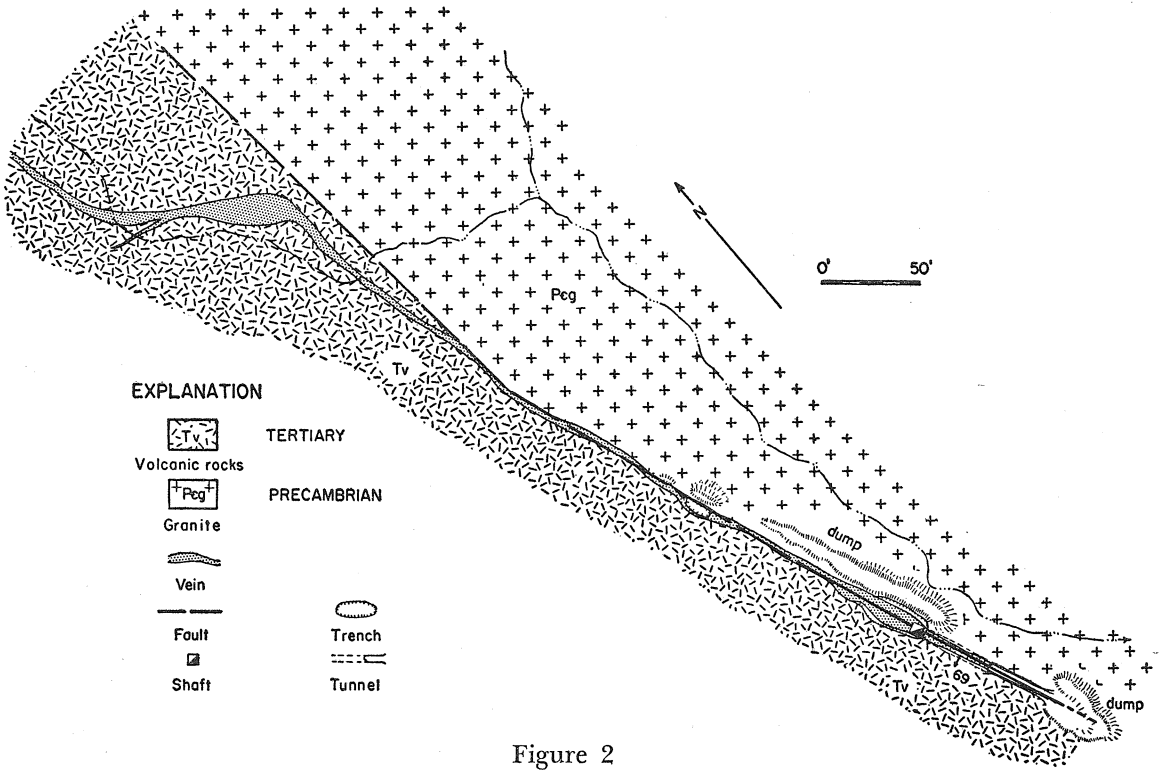

Figure 2

GEOLOGICAL SKETCH MAP OF THE BLACK EAGLE MINE

SW¼ sec. 6, T. 18 S., R. 18 W.

Development consists of an inclined adit about 75 feet long that connects with a vertical shaft from which small stopes extend (pl. 11B). The vein is also exposed in shallow trenches for 150 feet northwestward along the strike.

The manganese minerals appear to be concentrated for 100 feet along the southeast end of the vein and near the surface. In the vicinity of the shaft, about half the vein is manganese oxides, but to the northwest, the vein is almost completely calcite. This black, coarsely crystalline calcite, the most abundant vein mineral, contains veinlets, lenses, and nodules of psilomelane and lesser amounts of pyrolusite and wad. Lenses of pink, finely crystalline calcite are contained in the black calcite; both types are veined by white to gray calcite. A thinsection containing all three varieties of calcite and abundant manganese oxides shows that the pink calcite contains tiny anhedral grains of fluorite. The black calcite derives its color from numerous feathery inclusions of manganese oxides, some of which are a millimeter long. The black calcite cuts the pink variety, and both are veined by white calcite that is free of inclusions. The sequence of mineral deposition is shown by fluorite rimmed successively by pink calcite, black calcite containing included manganese oxides, and colorless calcite. Some veinlets of psilomelane that transect colorless calcite are probably supergene. The sequence of events that led to the formation of this deposit is:

1. Faulting of Tertiary volcanic rocks against Precambrian granite;
2. Deposition of the following minerals from low-temperature hydrothermal solutions (hot springs?):
   a. Small amounts of fluorite and pink calcite,
   b. Brecciation(?), followed by abundant black calcite and manganese oxides,
   c. White calcite, with small amounts of manganese oxides;
3. Near-surface concentration by supergene processes of manganese oxides disseminated in black calcite.

Radioactive Minerals

A rhyolite-jasper breccia from a claim that was located in NE¼ sec. 22, T. 18 S., R. 18 W., by Gerald Hunt, of Clifton, Arizona, is weakly radioactive. Burro Mountains granite underlies the area around this claim. A northwest-trending rhyolite dike that is nearly vertical extends southeastward from the claim for a little more than half a mile. Veins of dark-purple fluorite, pyrite, and cryptocrystalline quartz occur as fissure fillings along the southeast end of this dike. For a distance of about 75 feet, the dike has been brecciated and cemented with brown cryptocrystalline quartz. The rhyolite fragments range from a quarter of an inch to 6 inches; the matrix has irregular cavities up to half an inch long that are lined with drusy quartz. This breccia is well exposed in 2 pits from 6 to 8 feet deep (fig. 3). The attitude of the brecciated

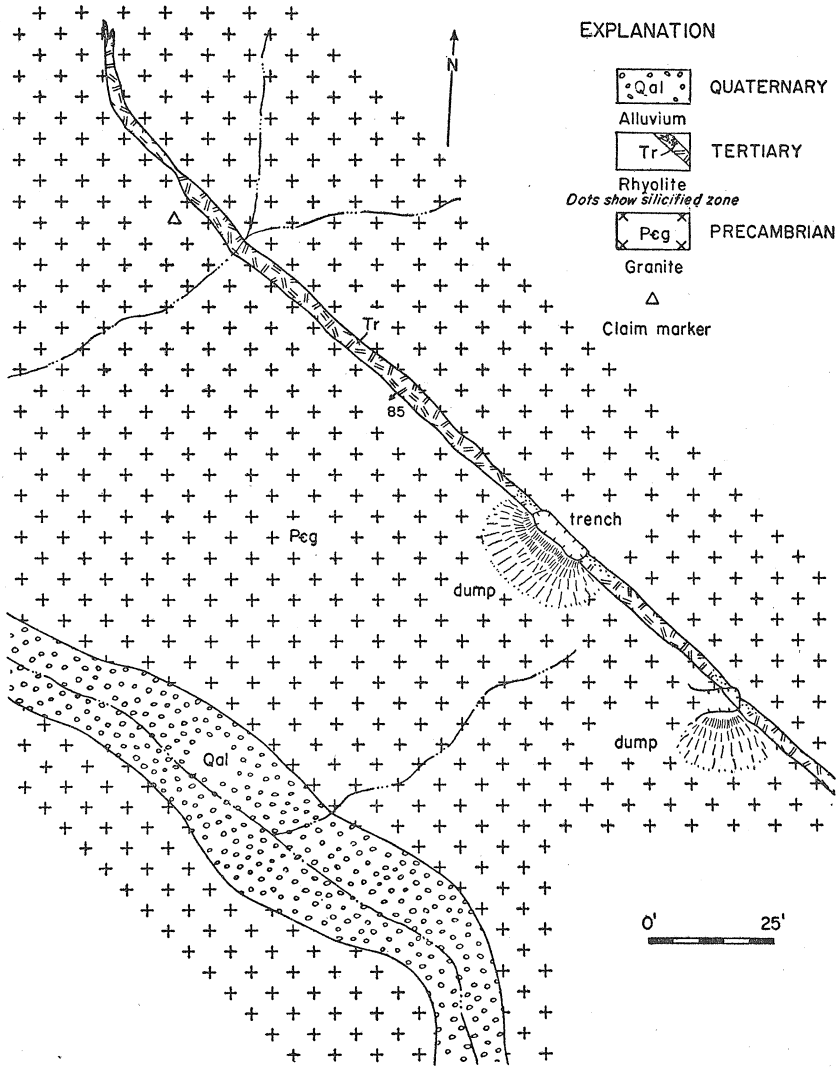

Figure 3

GEOLOGICAL SKETCH MAP OF RADIOACTIVE DEPOSIT
NE¼ sec. 22, T. 18 S., R. 18 W.

dike is N. 48° W., 85° SW. Weathering leaves the rhyolite a light pink and the quartz matrix a light tan. Dendritic manganese oxides stain the matrix around the margins of a few of the fragments. On a freshly broken surface, the fragments are red, and the matrix is brown.

Thinsection examination shows that the rhyolite fragments are silicified. Microphenocrysts of partly sericitized oligoclase are enclosed in an aphanitic matrix that contains abundant secondary microgranular quartz. The matrix is made up of fine- to microgranular quartz that is coarser grained around the edges of the cavities, some of which are partly filled with calcite.

The radioactivity in the prospect pits and on the dumps is about twice the background count. An autoradiograph exposed for 7 weeks showed that radioactive minerals are nonuniformly distributed in the cement (pl. 11C). Several small darkened areas in the fragments resulted from radioactive minerals deposited along fractures in the rhyolite fragments. An ultraviolet light reveals tiny specks that fluoresce a brilliant yellow green. According to Mr. Hunt, the owner of the claim, the mineral has been identified as uranophane. Not enough material could be isolated to confirm this identification.

The radioactive mineralization is clearly related to the deposition of cryptocrystalline quartz that cements the breccia. The presence of fluorite and the same type of cryptocrystalline quartz at the southeast end of the same rhyolite dike shows a genetic relationship between the fluorite and radioactive mineralization at this prospect. The hydrothermal deposition was probably at low temperature and under near-surface conditions.

LARAMIDE AND POST-LARAMIDE REPLACEMENT DEPOSITS

MAGNESITE

Small magnesite deposits are scattered along the western side of the tributary to Ash Creek that parallels a major northwest-trending fault in N½ sec. 17, T. 18 S., R. 18 W. (pl. 1 and 12). The magnesite is poorly exposed in a few prospect pits on the west slope of the tributary from its junction with Ash Creek northwestward for about half a mile. The northernmost and best exposed deposit crops out on a steep hillside, where it has been eroded into miniature badland topography (pl. 11A). The magnesite is faulted against Burro Mountains granite to the east and is covered by debris from the Gila conglomerate to the west. Magnesite is exposed in an area about 20 yards wide and 25 yards long.

This largest exposure contains horizontally bedded magnesite, cryptocrystalline quartz, and lenses of white, finely crystalline dolomite. On a weathered surface, the more resistant siliceous lenses and layers project from the softer carbonate. The magnesite weathers out as inch-long nodules that are hard, white, and stained light red along fractures. A

fresh surface of the siliceous layers shows veinlets of quartz and magnesite in a fine-grained matrix. Under the microscope, the siliceous layers appear as a matrix of tightly interlocked fine-grained quartz, cut by veinlets of slightly coarser grained quartz. Veinlets of magnesite transect the matrix and quartz veinlets. Magnesite in the nodules is too fine grained for optical determination. However, chemical tests on the weathered nodules served to identify the mineral as magnesite.

Veinlets and diffuse masses of magnesite transect dolomite. The dolomite and some of the fine-grained quartz originated as bedded sedimentary rocks that were veined first by quartz and then veined and replaced by magnesite. Two possibilities exist for the origin of the carbonate host rocks: (1) The sediments are of Paleozoic or Mesozoic age similar to the horse blocks north of the Gila River, in sec. 22, T. 18 S., R. 18 W. (pl. 1); (2) the sediments are Precambrian in age and are related to the Ash Creek xenoliths.

Both possibilities are supported by various lines of evidence. Yale and Stone (1921, 1922) reported magnesite from Ash Creek Canyon in blocks of limestone enclosed in granite and cut by dikes of diabase older than the granite. Their report does not clearly state on which side of the fault the magnesite occurs, but their description fits some of the smaller xenoliths of the Ash Creek serpentine-carbonate rocks on the east side of the tributary to Ash Creek.

The position of the magnesite on the downthrow side of a fault that transects Tertiary rocks supports an origin as horse blocks for the carbonate host rocks and a late age for their replacement by magnesite. The host rocks for the magnesite may be Precambrian or younger, but the replacement of dolomite by magnesite probably resulted from hydrothermal solutions circulating along the fault during middle or late Tertiary time.

ECONOMIC POTENTIAL OF THE MINERAL DEPOSITS

The northern Big Burro Mountains-Redrock area has been extensively prospected by professional as well as amateur geologists. The number of prospect pits in the area shows that many of the deposits have been at least superficially explored. Most of the deposits thus far discovered are too small to warrant economic consideration. Mining of any of the larger manganese, lead, or fluorite deposits under present economic conditions would be a marginal enterprise.

Future mineral development of the area lies in the discovery of new deposits at depth in veins already known, or in the discovery of new veins. The following features would serve to guide further exploration:

1. The known hydrothermal mineral deposits are localized in faults, shear zones, or breccia zones in rocks ranging in age from Precambrian to middle Tertiary.

2. The most common wall rock in the area is the Burro Mountains granite, which is characterized near the veins by kaolinization, sericitization, or silicification.
3. Many of the deposits occur in the vicinity of Laramide and post-Laramide stocks and dikes of intermediate composition.
4. Veins that transect Burro Mountains granite and Beartooth quartzite are most extensively mineralized in the granite below the quartzite contact or in brecciated quartzite just above the granite.

References

Anderson, E. M. (1942) *The dynamics of faulting,* London, Oliver & Boyd.

Billings, M. P. (1954) *Structural geology,* New York, Prentice-Hall, Inc.

Bowen, N. L. (1928) *The evolution of the igneous rocks,* Princeton, N. J., Princeton University Press.

———, and Tuttle, O. F. (1949) *The system MgO-SiO_2-H_2O,* Geol. Soc. Am. Bull., v 60, 439-460.

Callaghan, E. (1951) *Distribution of intermediate and basic igneous rocks in the Tertiary of Western United States* (abs.), Geol. Soc. Am. Bull., v 62, 1428.

Cannon, R. S., Jr., and Murata, K. J. (1944) *Estimating molybdenum content of scheelite or calcium tungstate by visual color of its fluorescence,* U. S. Patent 2,346,661.

Corle, Edwin (1951) *The Gila, river of the Southwest,* New York, Rinehart & Co., Inc.

Eardley, A. J. (1951) *Structural geology of North America,* New York, Harper & Bros.

Elston, W. E. (1955a) *Volcanic succession and possible mineralization in the Dwyer quadrangle, southwestern New Mexico* (abs.), Geol. Soc. Am. Bull., v 66, 1553.

——— (1955b) Unpublished reconnaissance map of the Virden quadrangle, N. Mex. Inst. Min. and Technology, State Bur. Mines and Mineral Res.

——— (1956) *Reconnaissance geology of the Virden quadrangle, Grant and Hidalgo Counties, New Mexico* (abs.), Geol. Soc. Am., Program 1956 annual meetings, 45.

Eskola, P. (1914) *On the petrology of the Orijärvi region in southwestern Finland,* Bull. Comm. Géol. Finlande, n 40.

——— (1915) *On the relation between chemical and mineralogical composition in the metamorphic rocks of the Orijärvi region,* Bull. Comm. Géol. Finlande, n 44.

Ferguson, H. G. (1920) *The Mogollon district, New Mexico,* U. S. Geol. Survey Bull. 715-L.

——— (1927) *Geology and ore deposits of the Mogollon mining district, New Mexico,* U. S. Geol. Survey Bull. 787.

Gabelman, J. W. (1955) *Geographic relation of uranium and fluorite in the regional tectonic pattern* (abs.), Abs. of AEC papers for AEC-USGS symposium, Mar. 8-11, 1955.

Gilbert, G. K. (1875) *Report on the geology of New Mexico and Arizona examined in 1873,* Rept. Geog. and Geol. Surveys West of 100th Meridian, v 3, Geology, 503-566.

Gillerman, Elliot (1951) *Fluorspar deposits of Burro Mountains and vicinity, New Mexico,* U. S. Geol. Survey Bull. 973-F.

———, and Whitebread, D. H. (1956) *Uranium-bearing nickel-cobalt-native silver deposits, Black Hawk district, Grant County, New Mexico,* U. S. Geol. Survey Bull. 1009-K.

Granger, H. C., and Bauer, H. L., Jr. (1950) *Results of diamond drilling, Merry Widow claim, White Signal, Grant County, New Mexico,* Oak Ridge, Tenn., U. S. Atomic Energy Comm., TEM 146-A, Tech. Inf. Service.

———, and ——— (1952) *Uranium occurrences on the Merry Widow claim, White Signal district, Grant County, New Mexico,* U. S. Geol. Survey Circ. 189.

Greenwood, Robert (1943) *Effect of chemical impurities on scheelite fluorescence,* Econ. Geol., v 38, 56-64.

Grim, R. E. (1953) *Clay mineralogy,* New York, McGraw-Hill Book Co., Inc.

Harker, Alfred (1939) *Metamorphism, a study of the transformation of rock-masses,* 2d ed., New York, E. P. Dutton & Co., Inc.

Harpum, J. R. (1954) *Formation of epidote in Tanganyika,* Geol. Soc. Am. Bull., v 65, 1075-1092.

Hayden, F. V. (1876) U. S. Geol. and Geog. Survey Terr. 8th Ann. Rept.

Heinrich, E. Wm. (1956) *Microscopic petrography,* New York, McGraw-Hill Book Co., Inc.

———, Levinson, A. A., Levandowski, D. W., and Hewitt, C. H. (1953) *Studies in the natural history of micas,* Univ. of Mich. Engineering Research Inst., Final Rept. of Project M978.

Hidden, W. E. (1893) *Two new localities for turquoise, New Mexico,* Am. Jour. Sci., 3d ser., v 46, 400-402.

James, H. L. (1955) *Zones of regional metamorphism in the Precambrian of northern Michigan,* Geol. Soc. Am. Bull., v 66, 1455-1488.

Johannsen, A. (1937) *A descriptive petrography of the igneous rocks,* 4 v, Chicago, Univ. of Chicago Press.

Johnston, W. D., Jr. (1928) *Fluorspar in New Mexico,* N. Mex. School of Mines, State Bur. Mines and Mineral Res. Bull. 4.

Jones, F. A. (1904) *New Mexico mines and minerals,* Santa Fe, N. Mex., World's Fair edition [cited in Northrop, 1942].

Kelley, V. C. (1949) *Geology and economics of New Mexico iron-ore deposits,* N. Mex. Univ. Pub., geol. ser., n 2.

Kennedy, G. C. (1947) *Charts for correlation of optical properties with chemical composition of some common rock forming minerals,* Am. Mineralogist, v 32, 561-573.

Kerr, Paul (1946) *Tungsten mineralization in the United States,* Geol. Soc. Am. Memoir 15.

King, P. B., and Flawn, P. T. (1953) *Geology and mineral deposits of Precambrian rocks of the Van Horn area, Texas,* Bur. Econ. Geol., Univ. of Texas Pub., n 5301.

Knechtel, M. M. (1936) *Geologic relations of the Gila conglomerate in southeastern Arizona,* Am. Jour. Sci., 5th ser., v 31, 81-92.

Krumbein, W. C., and Sloss, L. L. (1951) *Stratigraphy and sedimentation,* San Francisco, W. H. Freeman.

———, ———, and Dapples, E. C. (1949) *Sedimentary tectonics and sedimentary environments,* Am. Assoc. Petrol. Geol. Bull., v 33, 1859-1891.

Lang, S. S. (1906) *The Burro Mountain copper district,* Eng. Min. Jour., v 82, 395-396.

Lasky, S. G., and Wootton, T. P. (1933) *The metal resources of New Mexico and their economic features,* N. Mex. School of Mines, State Bur. Mines and Mineral Res. Bull. 7.

Leach, A. A. (1916) *Black Hawk silver-cobalt ores,* Eng. Min. Jour., v 102, 456.

——— (1927) *The mining of radium ore in New Mexico,* Min. Jour., v 10, n 22, 3-4.

Leach, F. I. (1920) *Radium ore discovered in White Signal district, New Mexico,* Eng. Min. Jour., v 109, 989.

Lindgren, W. (1933) *Mineral deposits,* New York, McGraw-Hill Book Co., Inc.

———, and Graton, L. C. (1906) *A reconnaissance of the mineral deposits of New Mexico,* U. S. Geol. Survey Bull. 285, 74-86.

———, ———, and Gordon, C. H. (1910) *The ore deposits of New Mexico,* U. S. Geol. Survey Prof. Paper 68.

Loewinson-Lessing, F., and Vorobjeva, O. (1929) *Contribution to the knowledge of orbicular structures in igneous rocks,* Compt. Rend. Acad. Sci., USSR (Academiia Nauk, Leningrad, Doklady), ser. A, 351-356.

Lovering, T. G. (1956) *Radioactive deposits in New Mexico,* U. S. Geol. Survey Bull. 1009-L, 327-355.

Mandarino, J. A. (1956) *A new technique for micrometric analysis of thin sections,* Am. Mineralogist, v 41, 786-789.

Mead, W. J. (1940) *Folding, rock flowage, and foliate structures,* Jour. Geol., v 48, 1007-1021.

Northrop, S. A. (1942) *Minerals of New Mexico,* N. Mex. Univ. Bull. 379, geol. ser., v 6, n 1.

Paige, Sidney (1911) *Metalliferous ore deposits near the Burro Mountains, Grant County, New Mexico,* U. S. Geol. Survey Bull. 470-C, 131-150.

———, (1912) *The origin of turquoise in the Burro Mountains, New Mexico,* Econ. Geol., v 7, 382-392.

———, (1916) *Silver City folio, New Mexico,* Geol. Atlas of the U. S., U. S. Geol. Survey Folio 199.

Phillips, A. H., and Hess, H. H. (1936) *Metamorphic differentiation at contacts between serpentinite and siliceous country rocks,* Am. Mineralogist, v 21, 333-362.

Poldervaart, Arie (1950) *Chrysotile asbestos produced by dolerite intrusions in dolomite,* Colonial Geology and Mineral Resources, v 1, n 3, 239-245.

Pringsheim, P., and Vogel, M. (1943) *Luminescence of liquids and solids and its practical applications,* New York, Interscience Publishers, Inc.

Ransome, F. L. (1919) *The copper deposits of Ray and Miami, Arizona,* U. S. Geol. Survey Prof. Paper 115, 71-75.

Ray, R. G. (1952) *Orbicular diorite from southern Alaska,* Am. Jour. Sci., v 250, 57-70.

Reid, G. D. (1902) *The Burro Mountain copper district,* Eng. Min. Jour., v 74, 778-779.

Rothrock, H. E., Johnson, C. H., and Hahn, A. D. (1946) *Fluorspar resources of New Mexico,* N. Mex. School of Mines, State Bur. Mines and Mineral Res. Bull. 21.

Sederholm, J. J. (1928) *On obicular granites, spotted granites, etc., and on the rapakivi texture,* Bull. Comm. Géol. Finlande, n 83.

Selfridge, G. C., Jr. (1936) *An X-ray and optical investigation of the serpentine minerals,* Am. Mineralogist, v 21, 463-503.

Snow, C. H. (1891)*Turquoise in southwest New Mexico,* Am. Jour. Sci., 3d ser., v 41, 511-512.

Somers, R. E. (1915) *Geology of the Burro Mountains copper district, New Mexico,* Am. Inst. Min. Met. Eng. Bull. 101, 957-996.

Stauber, I. J. (1910) *Burro Mountain mining district,* Mines and Minerals, v 30, 380-382.

Talmage, S. B., and Wootton, T. P. (1937) *The non-metallic mineral resources of New Mexico and their economic features,* N. Mex. School of Mines, State Bur. Mines and Mineral Res. Bull. 12.

Turner, F. J. (1948) *Mineralogical and structural evolution of the metamorphic rocks,* Geol. Soc. Am. Memoir 30.

Twenhofel, W. H. (1939) *Environments of origin of black shales,* Am. Assoc. Petrol. Geol. Bull., v 23, 1178-1198.

Vermaas, F. H. S. (1952) *South African scheelites and an X-ray method for determining members of the scheelite-powellite series,* Am. Mineralogist, v 37, 719-735.

Vogt, T. (1927) *Sulitelmafeltets geologi og petrografi* (with English summary), Norges geol. undersökelse, n 121.

von Chrustschoff, K. (1894) *Über holokrystalline makrovariolithische Gesteine,* Acad. Sci. St. Pétersbourg Mém., ser. 7, v 42, n 3.

Wade, W. R. (1907) *Burro Mountain copper district, New Mexico,* Eng. Min. Jour., v 84, 355-356.

Wahlstrom, E. E. (1950) *Introduction to theoretical igneous petrology,* New York, John Wiley & Sons, Inc.

Wargo, J. G. (1958) *Structure and volcanic stratigraphy in the Schoolhouse Mountain area, Grant County, New Mexico* (abs.), Geol. Soc. Am., Program of the Rocky Mountain Section, May 8-10, 1958, 34.

Wilmarth, M. G. (1938) *Lexicon of geologic names of the United States,* U. S. Geol. Survey Bull. 896.

Winchester, D. E. (1920) *Geology of Alamosa Creek valley, Socorro County, New Mexico,* U. S. Geol. Survey Bull. 716-A.

Yale, C. G., and Stone, R. W. (1921) *Magnesite,* U. S. Geol. Survey, Mineral Resources 1918, pt. 2, 149-150.

———, and ——— (1922) *Magnesite,* U. S. Geol. Survey, Mineral Resources 1919, pt. 2, 234.

Yoder, H. S., Jr. (1952) *The MgO-Al_2O_3-SiO_2-H_2O system and the related metamorphic facies,* Am. Jour. Sci., Bowen volume, pt. 2, 569-627.

——— (1955) *Role of water in metamorphism,* Geol. Soc. Am. Special Paper 62, 505-524.

Zalinski, E. R. (1907) *Turquoise in the Burro Mountains, New Mexico,* Econ. Geol., v 2, 464-492.

——— (1908) *Turquoise mining, Burro Mountains, New Mexico,* Eng. Min. Jour., v 86, 843-846.

Explanation of Plates 2-11

Plate 2

BURRO MOUNTAINS

A. View southeast of west flank of northern Big Burro Mountains. Precambrian complex in mountains; Gila conglomerate in foreground.
B. View northwest across Slate Creek Canyon, showing the Beartooth quartzite (middle skyline) overlying Burro Mountains granite.
C. View north across Ash Creek Canyon. Tertiary rhyolite (light) faulted down between the Burro Mountains granite to the west and the Colorado shale to the east.

Plate 3

GRANITE AND GNEISS

A. Contact of Burro Mountains granite (left) and layered hornblende gneiss (right) in a tributary to House Canyon, about 2 miles west of Bullard Peak.
B. Lenses of biotite-hornblende gneiss in migmatite. West flank of the Big Burro Mountains, 1 mile north of the Redrock-Silver City road.
C. Lenses of granite in migmatized hornblende gneiss. Potash feldspar metacrysts in hornblende gneiss near the granitic lenses. Head of Stein Canyon.

Plate 4

PHOTOMICROGRAPHS

A. Quartz-feldspar gneiss from east slope of Bullard Peak, showing coarse-grained muscovite, fine-grained biotite, quartz, and feldspar. Plane-polarized light. × 53.
B. Sillimanite gneiss from ridge southwest of Slate Creek. Andalusite, poikiloblastic with magnetite (lower), and sillimanite needles in quartz-biotite matrix. Plane-polarized light. × 124.

Plate 5

PHOTOMICROGRAPHS

A. Hornblende gneiss from ridge northwest of Brushy Canyon. Band of quartz and plagioclase between bands of granular hornblende and plagioclase. Plane-polarized light. × 28.
B. Andalusite-sericite schist from Ash Creek Canyon. Porphyroblasts of biotite (dark gray) and of andalusite (light gray) rimmed with biotite in quartz-sericite matrix. Plane-polarized light. × 53.

Plate 6

SERPENTINITE

A. Xenolith of banded talc serpentinite (S) and diopside quartzite (Q) in metadiabase (MD) and granite (G). West side of Ash Creek Canyon.
B. Banded talc serpentinite exposed in the bottom of Ash Creek Canyon near the ricolite quarry.
C. Lensoid core of ophicalcite (O) wrapped by serpentinite (S); coarsely crystalline calcite (C) along boundary of serpentinite (S) and ophicalcite (O) country rock. Mottled serpentinite in Ash Creek Canyon.

Plate 7

Photomicrographs

A. Spotted andalusite hornfels from Ash Creek Canyon. Discontinuous trains of biotite between clusters of andalusite and quartz (A) and quartz-sericite-chlorite matrix (B). Plane-polarized light. × 28.
B. Andesite porphyry from dike in Jacks Canyon. Corroded phenocrysts of andesine, containing slightly devitrified glass inclusions, in characteristically mottled matrix. Crossed nicols. × 28.

Plate 8

Igneous Rocks

A. Weathered exposure of anorthosite. Ridge west of Ash Creek Canyon.
B. Apophyses of fine-grained granite in metadiabase and xenoliths of metadiabase in granite. Ash Creek Canyon above the ricolite quarry.
C. Spheroidal weathering of Burro Mountains granite. Two miles southwest of Clarks Peak.

Plate 9

Migmatites

A. Banded migmatite containing orbicules in layers (right center) and in an irregularly shaped mass (left). Eccles Canyon.
B. Banded migmatite containing layers of orbicules. Eccles Canyon.
C. Irregular cluster of orbicules in banded migmatite. Orbicule with multiple rim (A); irregular lens of granular plagioclase and biotite (B). Eccles Canyon.

Plate 10

Gila Conglomerate

A. Characteristic outcrop of Gila conglomerate as cliffs. North of the Gila River, sec. 20, T. 18 S., R. 18 W.
B. Gila conglomerate. Large boulders are white rhyolite from Tertiary flows to the north; sand lens (left) cemented with white calcite. Tributary to Joe Harris Canyon, SW¼ sec. 24, T. 18 S., R. 18 W.
C. Dark, well-consolidated Gila conglomerate overlain by unconsolidated bajada deposits. Kelley Chimney Canyon.

Plate 11

Ore Minerals

A. Weathered outcrop of horizontally bedded magnesite and chert. N½ sec. 17, T. 18 S., R. 18 W.
B. View northeast along strike of black calcite-manganese oxide vein. The vein is exposed in the adit (left foreground) and in the trench (background). SW¼ sec. 6, T. 18 S., R. 18 W.
C. Negative print of an autoradiograph of radioactive rhyolite-jasper breccia, showing radioactivity essentially confined to the jasper matrix. Prospect in NE¼ sec. 22, T. 18 S., R. 18 W. Seven weeks' exposure.

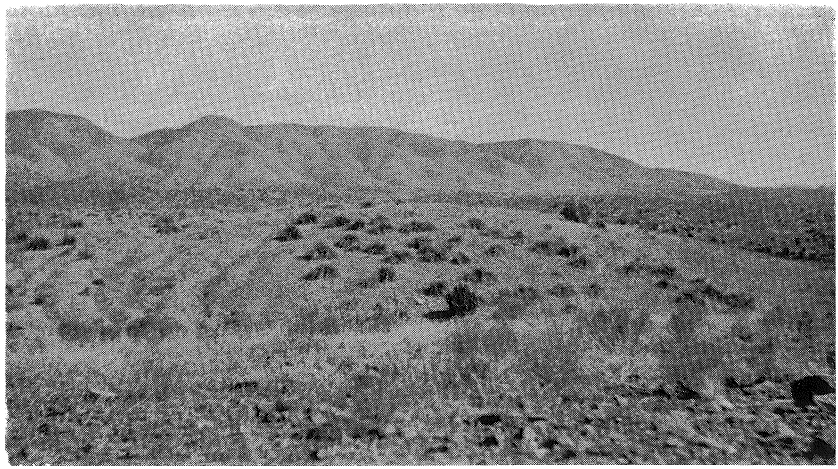

A

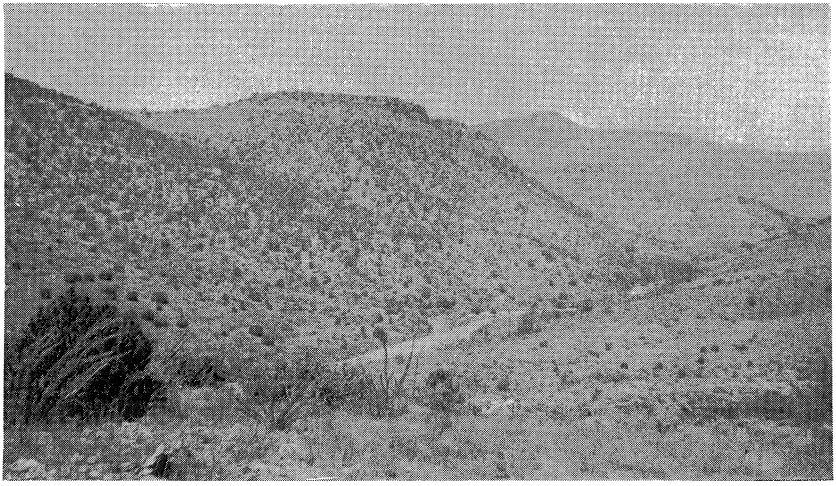

B

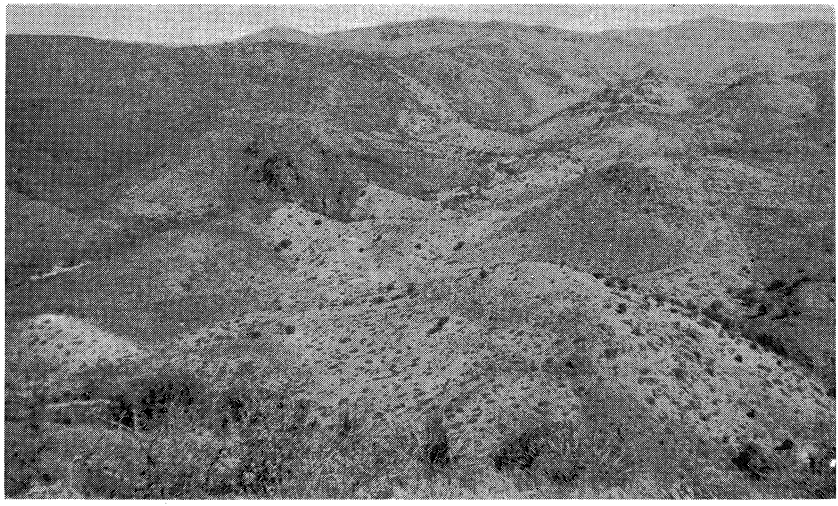

C

Plate 2

A

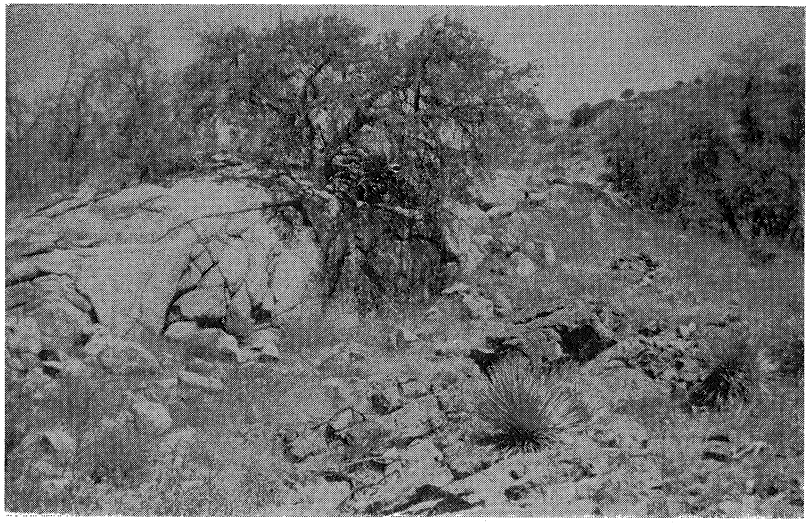

B

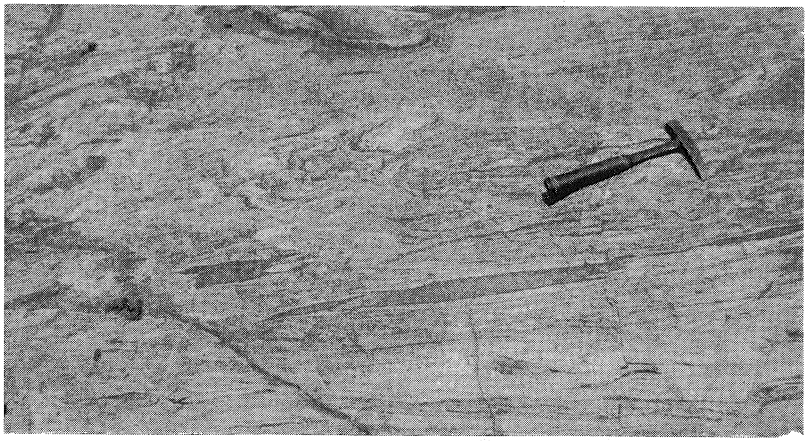

C

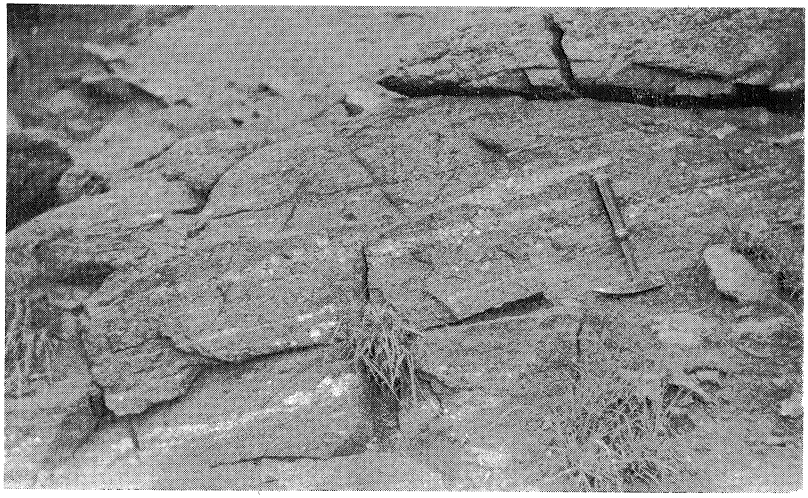

Plate 3

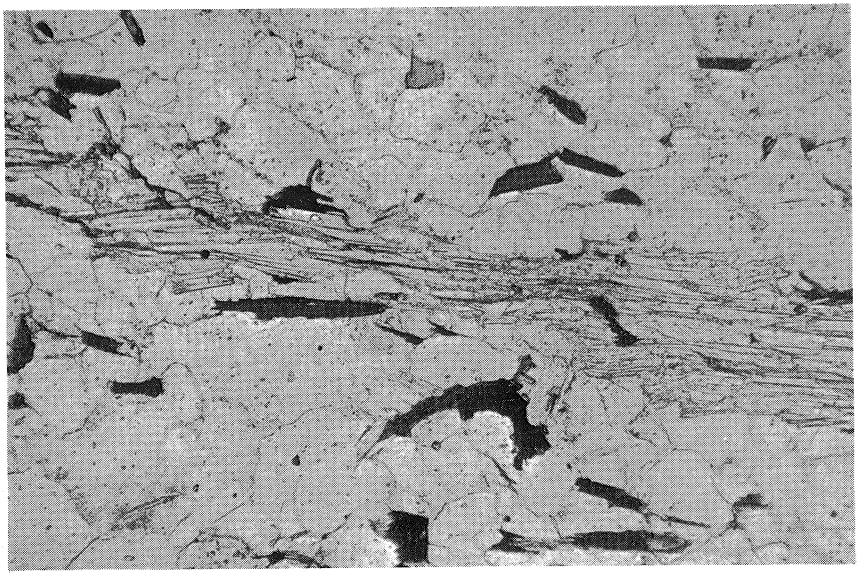

A

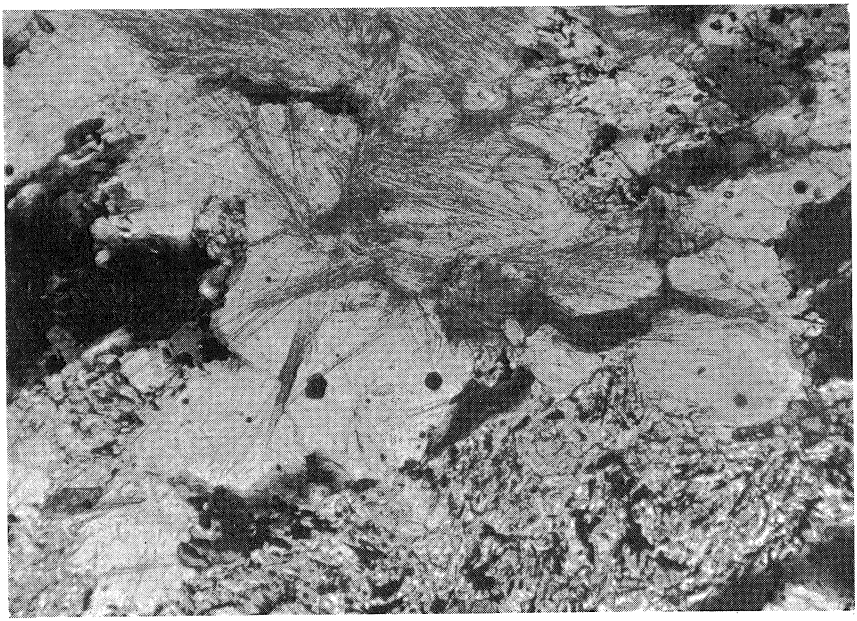

B

Plate 4

A

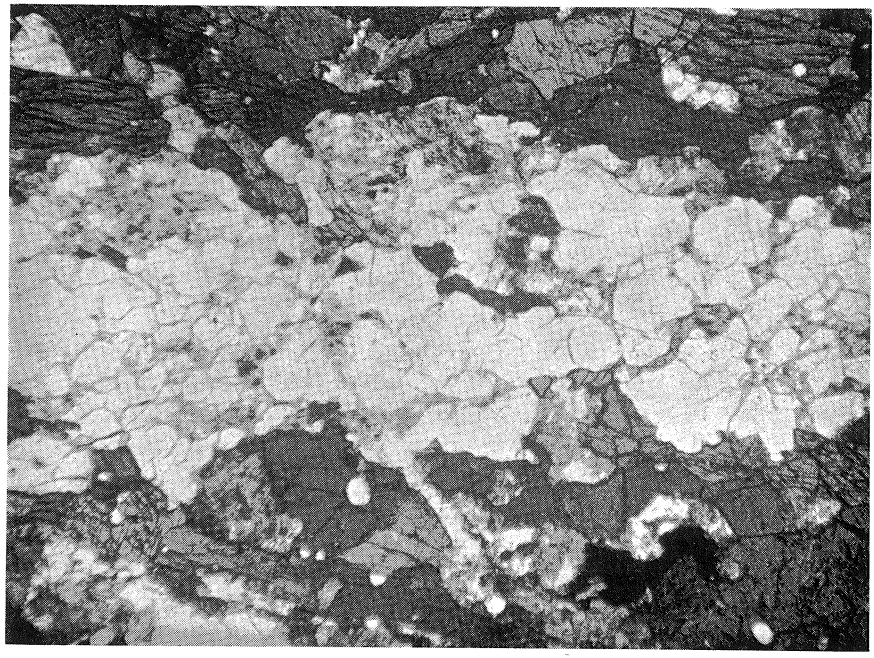

B

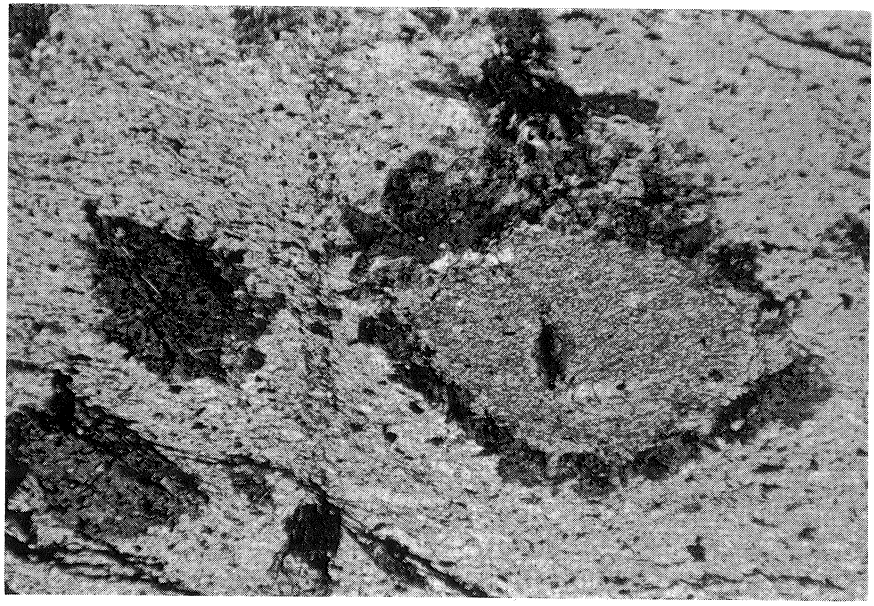

Plate 5

A

B

C

Plate 6

A

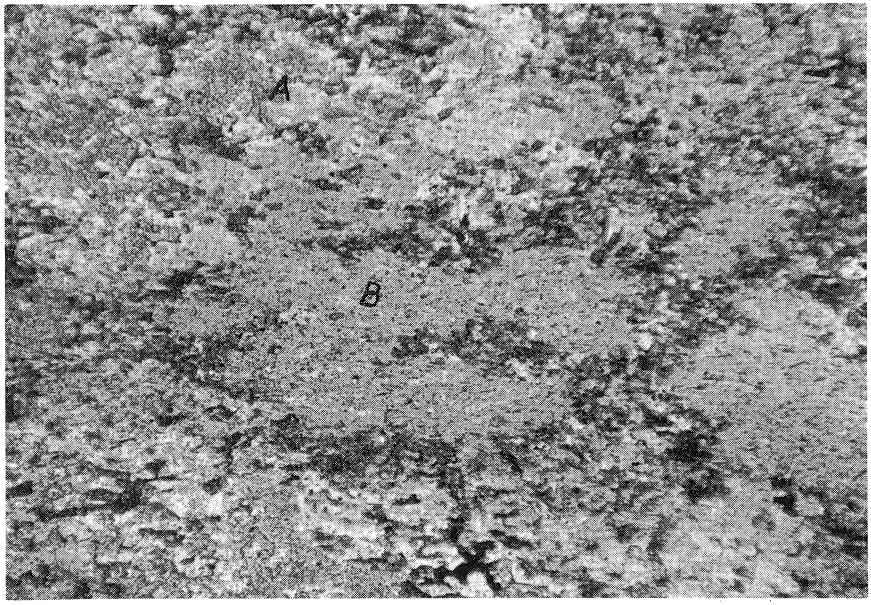

B

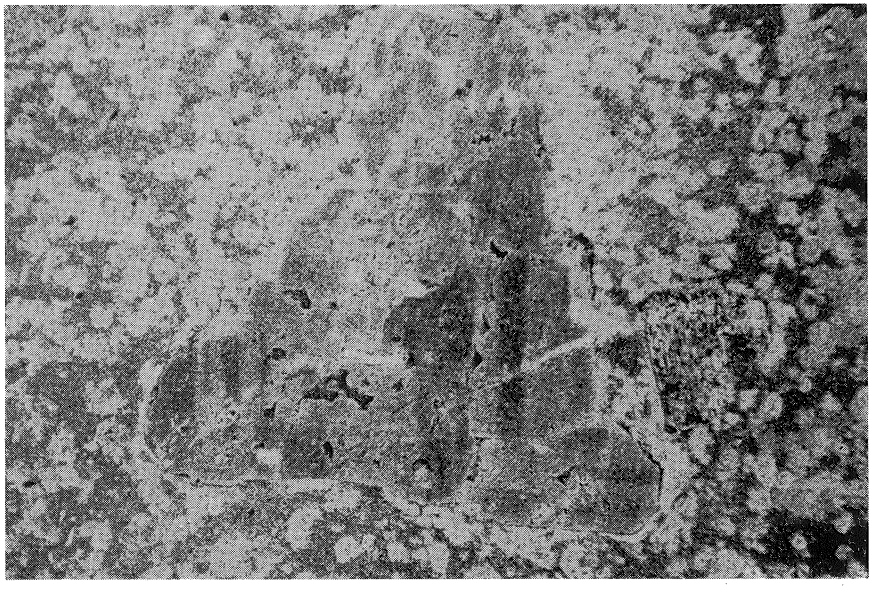

Plate 7

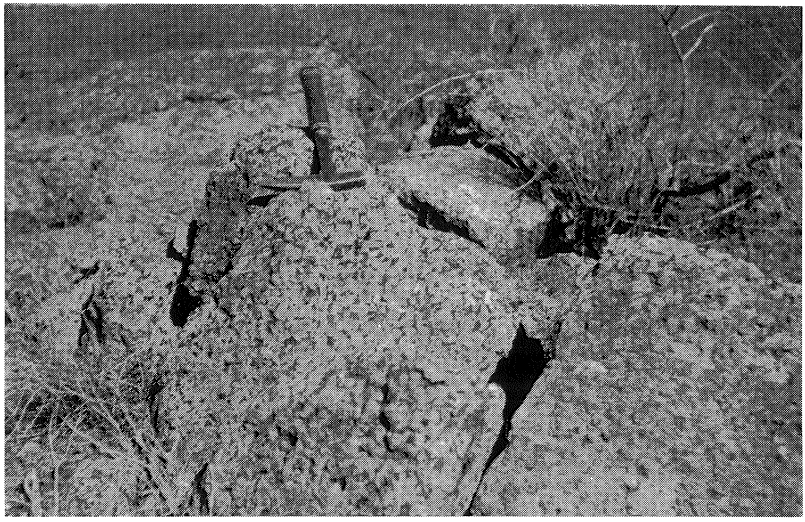

A

B

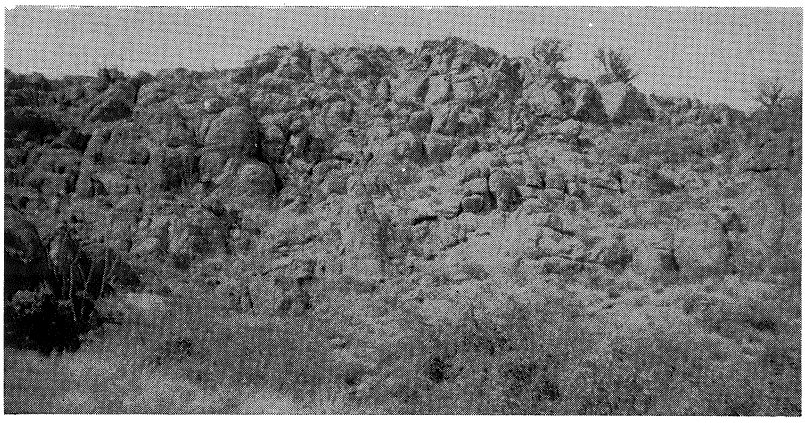

C

Plate 8

A

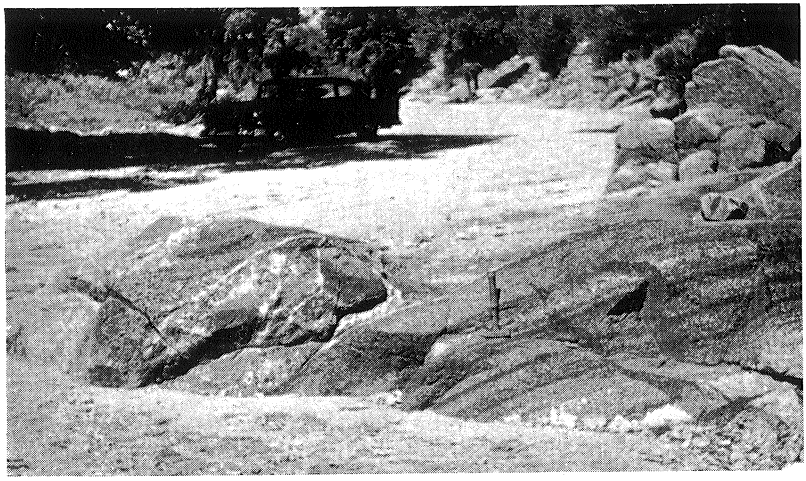

B

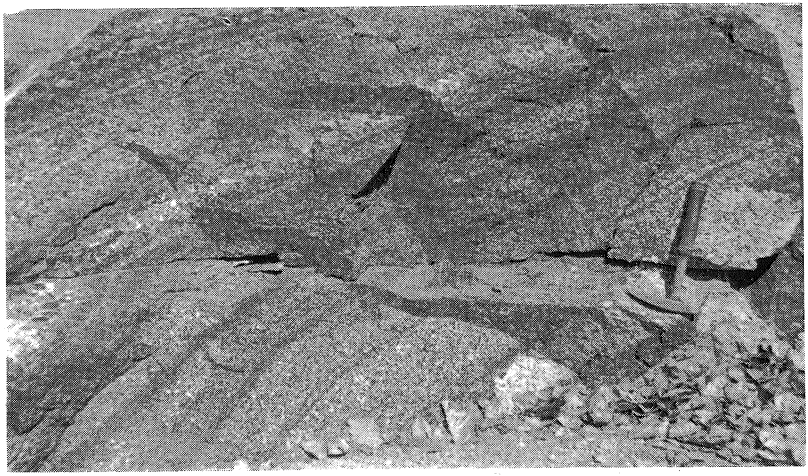

C

Plate 9

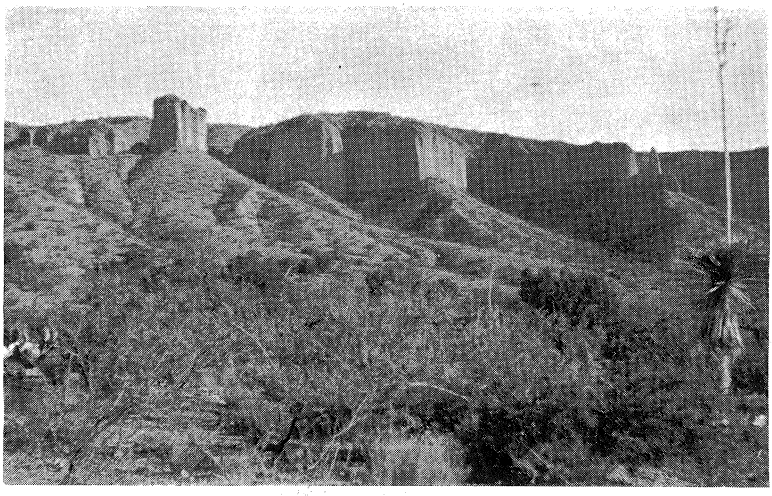

A

B

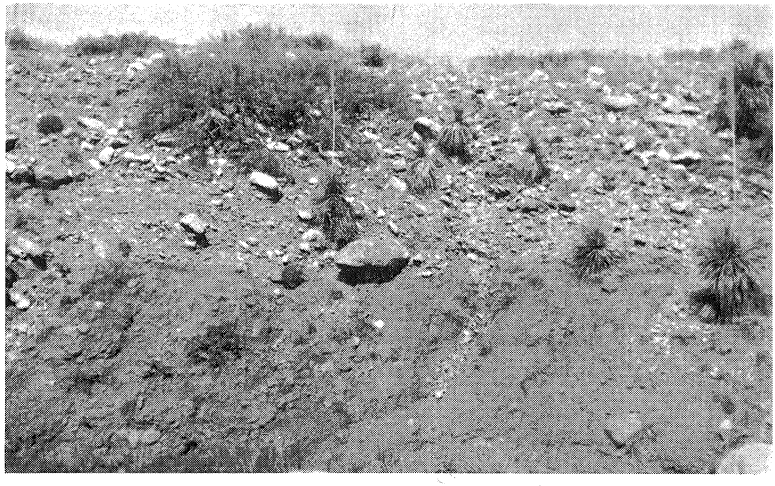

C

Plate 10

A

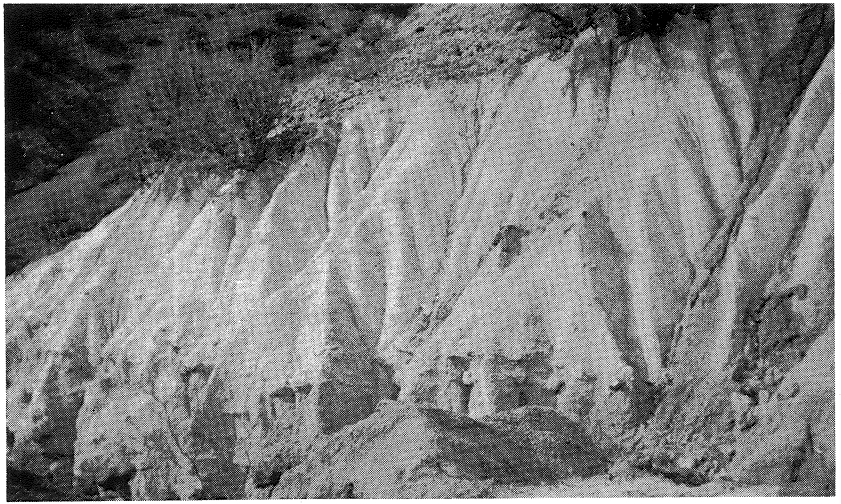

B

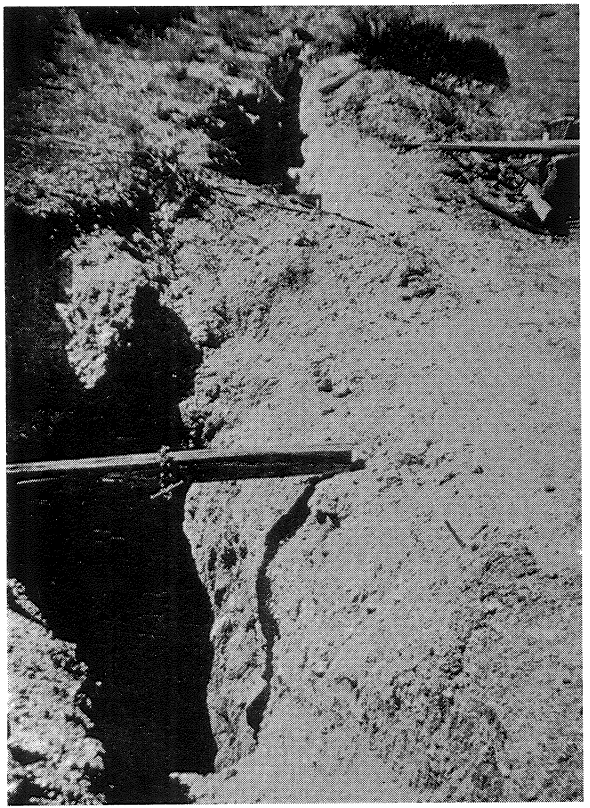

C

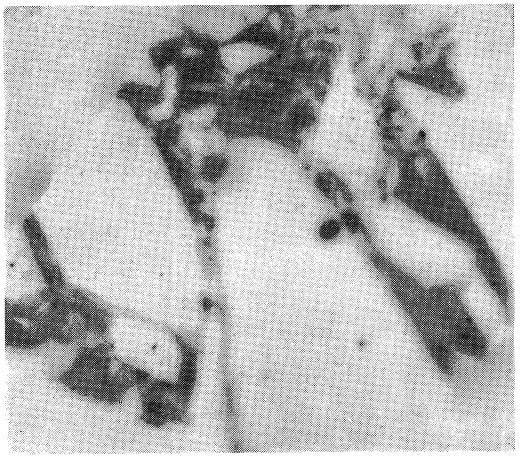

Plate 11

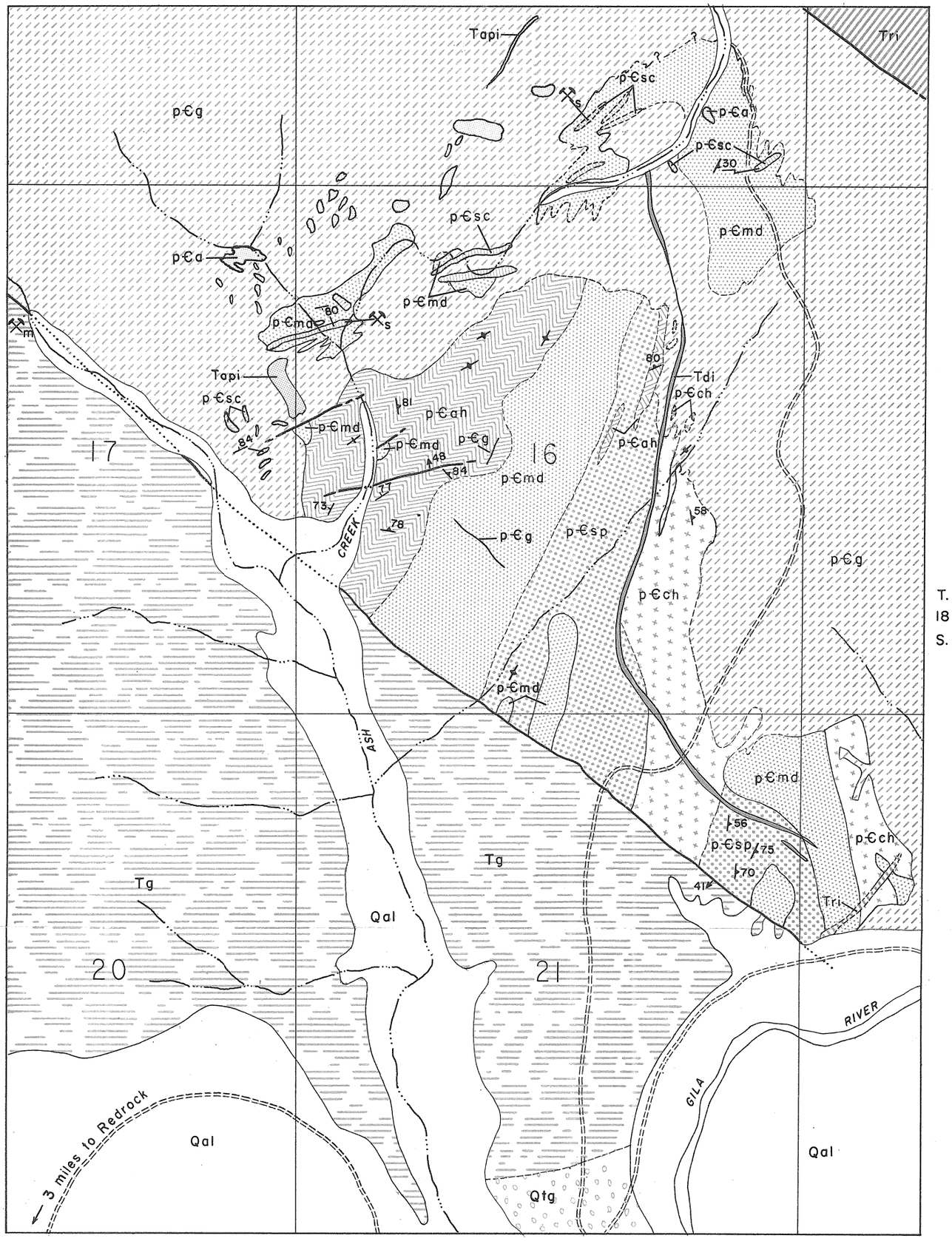

EXPLANATION

- Qal — Alluvium (QUATERNARY)
- Qtz — Terrace gravels (TERTIARY–QUATERNARY)
- Tg — Gila conglomerate (TERTIARY–QUATERNARY)
- Tri — Rhyolite (LATE CRETACEOUS–EARLY TERTIARY)
- Tapi — Andesite porphyry (LATE CRETACEOUS–EARLY TERTIARY)
- Tdi — Diabase (LATE CRETACEOUS–EARLY TERTIARY)
- p€g — Granite and aplite (PRECAMBRIAN)
- p€md — Metadiabase (PRECAMBRIAN)
- p€a — Anorthosite (PRECAMBRIAN)

Ash Creek Series (PRECAMBRIAN)

- p€sp — Sericite phyllite and andalusite–sericite schist
- p€ch — Cordierite hornfels
- p€ah — Spotted andalusite hornfels, biotite hornfels, and diopside quartzite
- p€sc — Serpentine–carbonate rocks

- Fault
- Strike of vertical joints
- Strike and dip of bedding
- Strike of vertical bedding
- Strike and dip of foliation
- Strike of vertical foliation
- Contact (dashed where approx.)
- Quarry (m–magnesite, s–serpentinite)

GEOLOGIC MAP OF THE ASH CREEK AREA, GRANT CO., NEW MEXICO

0 500 1000 2000 3000

SCALE IN FEET

Index

Access, 5
Actinolite, 44, 45, 60
Agglomerates, 11, 89, 90
Albite, 17, 31
Allanite, 67, 74, 76
Alluvium, **95**, 100, 106
Almandite, 15, 20, 21, 33, 34, 35, 75
Amethyst, 113
Amphibole, 61, 62
Amphibolite, 12, 13, 14, 20, 22, 24, 25, 26, 27, 30, 35, 58, 97
Andalusite, 21, 22, 33, 35, 37, 38, 40, 41, 42, 54, 133, 134
Andalusite-sericite schist, **37**
Anderson, Charley, Jr., 4
Anderson, E. M., cited, 83
Anderson, Fred, 4
Andesine, 15, 16, 31, 34, 35, 61, 65, 70, 77, 84, 85, 86, 90, 134
Andesite, 10, 11, **84-86**, 88, 101
Anorthosite, 56, 58, 59, 134
Anthophyllite, 56
Antigorite, 44, 45, 46, 47, 49
Apatite, 16, 18, 24, 25, 29, 31, 38, 41, 42, 59, 61, 62, 65, 67, 68, 69, 71, 85, 86, 87, 109
Aplite, 10, 31, 33, 40, 58, 60, 75, **76-77**, 98
Argentite, 116
Arkose, 79
Asbestos, **108**
Ash Creek, 10, 36, 46, 58, 63, 126
Ash Creek Canyon, 40, 41, 45, 46, 47, 58, 60, 61, 66, 68, 82, 87, 92, 97, 100, 101, 105, 108, 133, 134
Ash Creek series, 13, **33-58**
60, 62, 63, 73, 96, 98, 99, 104
andalusite-sericite schist, **37**
biotite hornfels, **41-42**
cordierite hornfels, **38-39**
diopside quartzite, **42-43**
sericite phyllite, **36**
serpentine-carbonate rocks, **44-53**
spotted andalusite hornfels, **39-41**
Astrologer mine, **116**
Augite, 24, 25
Azurite, 114

Bajada deposits, 11, **94**, 100, 106, 134
Balk, Robert, 4
Banding, **96-98**
Barite, 116
Bar Six Canyon, 12, 97
Basalt, 11, **88**
Batholith, Burro Mountains, 9, 10, 12, 19, 20, 21, 22, 27, 30, 32, 33, 63, 64, **77-78**, 98, 100, 104
Bauer, H. L., Jr., cited, 4
Bear Canyon, 14, 23, 86, 114
Beartooth quartzite, 10, 11, **78-80**, 81, 85, 86, 101, 102, 106, 113, 115, 121, 133
Bennett, E., 108
Biotite, 14, 15, 16, 17, 19, 20, 21, 22, 24, 25, 26, 27, 28, 29, 31, 32, 33, 34, 35, 37, 38, 40, 41, 42, 44, 45, 54, 55, 57, 58, 59, 60, 61, 62, 65, 66, 67, 68, 69, 70, 71, 74, 75, 77, 84, 86, 88, 90, 93, 133, 134
Biotite hornfels, **41-42**
Bismuthinite, 116
Black Eagle mine, **122-124**
Black Hawk Canyon, 14, 16, 17, 18, 30, 60, 61, 62, 63, 66, 74, 75, 100, 101, 109, 116
Black Hawk mining district, 64, 65, 66, 84, 85, 98, 103, 107, 110, **115-116**
Bliss sandstone, 105
Bolson deposits, 11, 92, **94**, 106
Bornite, 113
Bowen, N. L., cited, 50, 72
Briggs, L. I., 4
Bronx mine, 116
Brushy Canyon, 27, 28, 29, 73, 74, 133
Bullard Peak, 13, 14, 15, 16, 18, 19, 23, 24, 25, 27, 28, 29, 30, 58, 65, 86, 97, 98, 99, 100, 112, 133
Bullard Peak Canyon, 7, 14, 28, 29, 30, 31, 65, 69, 98, 99
Bullard Peak series, **12-33**, 34, **57-58**, 64, 65, 66, 69, 73, 96, 97, 98, 99, 101, 104, 105, 114
granite gneiss, **27-30**
quartz-feldspar gneiss, **14-21**
sillimanite gneiss, **21-22**
Burro Chief mine, 107
Burro Mountains:
batholith, 9, 10, 12, 19, 20, 21, 22, 27, 30, 32, 33, 63, 64, **77-78**, 98, 100, 104
granite, 9, 10, 21, 28, 33, 63, 99, 100, 101, 110, 113, 114, 115, 116, 118, 119, 120, 121, 124, 126, 133, 134
Burro Springs Canyon, 66, 68, 75, 92, 93, 100
Buzzard Canyon, 121

Calcite, 36, 43, 44, 45, 47, 49, 55, 66, 79, 84, 85, 88, 92, 93, 109, 114, 121, 122, 124, 133, 134

Callaghan, Eugene, cited, 4, 89
Cambrian, **105**
Cannon, R. S., Jr., cited, 112
Cauthen, J. H., 117
Chalcedony, 109, 117, 118, 119
Chalcocite, 116
Chalcopyrite, 110, 113, 114, 115, 116
Chambers, Roy, 122
Chert, 66, 79, 93, 109, 118, 119, 121, 134
Chlorite, 15, 16, 18, 19, 22, 26, 29, 34, 35, 36, 37, 38, 40, 41, 44, 46, 54, 55, 57, 59, 60, 66, 76, 83, 84, 85, 86, 88, 96, 109, 134
Chrysocolla, 92, 113
Chrysotile, 46, 49
Clarks Peak, 80, 81, 89, 102, 134
Climate, **5-6**
  precipitation, 5
  temperature ranges, 5
Clinozoisite, 43, 44, 45, 46, 52, 55
Clover Leaf prospect, 122
Colorado shale, 10, 11, 78, **80-81**, 85, 86, 87, 89, 91, 101, 106, 121, 133
Conglomerate, 11, 33, 79, 92, 93, 134
  Gila conglomerate, 6, 11, 33, 66, 81, 88, 91, **92-94**, 102, 106, 126, 133, 134
Conner, A. B., 117
Contact metamorphism, 22, 33, 37, 38, 39, 42, 43, 54, 55
Copper deposits, 107, **113**
Cordierite, 15, 17, 18, 19, 33, 34, 36, 37, 38, 42, 56
Cordierite hornfels, **38-39**
Corle, Edwin, cited, 6
Cretaceous, 10, 66, **78-81**, 86, 87, 89, **105**, **117**
  Colorado shale, 10, 11, 78, **80-81**, 85, 86, 87, 89, 91, 101, 106, 121, 133
  sedimentary rocks, **78-81**, 102

Dacite, 90
Denning, R. M., 4
Devonian, **105**
Diabase, 10, 11, 27, 33, 35, 37, 38, 50, 52, 56, 62, **82-84**, 86, 87
Dikes, 10, 11, 58, 62, 66, 73, 75, 76, 77, 82, 83, 84, 85, 86, 87, 88, 89, **102-103**, 110, 116, 119, 124, 126, 134
Diopside quartzite, 40, 41, **42-43**, 55, 133
Dolomite, 27, 43, 50, 52, 53, 55, 101, 126, 127
Dorothy mine, **113**
Drainage, **6-7**

Eardley, A. J., cited, 81, 89, 103
Eaton, H. R., 114
Eccles Canyon, 12, 14, 17, 19, 23, 27, 28, 61, 67, 68, 69, 73, 74, 75, 76, 82, 84, 86, 98, 99, 103, 110, 134
Economic geology, **107-128**
  asbestos, **108**
  Astrologer mine, **116**
  Black Eagle mine, **122-124**
  Black Hawk district, **115-116**
  copper, 107, **113**
  Dorothy mine, **113**
  economic potential, **127-128**
  fluorite, **116-122**
  Great Eagle mine, 107, 109, **117-119**
  Hope prospect, **119**
  hydrothermal veins, **109-126**
  Laramide, **109-126**, **126-127**
  lead, **113-115**
  Lead Mountain, **113**
  Little Bear Canyon, **114**
  Live Oak prospect, **114-115**
  Long Lost Brother prospect, 107, **120-122**
  magnesite, **126-127**
  magnetite, **108**
  manganese, **122-124**
  metamorphic deposits, **108-109**
  mica, **109**
  pegmatites, **109**
  post-Laramide, **109-127**
  Precambrian metamorphic deposits, **108**
  Precambrian pegmatites, **109**
  radioactive minerals, **124-126**
  Redrock area, **119-120**
  Rice-Graves claim, **110-112**
  ricolite, **108**
  Ruth mine, **113**
  serpentinite, **108**
  S. Harper claim, **112**
  silver, **115-116**
  Slate Creek Canyon, **113-114**
  Telegraph district, **115**
  tungsten, **110-112**
Edwards, John, 113
El Paso limestone, 105
Elston, W. E., cited, 4, 89, 92
Epidote, 16, 24, 25, 26, 27, 31, 34, 35, 42, 61, 67, 69, 71, 83, 84, 85, 112
Eschman, D. F., 4

Faults, 10, 11, 83, 86, 87, **100-102**
Ferguson, H. G., cited, 89
Flawn, P. T., cited, 26
Fluorite, 107, 109, 110, **116-122**
Fluorspar Milling Co., 117
Flying A ranch, 100, 101

Folds, **98-99**
Foliation, **96-98**
Forsterite, 45, 50, 52
Fox Tail Canyon, 21, 22, 80, 81, 90, 102
Fox Tail Creek, 79
Fusselman limestone, 105

Gabelman, J. W., cited, 110, 117
Galena, 110, 113, 114, 115, 116, 117
Garnet, 16, 21, 57, 58, 74, 75
Geography, **5-7**
Geologic history, **104-106**
  Laramide, **106**
  Mesozoic, **105-106**
  Paleozoic, **105-106**
  post-Laramide, **106**
  Precambrian, **104-105**
Geomorphology, **5-7**
Gila conglomerate, 6, 7, 11, 33, 66, 81, 88, 91, **92-94**, 102, 106, 126, 133, 134
Gila River, 6, 7, 21, 60, 66, 92, 100, 101, 102, 113, 115, 117, 119, 134
Gilbert, G. K., cited, 3, 91
Gillerman, Eliot, cited, 4, 12, 64, 65, 84, 85, 88, 92, 98, 101, 103, 107, 110, 115, 116, 117, 120, 121, 122
Gneiss, 9, 10, 13, 14, 15, 16, 17, 18, 19, 20, 21, 22, 24, 25, 26, 27, 28, 30, 31, 32, 33, 34, 35, 65, 66, 73, 97, 98, 99, 100, 110, 111, 120, 121, 133
  granite, **27-30**
  quartz feldspar, **14-21**
  sillimanite, **21-22**
Goat Canyon, 24, 101
Granfel, N. P., 114
Granger, H. C., cited, 4
Granite, 10, 11, 12, 18, 19, 21, 23, 31, 32, 33, 34, 35, 38, 40, 42, 44, 50, 52, 56, 58, **63-64**, 65, **66-69**, 73, 76, 79, 81, 87, 98, 99, 101, 109, 113, 117, 133, 134
  Burro Mountains granite, 9, 10, 14, 21, 28, 33, 63, 99, 100, 101, 110, 113, 114, 115, 116, 118, 119, 120, 121, 124, 126, 133, 134
Granite gneiss, **27-30**
Granodiorite, 10, 63, **68-69**
Graton, L. C., 3, 115
Graves, G., 110
Great Eagle mine, 107, 109, **117-119**
Greenwood, Robert, cited, 112
Grim, R. E., cited, 36
Grossularite, 75

Hahn, A. D., cited, 4
Harker, Alfred, cited, 19, 37, 50, 63, 97
Harper, Sherman, 112
Harrison, John, 121
Hayden, F. V., cited, 80
Hazen, C. C., 121
Heinrich, E. Wm., cited, 4, 33
Hematite, 17, 18, 21, 36, 37, 40, 41, 66, 79, 86, 87
Hess, H. H., cited, 44, 51
Hewitt, Janice L., 4
Hidden, W. E., cited, 3
History:
  geologic, *see* Geologic history
  mining, **107**
Hope prospect, **119**
Hornblende, 24, 25, 26, 27, 29, 30, 32, 33, 35, 43, 58, 59, 60, 61, 62, 63, 66, 67, 68, 70, 71, 73, 84, 85, 86, 112, 133
Hornblende gneiss, 22, 23, 24
Hornfels, 10, 22, 33, 34, 35, 36, 38, 40, 41, 42, 54, 96, 97, 134
  cordierite, **38-39**
  spotted andalusite, **39-41**
  biotite, **41-42**
House Canyon, 21, 98, 100, 133
Hunt, Gerald, 124, 126
Hyalite, 76
Hydrothermal alteration, 27, 55, 63
Hydrothermal veins, **109-126**

Illite, 19, 20, 27, 36, 40, 43
Ilmenite, 38, 67, 68

Jacks Canyon, 66, 101, 110, 134
James, H. L., 57
Jasper, 109, 118, 119, 120, 121, 134
Joe Harris Canyon, 14, 15, 19, 21, 60, 62, 66, 92, 99, 100, 102, 109, 113, 119, 134
Johannsen, A., cited, 59, 72
Johnson, C. H., cited, 4
Johnston, W. D., Jr., cited, 4, 116, 117
Jones, F. A., 48

Kaolinite, 15, 16, 17, 20, 24, 25, 27, 28, 31, 36, 70, 71, 76, 84, 85, 86, 87, 90
Kelley Chimney Canyon, 14, 30, 31, 73, 134
Kelley, V. C., cited, 4, 108
Kennedy, G. C., cited, 45, 75
Kerr, Paul, cited, 112
King, P. B., cited, 26
Knechtel, M. M., cited, 91, 94
Krumbein, W. C., cited, 53, 80

Labradorite, 25, 27, 35, 59, 60, 62, 83, 84
Lang, S. S., cited, 3

Laramide and post-Laramide, 10-11, 66, **81-91, 100-103, 106, 109-127**
andesite, **84**
andesite porphyry, **85-86**
basalt, **88**
diabase, **82-84**
history, **106**
hydrothermal veins, **109-126**
monzonite porphyry, **85**
replacement deposits, **126-127**
rhyolite and rhyolite porphyry, **87-88**
structural features, **81-91, 100-103**
Lasky, S. G., cited, 4, 116
Leach, A. A., cited, 4
Leach, F. I., cited, 4
Lead, **113-115**
Lead Mountain, **113**
Leucoxene, 16, 38, 67, 71
Limestone, 53, 55, 81, 101, 105
Limonite, 17, 40, 41, 61, 75, 79, 86, 87, 114, 115
Lindgren, W., cited, 3, 107, 112, 114, 115, 116
Lineation, **98**
Little Bear Canyon, 14, 18, 23, 76, 86, 110, 114
Little Burro Mountains, 6, 9, 102
Live Oak prospect, **114-115**
Location, **5**
Loewinson-Lessing, F., cited, 71
Long Lost Brother prospect, 107, **120-122**
Lovering, T. G., cited, 4

McCabe, D. F., 117
McCray, H. E., 122
Magnesite, 101, **126-127**, 134
Magnetite, 15, 16, 17, 18, 19, 20, 21, 22, 24, 25, 26, 29, 31, 37, 38, 40, 41, 42, 45, 46, 47, 48, 49, 50, 52, 55, 59, 60, 61, 62, 63, 65, 67, 68, 69, 71, 74, 75, 76, 77, 83, 84, 85, 86, 87, 88, 90, 93, **108**, 109, 133
Malachite, 113, 114
Malone fault, 101
Mandarino, J. A., cited, 70
Manganese, **122-124**
Mangas Valley, 6
Marble, 44
Mead, W. J., cited, 97, 98
Meander scars, 6
Mesozoic, **105-106**
Metadiabase, 10, 33, 36, 37, 40, 41, 42, 44, 45, 50, 56, 58, **60-63**, 113, 133
Metamorphic deposits, **108-109**
Metamorphism
contact, 19, 27, 38, 43, 60
hydrothermal, 63
regional, 18, 20, 21, 26, 29, 32, 33, 39, 40, 41, 42, 53, 54, 55, 56, 57, 58
thermal, 22, 32, 37, 40, 41, 48, 50, 52, 53, 56, 63
Metasomatism, 22, 52
Mica, *see also* Biotite and Muscovite, **109**
Microcline, 15, 17, 22, 28, 29, 30, 31, 32, 33, 34, 35, 43, 65, 67, 68, 69, 70, 71, 74, 75, 76, 77, 93, 122
Microperthite, 28, 29, 32, 67, 68, 77
Migmatite, 9, 13, 14, 23, 29, 66, 69, 99, 133, 134
Mining history, **107**
Mississippian, **105**
Modes:
amphibolite, 25
anorthosite, 59
granite, 29, 68
granodiorite, 69
hornblende gneiss, 25
metadiabase, 61
migmatite, 70
Precambrian gneiss, 25, 29
tonalite, 65
Molybdenite, 74, 75
Montmorillonite, 19, 20, 27, 36
Montoya limestone, 105
Monzonite porphyry, 10, 11, **85**, 86, 87, 88, 102, 110, 116
Moreland, J. A., 119
Murata, K. J., cited, 112
Muscovite, 14, 15, 16, 17, 18, 19, 21, 22, 33, 35, 36, 38, 40, 41, 54, 55, 74, 75, 77, 93, 109, 133
Myrmekite, 28, 30, 31, 65

Niccolite, 116
Northrop, S. A., 48

Oligoclase, 15, 16, 28, 29, 31, 34, 35, 41, 55, 65, 67, 68, 69, 70, 71, 74, 76, 87, 90, 93
Olivine, 52
Opal, 74, 76
Orbicular rock, **69-73**
Ordovician, **105**
Orthoclase, 21, 41, 85, 87

Paige, Sidney, cited, 3, 4, 12, 63, 64, 78, 80, 81, 85, 89, 91, 105, 106
Paleozoic, **105-106**
Pediments, **7**, 106
Pegmatite, 10, 27, 31, **73-76**, 98, **109**, 116
Pennine, 31, 45, 46, 62, 67
Pennsylvanian, **105**

Percha shale, 105
Perthite, 68
Petrology, **12-78**
  andalusite-sericite schist, **37**
  anorthosite, **58-60**
  aplite, **76-77**
  Ash Creek series, **33-58**
  biotite hornfels, **41-42**
  Bullard Peak series, **12-33, 57-58**
  Burro Mountains batholith, **77-78**
  cordierite hornfels, **38-39**
  diopside quartzite, **42-43**
  granite, **63-66**
  granodiorite, **68-69**
  hornblende gneiss, **22-27**
  igneous rocks, **12**
  metadiabase, **60-63**
  metamorphic rocks, **12**
  orbicular rock, **69-73**
  pegmatite, **73-76**
  Precambrian, **12**
  Precambrian igneous, **58-78**
  quartz-feldspar gneiss, **14-21**
  sericite phyllite, **36**
  serpentine-carbonate rocks, **44-53**
  sillimanite gneiss, **21-22**
  spotted andalusite hornfels, **39-41**
  tonalite, **65-66**
Phelps Dodge Corp., 107
Phillips, A. H., cited, 44, 51
Phyllite, 33, **36**, 37, 42, 54, 96
Pigeonite, 83, 84
Pinite, 42, 54
Pitchblende, 116
Plagioclase, 70, 84
Pliocene, 106
Plugs, 10, 62, 86, 89, 91, 102
Poldervaart, Arie, cited, 51
Polymetamorphism, 39
Precambrian, **58-78**
  anorthosite, 58-60
  aplite, 75, **76-77**
  granite, 40, 62, **63-64, 66-69**, 78, 81, 82, 84, 85, 86, 87, 88, 89, 117
  granodiorite, 68-69
  history, **104-105**
  igneous rocks, **58-78**
  metadiabase, **60-63**
  metamorphic and igneous rocks, **12**, 92
  metamorphic deposits,**108-109**
  orbicular rock, **69-73**
  pegmatite, **73-76, 109**
  tonalite, **65-66**
  structural features, **96-100**
Pringsheim, P., cited, 76
Psilomelane, 110, 122, 124
Purple Heart deposit, 107, 121
Pyrite, 65, 110, 113, 114, 115, 116, 117, 119, 120
Pyrolusite, 124
Pyroxene, 24, 27, 60, 62, 63, 83, 84

Quartz, 15, 16, 17, 18, 19, 20, 21, 22, 23, 24, 25, 28, 29, 30, 31, 33, 34, 35, 36, 37, 38, 40, 41, 43, 46, 53, 54, 55, 65, 66, 67, 68, 69, 70, 71, 74, 75, 76, 77, 79, 87, 90, 93, 101, 109, 112, 113, 114, 115, 116, 117, 118, 121, 122, 126, 127, 133, 134
Quartz-feldspar gneiss, **14-21**
Quartzite, 12, 13, 14, 15, 20, 33, 42, 43, 55, 78, 97, 101
  Beartooth, 10, 11, **78-80**, 81, 85, 86, 102, 106, 113, 115, 133
  diopside, 40, 41, **42-43**, 55
Quartz latite, **89-91**
Quaternary, 11, **91-95, 106**
  alluvium, **95**
  bajada deposits, **94**
  bolson deposits, **94-95**
  Gila conglomerate, **92-94**
  sedimentary rocks, **91-95**
  terrace gravels, **94**

Radioactive minerals, **124-126**
Ramsdell, L. S., 4
Ransome, F. L., cited, 91
Ray, Charles, 116, 120
Ray, R. G., cited, 72
Redrock area, **119-120**
Regional geology, **8**
Regional metamorphism, 18, 20, 21, 26, 29, 33, 39, 40, 41, 42, 53, 54, 55, 56, 57, 58
Reid, G. D., cited, 3
Replacement deposits, **126-127**
Retrograde metamorphism, 39, 54
Rhyolite, 10, 11, 84, 86, **87-91**, 101, 133, 134
Rice, F., 110
Rice-Graves claim, **110-112**
Ricolite, 41, 45, 46, 47, 48, **108**, 133
Rothrock, H. E., cited, 4, 116, 118
Rough Canyon, 14, 60
Ruth mine, **113**

Saddle Rock Canyon, 27, 75, 85
Sandstone, 18, 20, 34, 35, 42, 43, 53, 55, 79, 81, 90, 93, 101, 105
Sanidine, 90
Saussurite, 24, 26, 62, 84
Scheelite, 107, 109, 110, 112

Schists, 9, 10, 12, 13, 14, 16, 17, 18, 19, 20, 30, 31, 33, 34, 35, 37, 54, 56, 65, 66, 133
Sederholm, J. J., cited, 72
Selfridge, G. C., Jr., cited, 48
Sericite, 15, 16, 17, 18, 19, 24, 25, 26, 28, 31, 33, 36, 37, 38, 40, 41, 42, 43, 54, 56, 61, 62, 70, 71, 76, 77, 84, 85, 86, 88, 90, 96, 109, 133, 134
Sericite phyllite, **36**
Serpentine, 19, 20, 33, 36, 44, 45, 46, 47, 48, 49, 50, 52, 53, 55, 56, 83, 84
Serpentine-carbonate rocks, **44-53**
Serpentinite, 10, 42, 43, 44, 45, 46, 47, 48, 49, 50, 52, 96, **108**, 133. *See also* Ricolite.
Shale, 20, 34, 35, 36, 37, 40, 41, 53, 54, 86, 101, 105
  Colorado shale, 10, 11, 78, **80-81**, 85, 86, 87, 89, 91, 101, 106, 121, 133
  Percha shale, 105
S. Harper claim, **112**
Shrine mine, 107
Silicification, 101, 109
Sillimanite, 14, 15, 16, 18, 19, 20, 21, 22, 32, 33, 34, 35, 57, 58, 133
Sillimanite gneiss, **21-22**
Siltstone, 20, 34, 53
Silurian, **105**
Silver, 107, **115-116**
Silver City range, 8, 9, 102
Sisco, Ernest, 119
Skutterudite, 116
Slate Creek, 79, 100, 113, 133
Slate Creek Canyon, 78, 80, 81, 89, 101, 102, 113, 133
Slawson, C. B., 4
Sloss, L. L., cited, 80
Snow, C. H., cited, 3
Somers, R. E., cited, 3
Southwestern Mining Co., 118
Spessartite, 75
Sphalerite, 110, 113, 114, 115, 116
Sphene, 16, 24, 29, 38, 41, 43, 44, 45, 67, 68, 69, 71
Spinel, 45
Spotted andalusite hornfels, **39-41**
Stauber, I. J., cited, 3
Staurolite, 57
Stein Canyon, 30, 31, 73, 99, 133
Stone, R. W., cited, 4, 127
Streams, intermittent, 6
Structural geology, **96-103**
  banding, **96-98**
  dikes, **102-103**
  faults, **100-102**
  folds, **98-99**
  foliation, **96-98**
  fractures, **100-102**
  igneous-metamorphic relations, **99**
  joints, **100-102**
  Laramide, **100-103**
  lineation, **98**
  post-Laramide, **100-103**
  Precambrian, **96-98, 103**
  stocks, **102-103**
  xenoliths, **99-100**
Swan Canyon, 100

Talc, 42, 43, 44, 45, 46, 47, 48, 49, 50, 52, 53, 55, 56, 133
Talmage, S. B., cited, 4, 105, 108, 116
Telegraph mining district, 107, **115**
Terrace gravels, 11, 94
Terraces, 6, 106
Tertiary:
  andesite, 86
  bajada deposits, **94**
  bolson deposits, **94-95**
  Gila conglomerate, **92-94**
  quartz latite, **89-91**
  Quaternary alluvium, **95**
  rhyolite, **89-91**, 119
  sedimentary rocks, **91-95**
  terrace gravels, **94**
  volcanic rocks, **89-91**, 101, 102, 110, 117, 122
Thermal metamorphism, 22, 37, 40, 41, 48, 50, 52, 53, 56, 63
Tonalite, 10, 63, 98
Topography, **6-7**
Travertine, 93
Tridymite, 90
Tucker, J. B., 121
Tuffs, 11, 89, 90, 91
Tungsten, 107, 110
Turner, F. J., cited, 19, 21, 36, 37
Turquoise, 107
Tuttle, O. F., cited, 50
Twenhofel, W. H., cited, 81
Twin Peaks, 85
  monzonite porphyry stock, 10, 11, **85**, 86, 87, 88, 102, 110, 116
Tyrone mining district, 107

Uralite, 63
Uranium, 110
Uranophane, 126

Vegetation, **5-6**
Vermaas, F. H. S., cited, 112
Vogel, M., cited, 76
Vogt, T., cited, 36

von Chrustschoff, K., cited, 71
Vorobjeva, O., cited, 72

Wad, 124
Wade, W. R., cited, 3
Wahlstrom, E. E., cited, 30, 68
Wargo, J. G., cited, 4, 89
Watson, Sid, 120
Whitebread, D. H., cited, 4, 12, 64, 84, 85, 98, 103, 110, 115, 116
White Signal mining district, 107
Wild Horse Canyon, 68, 80, 81
Wild Horse Mesa, 23, 78, 79, 80, 90, 101, 102, 121, 122
Winchester, D. E., cited, 89
Wootton, T. P., cited, 4, 105, 108, 116

Yale, C. G., cited, 4, 127
Yoder, H. S., Jr., cited, 19, 36, 57

Zalinski, E. R., cited, 3
Zircon, 15, 16, 18, 24, 25, 29, 31, 38, 59, 65, 67, 68, 69, 71, 86, 87, 90, 93